Catch, Effort, and Ecosystem Impacts of Tropical Tuna Fisheries

(CECOFAD II)

European Maritime and Fisheries Fund (EMFF)

[Written by Daniel Gaertner (IRD), Maitane Grande (AZTI), Pedro Pascual (IEO), David Kaplan (IRD), Josu Santiago (AZTI), Yannick Baidai (IRD), Francisco Abascal (IEO), Taha Imzilen (IRD), Gipsy Deledda-Tramoni (IRD), Anis Diallo (CRODT – ISRA), Francis Marsac (IRD), Blanca Orue (CLS Group), Camille Deslias (Univ. La Rochelle), Manuella Capello (IRD), Isidora Katara (CEFAS), Santiago Deniz (IEO), Maria Lourdes Ramos (IEO), Iván Casañas Machín (IEO), Jose Carlos Báez (IEO), Laurent Floch (IRD), Pascal Cauquil (IRD), Mathieu Depetris (IRD), Antoine Duparc (IRD), Lyndsay Clavareau (Univ. Montpellier), Bastien Mérigot (Univ. Montpellier), Jon Uranga (AZTI), Gorka Merino (AZTI), Hilario Murua (ISSF), Agurtzane Urtizberea (AZTI), Lauren Dagorn (IRD), Haritz Arrizabalaga (AZTI) [October – 2020]

This report should be cited as:

Gaertner D., Guéry L., Grande M., Pascual P., Kaplan D., Santiago J., Badai Y., Abascal F., Imzilen T., Deledda G., Diallo A., Marsac F., Orue B., Deslias C., Capello M., Katara I., Deniz S., Ramos Ma-L., Casañas Machín I., Baez J-C., Floch L., Cauquil P., Depetris M., Duparc A., Clavareau L., Merigot B., Uranga J., Merino G., Murua H., Urtizberea A., Dagorn L., Arrizabalaga H. (2019). Catch, effort and ecosystem impacts of Tropical Tuna fisheries (CECOFAD2). Final Report. European Commission. Specific Contract No. 9 under Framework Contract No. EASME/EMFF/2016/008. pp + Annexes.

EUROPEAN COMMISSION

Executive Agency for Small and Medium-sized Enterprises (EASME)

Unit Department A - COSME, H2020 SME and EMFF

Unit A3 EMFF

Contact: EASME EMFF A.3

E-mail: EASME-EMFF-CONTRACTS@ec.europa.eu

European Commission
B-1049 Brussels

Specific Contract No 9

EASME/EMFF/2017/1.3.2.6

FRAMEWORK CONTRACT EASME/EMFF/2016/008

Provision of Scientific Advice for Fisheries Beyond EU Waters

Catch, Effort, and Ecosystem Impacts of Tropical Tuna Fisheries (CECOFAD II)

Final Report

Europe Direct is a service to help you find answers to your questions about the European Union.

Freephone number (*)**:**

00 800 6 7 8 9 10 11

(*) The information given is free, as are most calls (though some operators, phone boxes or hotels may charge you).

Luxembourg: Publications Office of the European Union, 2020

PDF ISBN 978-92-9460-215-2 doi: 10.2826/621446 EA-02-20-650-EN-N

Contents

1 Summary

The Specific Contract n°9 " Catch, Effort, and Ecosystem impacts of tropical tuna fisheries" (CECOFAD2) of SAFEWATERS2 set out to (1) improve our understanding of the use of drifting fish-aggregating devices (dFADs) in tropical purse seine tuna fisheries and (2) to assess the impact of this fishing practice on associated pelagic species and on vulnerable ecosystem.

In association with the European project (RECOLAPE), new information on technological changes over time in terms of echo sounder buoys brands and models type has been collected. In addition, the analysis of the dFAD fishing activities of the European baitboats operating from Dakar (Senegal) showed an increase in catch due to the sharing of the buoys (about 300 buoys per group of 3-4 baitboats). With the aim to explore the effect of the total density of dFADs equipped with buoys, i.e. summing the density from available EU buoys trajectories data and the density of buoys without trajectories data (some Spanish and non-EU) on the catch per set, identified buoys without available trajectories from the French fleet capture data have been used in Spatial Capture-Recapture (SCR) models to estimate this second part of buoys density, i.e., those without trajectories data. Since change in abundance of tropical tunas over time may be due to change in the density of tuna schools and/or in the size of the school, the European purse seiner CPUE standardization for large yellowfin in free schools was based on a 3-components model at the set scale level. The standardized index was used in the yellowfin stock assessment models in ICCAT and in a sensitivity analysis for the same species and fishing mode in IOTC. The CPUE standardization for FAD-fishing is still in progress due to the difficulties to obtain information on the ownership of the buoys which could be used to discriminate the part of the fishing effort devoted to setting on dFAD belonging to each vessel (i.e., when the purse seiner is using the GPS of the buoy and goes directly towards the dFAD) to the proportion of foreign dFADs (i.e., encountered randomly), as well as to integrate the effect of the assistance provided by the support vessels to each purse seiner.

Direct indices of juvenile tuna abundance through the use of echo sounder buoys attached to dFADs in the Spanish fleet were investigated. A delta-lognormal distribution was used to estimate the "alternate" Buoy-derived Abundance Index (BAI) as the product of the probability of presence of tuna and the mean relative abundance where there was a positive observation. The derived BAI was integrated in the 2019 yellowfin stock assessment models conducted by ICCAT and IOTC 2019. From echo sounder data collected on French purse seiners from Marine Instruments buoys, the average colonization time of a dFAD by tuna in the Atlantic Ocean was estimated at 20.5 days. The results also revealed that the residence time of a tuna aggregation around a single dFAD is about 9 days and that dFADs spend on average 7 days without tuna. These values could be variable depending on the buoy model used, algorithm developed and ocean.

An analysis conducted from the French observer data on the potential impact of dFAD-fishing revealed that silky shark catches appeared mostly localized around the Gabon and Angola coasts in the Atlantic Ocean while their distribution appeared more spread across all fishing regions in the Indian Ocean. The temporal series (2007-2018) of the relative abundance indices globally showed an increasing trend of silky shark. From data collected by the scientific Spanish Observer program, several indices related to biodiversity of bony fishes, showed no trend, or only small differences, over the 11-years period analyzed. With regard to the IUCN conservation status, only 4% of the total number of species/taxa found under dFADs are considered as vulnerable. Trajectory data from dFADs deployed by French purse-seiners over the period 2008-2017 were used to assess the impact of lost dFADs on vulnerable coastal ecosystems. Maps of beaching locations clearly identify coastal hotspots, such as the coasts of Africa (Guinea-Sierra Leone and Cameroun-Gabon), Brazil and the Caribbean, for the Atlantic Ocean, Somalia, Maldives, Sri Lanka and Seychelles, for the Indian Ocean. By backtracking from beaching locations, maps identifying areas for which buoys crossing an area have a high beaching event probability within the next 3 months have been produced.

In order to improve an effective dFAD time area closure for protecting juvenile of bigeye in the Atlantic 0cean, an analysis of global and local Moran's indicators of spatial association permitted to identify hotspots from September to January in the center of the Atlantic Ocean and then from November to January in the Gulf of Guinea. Spanish support vessel activities before, during and after the January-February dFAD moratoria season established by ICCAT between 2016 and 2018[1] was monitored in order to explore the efficiency of the assistance provided by these vessels to the purse seiners. There were slight drops in the number of FADs deployed and serviced or checked by supply vessels, as well as minor increases in the number of dFAD retrievals as compared to the months immediately preceding and following the January-February period. In addition, the efficiency of the current dFAD fishing moratorium Rec [15-01] was assessed using tagging data from the AOTTP for both yellowfin and bigeye juveniles. It was showed that recapture rates when juvenile yellowfin tunas were tagged outside the moratorium area is equal to 18 times the recapture rate of tunas that were tagged inside the moratorium area (2017 and 2018 confounded). This suggests that the moratorium has been effective for protecting juveniles of yellowfin. Due to the low number of release-recapture observations, the result is unclear for bigeye tunas. We conclude CECOFAD2 by proposing a guideline for implementing an adaptive management (AM) approach for facilitating decision making in terms of management objectives of highly migratory species (HMS) resources to support an ecosystem approach to fisheries.

[1] The moratorium implemented by ICCAT in January-February 2016 was based on Rec. 2014-01. The next moratorium (Rec. 2015-01) entered into in force in June 2016 and consequently was effective for the first time in January-February 2017.

2 Title of the project

Catch, Effort, and Ecosystem impacts of tropical tuna fisheries (CECOFAD2)

3 Objectives

The Specific Contract No. 9 under Framework Contract EASME/EMFF/2016/008 provisions of Scientific Advice for Fisheries Beyond EU Waters started on the 27th of April 2018, the day the contract was signed. As per Terms of Reference, originally the overall duration of the project was 16 months. However, to allow for a full implementation and achievement of objectives, a four months extension of the contract has been agreed.

The aim of this specific study is to provide the Directorate-General for Maritime Affairs and Fisheries (DG MARE) with technical and scientific analyses on the use of drifting Fish Aggregating Devices (dFADs) by the European tropical tuna purse seine (PS) fisheries and on their impact on the tuna resource and the environment of the Atlantic and Indian oceans.

With these considerations in mind, this study has three specific objectives:

- Estimate the contribution of the new fishing technologies, implemented by the tropical tuna PS fisheries, to fishing mortality;
- Estimate the accuracy and precision of direct indices of abundance based on echosounder buoys records;
- Improve the knowledge of the environmental impact of tropical tuna fisheries and develop management measures accounting for ecosystem considerations.

To achieve these objectives, CECOFAD2 was organized into 3 Work Packages (WPs), as follows:

- WP 1 - Contribution to fishing mortality of new fishing technologies implemented by tuna PS fisheries (Objective 1 of the project),
- WP 2 - Direct abundance indices from echosounder buoys (Objective 2),
- WP 3 - Impact of drifting FADs (dFADs) on the ecosystem (Objective 3).

4 Executive summary

4.1 Executive summary

The Specific Contract n°9 " Catch, Effort, and Ecosystem impacts of tropical tuna fisheries" (CECOFAD2) of SAFEWATERS2 set out to (1) improve our understanding of the use of drifting fish-aggregating devices (dFADs) in tropical purse seine tuna fisheries and (2) to assess the impact of this fishing practice on associated pelagic species and on vulnerable ecosystem.

As there are no suitable procedures for the standardization of purse-seiner CPUE indices, most of the assessments of tropical tuna stocks worldwide are based on longline CPUE indices which rarely take account of the implementation of new technology in the standardization process and only reflect the biomass of the older fraction of tuna populations. Consequently, one of the main tasks defined in CECOFAD2 was to provide insights into potential explanatory factors used in the calculation of European purse-seiner dFAD and free school CPUEs standardized indices of abundance for juvenile and adult tropical tuna in the Atlantic and Indian Oceans. Data from unofficial technology information related to FAD-fishing were retrieved during the first 12 months of the project thorough the European companion research project (RECOLAPE). Important data, such as the link between individual purse seiners and supply vessels, are still lacking for some fleets but new information on technological changes over time in terms of echo sounder buoys brands and models type are now available.

One of the variable which potentially might affect the school size under dFAD, and consequently the catch rate, is the density of floating objects ("FOB", that is to say dFADs plus natural or artificial logs). Estimating the density of dFADs as a proxy of the density of FOBs has been considered as an important issue in this project. For the French fleet, dFAD-associated purse-seiners monitored all buoys (i.e. belonging to any flag) GPS positions' and trajectories' to produce a density map since 2010. For the Spanish fleet, data recovery was still on-going at the time of the first analyses during 2018 and was completed later during 2019. The remaining part of buoys density (i.e., those without available trajectories) from non-European purse seiner fisheries (e.g., Ghana, Seychelles) still needs to be estimated. Using buoys IDs recorded in fine-scale operational data of observer and captain logbooks, identified buoys but for which trajectories data are not available (e.g. some of the Spanish flag and other non-European flags) can be used in Spatial Capture-Recapture (SCR) models to estimate remaining dFADs spatial and temporal distribution, time-at-sea density and probability of detection. These models are based on classical capture-recapture techniques, using individual encounter history data, where auxiliary spatial information is also obtained. In these models, the varying exploration effort is taken into account. Preliminary results obtained only with activities on non-tracked buoys reported by the French

purse seiners showed that this method can be useful to evaluate the density of buoys used by the other fleets of purse seiners.

In addition to the fishing technology developed by the European purse seiners, an analysis on the fishing activities related to dFADs by the European pole and line fishery operating from Dakar (Senegal) has been conducted. In the early 1990s, this baitboat fleet has implemented a new fishing strategy (i.e., the "vessel associated-school") where a baitboat acted as a floating object to attract tunas, then changed over time towards the increasing use of dFADs for aggregating tropical tunas with a concomitant wider fishing ground in the Eastern Atlantic Ocean. Depending on the season of the year, each group of baitboats may use up to more than 300 operational buoys. The total catch per group increased with the number of operational buoys but conversely the catch rate (catch per number of buoys) decreased.

European purse seiner CPUE standardization was successfully conducted for large yellowfin in free schools at the set scale level. To account for the fact that tropical tunas are spatially structured in schools and in clusters of schools and that in consequence any change in abundance may be influenced by change in the number (or density) of schools at sea, by change in the size of the school or by both, we developed an extension of the Delta-log model which takes the form of three sub-models as follows: (1) a Poisson GLMM that standardizes the number of positive and null sets, by vessel and unit of time and location, (2) a binomial GLMM that takes into account the fraction of positive sets with large yellowfins, (3) a lognormal LMM to describe the catch conditional to positive set (i.e., the size of the school). Standardized CPUE for free schools was thus defined as the product of the number of sets (positive and null) by spatio-temporal strata, the proportion of sets with large yellowfin (>10 kg) and the catch of large yellowfin per positive set. The originality of this work relied on the inclusion of i) null sets, considered as presence of schools of yellowfin, ii) fishing days (i.e., days on the fishing grounds for which the purse seiner is fishing) without set, considered as absence of FSC, and iii) searching time spent at sea by boat by day by cell of 1°*1° to take into account the heterogeneity in cells exploration. This new standardization approach, therefore, represents a significant advance over previous efforts and the standardized index has been used into the Yellowfin stock assessment in the Atlantic Ocean and in the sensitivity analysis for the Indian Ocean. The CPUE standardization for FAD-fishing has been limited to one component and is still in progress due to the difficulties to (1) discriminate the part of the fishing effort devoted to setting on dFAD belonging to each vessel (i.e., not detected randomly) to the proportion of foreign dFAD (i.e., encountered randomly) and (2) to account for not conventional variables such as the assistance provided by support vessels to purse seiners which have been identified as a clear component of the fishing

effort (i.e., ICCAT-Rec[16-01][2]). In the same way as for the free schools CPUE standardization, the integration of environmental factors in the model as well as spatial clustering methods, with the aim to reduce the amount of time for the computation due to the large database, should be investigated (i.e., how to account for the spatial and time dimensions with a moderate number of parameters to estimate). However, progress in dFAD CPUE standardization accomplished during CECOFAD2 will benefit in the ongoing Specific Contract N°14.

As an alternative to dFAD CPUE, direct indices of tuna abundance through the use of echo sounder buoys attached to dFADs in the Spanish fleet were investigated during CECOFAD2. Estimating the abundance of tuna and non-tuna species directly using echo sounder buoy acoustic biomass data requires gathering and processing heterogeneous echo sounder buoy information from different brands and models. For this reason, developing a consistent echo sounder buoy database required cleaning datasets before standardizing an abundance index derived from echo sounder buoy data. Because the factor of proportionality between the buoy-derived Abundance Index (BAI) and the unknown abundance is not constant, nominal measurements from echo sounder buoy records were standardized using a generalized linear mixed model (GLMM) approach and a delta-lognormal distribution was used to estimate BAI as the product of the probability of presence of tuna and the mean relative abundance where there was a detection of tuna. The derived BAI, assumed to depict change over time of juvenile tunas, was integrated in the 2019 yellowfin stock assessment models conducted by ICCAT and IOTC in 2019.

The analyses of the continuous process of association and disassociation, as well as the residence time under dFADs, were also conducted from echosounder data collected on French purse seiners. From this study it has been showed that newly deployed dFADs, equipped with a Marine Instruments buoy, are colonized by tuna aggregations after an average of 20.5 days in the Atlantic Ocean. The results also revealed, for the first time, that the continuous residence time of a tuna aggregation around a single dFAD is about 9 days and that an average of 7 days elapses between the aggregation departure and the later repopulation of the dFAD by other tunas. The ratio of the sum of all continuous residence times of tuna aggregations measured under a dFAD to its total soak time after colonization was estimated based on individual dFAD observations. On average, DFADs were shown to be occupied by tuna aggregation about 50 % of their soaking time after colonization. These metrics can be affected by seasonal variations. It should be noted however for this buoy model (M3I), current performances of the algorithms developed for assessing presence/absence of tuna are satisfactory, whereas the biomass estimates are weakly correlated with the catches done on the same dFAD. The same conclusion was drawn from the BAI Spanish study. The catch at the buoy

[2] "*FURTHER NOTING that the activities of **supply vessels** and the use of FADs are an integral **part** of the **fishing effort** exerted by the purse seine fleet"* (ICCAT Rec[16-01]

showed a positive trend with the estimated biomass, but the correlation coefficient is low due to the variability of the data and seems to be dependent of the amount of tuna catch in the set. Also, other factors as environmental factors (e.g., sea surface temperature), area or season could be affecting to this relationship and their impact on the buoy biomass and catch relationship should be further explored.

In order to improve knowledge of the environmental impact of tropical tuna fisheries and develop ecosystem management measures accounting for ecosystem considerations, we explored the risks of FAD-fishing on protected and endangered species as well as on vulnerable habitats, and the potential regulatory measures to reduce this impact. An analysis conducted from the French observer data on the potential impact of dFAD-fishing revealed that silky shark (*Carcharhinus falciformis*) catches appeared mostly localized around the Gabon and Angola coasts in the Atlantic Ocean while their distribution appeared more spread across all fishing regions in the Indian Ocean. In parallel, a novel approach to derive an abundance index for the silky sharks in the Indian Ocean, based on an empirical model that accounts for their association dynamics at dFADs, has been developed. The temporal series (2007-2018) of the relative abundance indices globally showed an increasing trend with a magnitude depending on the area. This increase in shark abundance could be a result of a combination of factors that took place as from 2010 (e.g. introduction of non-entangling FADs, Chagos MPA, shift of fishing effort due to piracy, Maldivian shark fishing ban). Nevertheless, it important to note that this relative index reflects a trend and is not a population estimate, which means that the observed upward trends should not be interpreted as an indication of a healthy population.

With the aim to assess the potential Impact of FAD-fishing on bony fishes and other marine species, a comparative analysis of biodiversity index, abundance, dominance curves and accumulation of species, was conducted from data collected by the scientific Spanish Observer program. On the information collected for each of the taxa (i.e. species or family), a descriptive analysis of each taxa, abundance, type habitat, biology, distribution and social behavior and IUCN status was performed. With regards to the natural habitat, the fauna associated to dFADs are mainly species classified as "reef-associated" and "oceanic pelagic" habitats (38% and 27%, respectively). The remaining 35% are species classified as benthopelagic and pelagic coastal. On the basis on the number of individuals caught during the set, 54% of the species were observed with one individual. 31% are species that swim in small groups and only 15% of the observed species swim forming large groups around the dFADs (such as tuna and tuna like species). With regards to the IUCN conservation status situation 76% of taxa are in a low concern situation, 16% of taxa have not been evaluated, 4% of taxa lack data and only 4% of taxa are considered as vulnerable. These vulnerable species correspond to two species of marlins (the Atlantic white marlin: *Kajikia albida* and the Atlantic blue marlin: *Makaira nigricans*), a tuna (the bigeye tuna: *Thunnus obesus*), a sunfish (*Mola mola*) and

two crossbow fish (*Balistes punctatus* and *Balistes capriscus*). Over the 19-years period analyzed, indices showed no trend over time (e.g., richness's index) or small differences (similarity MDS, dominance curves, Shannon's index). However, the information and results provided in the present study must be taken with great caution, since the balance and equality in the observer on board sampling have not been the same throughout the entire study period. Consequently, these differences might be explained by changes in fishing strategies to dFADs over time and/or by methodological differences between old and current observation programs. With this limitation in mind, there is no evidence of significant impact of dFAD-fishing on the community of bony fishes associated with dFADs.

Another important aspect is the potential damage of lost DFADs on vulnerable coastal ecosystems. From trajectory data from dFADs deployed by French purse-seiners over the period 2008-2017 it was evidenced that the number of deployed buoys has continued to increase dramatically in recent years especially in the Indian Ocean. It must be noted that the percentage of the deployed dFADs that end up beaching increased until 2013, but surprisingly remains stable or even slightly decreases after 2013. Maps of beaching locations clearly identify coastal hotspots, such as the coasts of Africa (Guinea-Sierra Leone and Cameroun-Gabon), Brazil and the Caribbean, for the Atlantic Ocean, Somalia, Maldives, Sri Lanka and Seychelles, for the Indian Ocean. By backtracking from beaching locations, maps identifying areas for which buoys crossing an area have a high beaching event probability within the next 3 months have produced. To highlight the potential impact of dFAD beaching in vulnerable areas, the same backtracking approach has also been conducted exclusively on buoys that beach into Coral reefs. In the case of the Indian Ocean, it was clearly showed that risky areas in terms of probability of beaching events change with seasons and depend on the Monsoon regimes.

In order to better definition of an effective dFAD time area closure for protecting juvenile of bigeye in the Atlantic 0cean, a study was conducted to detect hotspots of catch of small bigeye. Total dFAD catch by 1°square*month for the purse seine fleets operating in the Eastern Atlantic were reconstituted from the ICCAT task II catch/effort data (e.g., EU fleet), or raised to ICCAT task I and re-estimated by month and 1°square for the other fleets (e.g., in case of Ghana task II by fishing mode submitted to ICCAT is significantly lower than task I), It was also assumed that for each 1°square*month strata explored by the European purse seiners and the Ghanaian fleet, it was better to use the sampling done on the European dFADs sets at landings than the data submitted to ICCAT secretariat in order to re-estimate the amount of juvenile bigeyes caught on dFAD by the Ghanaian fleet. The results of the spatio-temporal analysis showed that the major dFADs catches of juvenile bigeyes are observed from September to January. Following this, an analysis of global and local Moran's indicators of spatial association permitted to identify hotspots from September to January in the center of the Atlantic Ocean and then from November to January in the Gulf of Guinea. This seasonal pattern

was in agreement with an analysis of monthly purse seiner catches of small bigeyes on dFAD over the period 2014-2018. There is no evidence of an effect of the dFAD moratorium on a change in proportion of bigeye tuna caught in free schools. It should be recalled that the main species caught in free school is the yellowfin and that the largest monthly bigeye catch (June-July) do not exceed 10% of the total free school catch.

An analysis of Spanish support vessel activities before, during and after the 2 months of moratorium for the three moratoria established by ICCAT between 2016 and 2018 was done in order to explore the efficiency of the assistance provided by these vessels to the purse seiners during these regulation periods. The pattern of vessels' activity during the FAD closures differed significantly between 2016 and the other two years, possibly due to the fact that the recommendations 14-01, 15-01 and 16-01 affected different areas. There were slight drops in the number of FADs deployed and serviced or checked by supply vessels, as well as minor increases in the number of FAD retrievals as compared to the months immediately preceding and following the January-February moratorium period; though the series show high variability throughout the year. An important issue when analyzing dFAD data from FAD logbooks is the difficulty in tracking unique dFADs without the actual buoy transmission information, due to several circumstances; including the activity of non-Spanish flagged vessels over this dFADs and issues related to dFAD coding and recording. As a consequence, the number of FADs deployed by supply vessels and later set by a purse seiner was unexpectedly low. The combination of FAD logbooks from purse seiners and supply vessels suggests that FADs deployed in January and February out of the closed areas are not fished once the closure finishes in these areas. On the contrary, FADs deployed in November-December can drift out of the closed areas and be fished in January-February. It seems however the impact of the closures in supply vessels' activity is limited.

In addition, the efficiency of the current dFAD fishing moratorium Rec [15-01] was assessed using tagging data from the AOTTP (2016-2018) for both yellowfin and bigeye juveniles (Fork length <70 cm) by (1) comparing the rate of recapture of juveniles within and outside the moratorium strata through the use of relative risk of recapture, (2) shortest distance in kilometers at sea, cardinal directions and time at sea were computed for individuals tagged inside the moratorium area in 2017. It was showed that recapture rates when juvenile yellowfin tunas were tagged outside the moratorium area is equal to 18 times the recapture rate of tunas that were tagged inside the moratorium area (2017 and 2018 confounded). This suggests that the moratorium has been effective for protecting juveniles of yellowfin. Due to the low number of release-recapture observations, the result is still unclear for bigeye tunas. An additional step dedicated to testing a border effect showed that 50% of the yellowfin tuna tagged inside the moratorium were marked within 100 km of the northern edge of the moratorium (North Latitude = 5°). From the circular diagram analysis, we showed that since the beginning of the

moratorium period juvenile yellowfin tuna were mainly recaptured in the east and west/northwest with relatively long distances covered (keeping in mind the 1 to 2 months' time at liberty considered). The release-recapture data of the AOTTP offer many promising perspectives to understand why juvenile yellowfin and bigeye tuna juveniles migrate in some parts preferentially in the Eastern Atlantic Ocean.

Today fishery managers are not faced only with the sustainable exploitation of the tropical tuna resources but also with the conservation of the ecosystems while providing food income and safeguarding fishermen's livelihoods in a sustainable way. As a consequence, multi-species management, bycatch mitigation, protection of vulnerable ecosystems must be integrated to achieve ecological and socio-economic objectives. Because the application of conventional research methods is often insufficient to support effective decision-making when decisions must be made regardless of the level of knowledge or uncertainty we propose a guideline for implementing an adaptive management (AM) approach for facilitating decision making in terms of management of highly migratory species (HMS) resources to support an ecosystem approach to fisheries.

Instead of focusing on tropical tuna management by using Management Strategy Evaluation (MSE) which omits the collateral effect of tropical fisheries on the epipelagic ecosystem, an AM process could offer an alternate approach to enable value judgments about how to control a sustainable use of the FAD-fishery within the frame an ecosystem approach to fisheries. Based on the fact that AM is "learning by doing", the guideline proposes a methodology to integrate the opinions of different stakeholders (scientists, fishermen, government officials, and NGO representatives) since the co-design of common objectives and indications where actions could be applied, to the assessment of the progress resulting from the implementation of management measures. The AM iterative decision-making process uses computer models (e.g., simulation tools such as Multi-agent systems) parameterized with stakeholder knowledge to synthesize and build alternatives management strategies to reach a consensus for a natural resource management. The confrontation of the model with real circumstances leads to revise and to re-build it, taking gradually into account the uncertainty features of the tropical tuna fisheries. Depending on the level of information and data available, the AM implementation can be based on simpler operative models than in MSE, using an optimum function. AM can be validated by statistical methods to assess if the regulation measure answers to the objectives fixed by the stakeholders.

4.2 Résumé Exécutif

Le contrat spécifique n° 9 « Catch, Effort, and Ecosystem impacts of tropical tuna fisheries » (CECOFAD 2) de SAFEWATERS2 vise à (1) améliorer notre compréhension de l'utilisation des dispositifs de concentration de poissons dérivants (DCPd) dans la pêcherie du thon tropical à la senne et (2) évaluer

l'impact de cette pratique de pêche sur les espèces pélagiques associées et sur les écosystèmes vulnérables.

Comme il n'y a pas de procédures appropriées pour la standardisation des indices de CPUE des senneurs, la plupart des évaluations des stocks de thons tropicaux dans le monde sont basées sur des indices de CPUE des palangriers qui tiennent rarement compte de la mise en œuvre de nouvelles technologies dans la standardisation et ne reflètent que la biomasse de la fraction la plus âgée des populations de thons. Par conséquent, l'une des tâches principales définies dans CECOFAD 2 était de fournir des informations sur les facteurs explicatifs potentiels utilisés dans le calcul de la standardisation des CPUE de thons tropicaux juvéniles et adultes des senneurs européens pour la pêche sur DCPd et en bancs libres dans les océans Atlantique et Indien. Des informations non conventionnelles sur la technologie utilisée pour la pêche sur DCP ont été récupérées au cours des 12 premiers mois de CECOFAD2 dans le cadre d'un autre projet européen de recherche (RECOLAPE), complémentaire à cette étude. Des données importantes, telles que le lien entre chaque senneur et les navires baliseurs font encore défaut pour certaines flottes, mais de nouvelles informations sur les évolutions technologiques au cours du temps en termes de marques et de types de bouées pour échosondeurs sont désormais disponibles.

L'une des variables susceptibles d'affecter la taille du banc sous DCPd, et par conséquent le taux de capture, est la densité des objets flottants («FOB», c'est-à-dire les DCPd plus les objets flottants naturels ou artificiels). L'estimation de la densité des DCPd comme indicateur « proxy » de la densité des FOB a été considérée comme un problème important dans ce projet. Pour la flotte française, les senneurs associés aux DCPd ont fournis des informations sur les positions et trajectoires GPS de toutes les bouées (c'est-à-dire appartenant à n'importe quel pavillon) qui ont permis de produire une carte de densité depuis 2010. Pour la flotte espagnole, la récupération des données était toujours en cours au moment des premières analyses en 2018 et s'est terminée plus tard en 2019. Le reste de la densité des bouées (celles pour lesquelles la trajectoire n'est pas disponible) pour les senneurs non européens (Ghana, Seychelles, par exemple) doit encore être estimée. En utilisant les ID de bouées enregistrées dans les opérations de pêche à petite échelle par les observateurs et dans les livres de bord remplis par les capitaines, les bouées identifiées mais pour lesquelles les trajectoires ne sont pas disponibles (certains senneurs espagnols et d'autres non européens) peuvent être utilisées dans les modèles spatiaux de capture-recapture (« SCR ») pour estimer la distribution spatiale et temporelle des DCPd restants, le temps en mer et la probabilité de détection. Ces modèles sont basés sur des techniques classiques de capture-recapture et utilisent des données historiques de rencontres individuelles où des informations spatiales sont également obtenues. Dans ces modèles, le niveau pris par l'effort d'exploration est pris en compte. Les résultats préliminaires, obtenus seulement à partir des activités sur les bouées non suivies reportées par les senneurs français, ont montré que cette méthode peut

être utile pour évaluer la densité des bouées utilisées par les autres flottes de senneurs.

En plus de la technologie de pêche développée par les senneurs européens, une analyse des activités de pêche liées aux DCP par les canneurs européens opérant à partir de Dakar (Sénégal) a été réalisée. Au début des années 1990, cette flotte de canneurs a mis en place une nouvelle stratégie de pêche (dite de la « matte » associée au canneur), où le canneur agissait comme un objet flottant pour attirer les thons, puis a évolué au cours du temps vers l'utilisation croissante de DCP pour agréger des thons tropicaux, ce qui s'est réalisé de manière concomitante avec une extension de leur zone de pêche dans l'Atlantique oriental. Selon la saison de l'année, chaque groupe de canneurs peut utiliser jusqu'à plus de 300 bouées opérationnelles. La capture totale par groupe de navires a augmenté avec le nombre de bouées opérationnelles utilisées, à l'inverse le rendement (capture par nombre de bouées) qui a diminué.

La standardisation des CPUE des senneurs européens a été menée avec succès pour les grands albacores en bancs libres à l'échelle du coup de senne. Pour tenir compte du fait que les thons tropicaux sont structurés spatialement en bancs et en concentrations de bancs et qu'en conséquence tout changement d'abondance peut être influencé soit par le nombre (ou la densité) de bancs, soit par la taille du banc ou soit par les deux, nous avons développé une extension du modèle Delta-log qui prend la forme de trois sous-modèles comme suit: (1) un GLMM de Poisson qui standardise le nombre de coups de senne positifs et nuls, par navire et unité de temps et de lieu, (2) un GLMM binomial qui prend en compte la fraction des calées positives avec des captures de grands albacores, (3) un LMM lognormal pour décrire la capture par calée positive (représentant la taille du banc). La CPUE standardisée pour les bancs libres a donc été définie comme le produit du nombre de calées (réussies et nulles) par strates spatio-temporelles, de la proportion de calées avec du gros albacore (> 10 kg) et de la capture de gros albacores par coup de senne positif. L'originalité de ce travail reposait sur l'inclusion i) des coups nuls, considérés comme indicateurs de la présence de bancs d'albacores, ii) des jours de pêche (c'est-à-dire les jours de pêche ou le senneur est actif) mais sans faire de calée, considérés comme caractérisant une absence de bancs libres, et iii) le temps de recherche par bateau, par jour, par cellule de 1° * 1° pour prendre en compte l'hétérogénéité dans le temps passé à explorer chaque cellule. Cette nouvelle approche de standardisation représente donc une avancée significative par rapport aux travaux antérieurs et l'indice standardisé a été utilisé dans l'évaluation des stocks d'albacores de l'océan Atlantique et dans l'analyse de sensibilité pour l'océan Indien. La standardisation des CPUE pour la pêche sur DCP a été limitée à une composante et est toujours en cours d'analyse en raison des difficultés à (1) discriminer la part de l'effort de pêche consacrée à la recherche des DCP appartenant à chaque navire (et qui ne sont pas détectés au hasard) et celle concernant les DCP étrangers (rencontrés au hasard) et enfin (2) pour tenir compte des variables non conventionnelles telles que l'assistance fournie aux

senneurs par les baliseurs qui ont été identifiés comme une composante essentielle de l'effort de pêche (ICCAT-Rec [16-01][3]). De la même manière que pour la standardisation des CPUE des bancs libres, l'intégration des facteurs environnementaux dans le modèle ainsi que les méthodes d'agrégation spatiale des cellules de 1°, dans le but de réduire le temps de calcul dû à la taille de la base de données, devraient être étudiées (par ex. comment prendre en compte les dimensions spatiales et temporelles à une échelle fine tout en limitant le nombre de paramètres à estimer). Il est à noter toutefois que les progrès réalisés lors de la standardisation de la CPUE sous DCPd au cours de CECOFAD2 bénéficieront au contrat spécifique n ° 14 en cours.

Comme alternative à la standardisation des CPUE commerciales sous DCPd, des indices d'abondance directs par l'utilisation de bouées munies échosondeurs attachées aux DCP ont été analysés au cours de CECOFAD2 sur la flotte espagnole. L'estimation directe de l'abondance de thons et d'espèces associées à l'aide des données acoustiques sur la biomasse nécessite la collecte et le traitement d'informations hétérogènes sur des échosondeurs de différentes marques et modèles. Pour cette raison, le développement d'une base de données cohérente sur les bouées munies d'échosondeur a nécessité un nettoyage des données avant de standardiser un indice d'abondance. Étant donné que le facteur de proportionnalité entre l'indice d'abondance dérivé de la balise (BAI) et l'abondance inconnue n'est pas constant, les mesures nominales des enregistrements des échosondeurs ont été standardisées à l'aide d'un modèle mixte linéaire généralisé (GLMM) et une distribution delta-lognormale a été utilisée pour estimer le BAI comme le produit de la probabilité de présence de thons et de l'abondance relative moyenne en cas de détection de thons. Le BAI, supposé représenter le changement dans le temps de l'abondance des thons juvéniles, a été intégré dans les modèles d'évaluation des stocks d'albacores de 2019 menés par l'ICCAT et la CTOI en 2019.

Une analyse du processus continu d'association et de dissociation, ainsi que le temps de séjour sous un DCPd, a également été réalisée à partir de données recueillies sur les bouées-échosondeurs des senneurs français. Grace à cette étude, il a été montré que les DCPd nouvellement déployés, équipés d'une bouée Marine Instruments, sont colonisés par des agrégations de thons en moyenne au bout de 20,5 jours dans l'océan Atlantique. Les résultats ont également révélé, pour la première fois, que le temps de séjour continu d'un banc de thon sous un DCPd est d'environ 9 jours et qu'il s'écoule en moyenne 7 jours entre le départ du banc et le repeuplement ultérieur du DCPd par d'autres thons. Le ratio de la somme de tous les temps de séjours continus des agrégations de thons mesurés sous un DCPd, à son temps de séjour en mer après colonisation a été estimé sur

[3] " *NOTANT EN OUTRE que les activités des* ***navires ravitailleurs*** *et l'utilisation des DCP font partie* ***intégrante*** *du* ***effort de pêche*** *exercé par la flottille de senneurs"* (Rec. ICCAT [16-01]

la base des observations faites sur chaque DCPd. En moyenne, les DCPD ont été occupés par un banc de thons environ 50% de leur temps de mer après colonisation. Ces estimations peuvent être affectées par des variations saisonnières. Il faut noter toutefois que si pour le modèle d'échosondeur (M3I) utilisé, et les performances actuelles des algorithmes développés, la détection de l'absence/présence de thons est satisfaisante, les estimations de biomasse sont faiblement corrélées avec les captures réalisées sur le même DCPd. La même conclusion est tirée de l'étude Espagnole portant sur le BAI. La capture sur la bouée montre une tendance croissante avec l'estimation de la biomasse faite à partir du signal de l'échosondeur mais le coefficient de corrélation reste faible et semble dépendre de la quantité de thons capturés dans le coup de senne correspondant. De plus, d'autres facteurs comme les facteurs environnementaux (par ex., la température de la surface de la mer), la zone ou la saison pourraient affecter ces estimations et leur impact sur la relation entre la biomasse estimée sur la bouée et la capture devrait être exploré plus avant.

Afin d'améliorer la connaissance de l'impact environnemental de la pêche des thonidés tropicaux et d'élaborer des mesures de gestion des écosystèmes qui tiennent compte de considérations écosystémiques, nous avons exploré les risques causés par la pratique de pêche sur DCP sur les espèces protégées et en voie de disparition, ainsi que sur les habitats vulnérables, et les mesures réglementaires possibles pour réduire cet impact. Une analyse réalisée à partir des données récoltées à bord des senneurs français par des observateurs sur l'impact potentiel de la pêche aux DCP dérivants a révélé que les captures de requins soyeux (*Carcharhinus falciformis*) sont principalement localisées au niveau des côtes du Gabon et de l'Angola dans l'océan Atlantique, tandis qu'elles semblent plus réparties dans toutes les zones de pêche de l'Océan Indien. En parallèle, une nouvelle approche pour dériver un indice d'abondance des requins soyeux de l'océan Indien, basée sur un modèle empirique qui tient compte de leur dynamique d'association aux DCPd a été développée. La série temporelle (2007-2018) de ces indices d'abondance relatifs a montré une tendance globale à la hausse avec une amplitude qui dépendait de la zone. Cette augmentation de l'abondance des requins pourrait résulter d'une combinaison de facteurs qui ont eu lieu à partir de 2010 (par exemple, l'introduction de DCP non-maillants, l'AMP des Chagos, le déplacement de l'effort de pêche en raison de la piraterie, l'interdiction de pêche au requin des Maldives). Néanmoins, il est important de noter que cet indice relatif ne reflète qu'une tendance et n'est pas une estimation de la population, ce qui signifie que les tendances observées à la hausse ne doivent pas être interprétées comme une indication d'une population en bonne santé.

Dans le but d'évaluer l'impact potentiel de la pêche des DCP sur les poissons osseux et d'autres espèces marines, une analyse comparative d'indice de biodiversité, d'abondance, des courbes de dominance et d'accumulation des espèces a été réalisée à partir des données collectées par le programme scientifique Espagnol d'observateurs à bord. Sur la base des

informations collectées pour chaque taxon (c'est-à-dire, les espèces ou les familles), une analyse descriptive par taxon, de l'abondance, du type d'habitat, de la biologie, de la distribution, du comportement social et de son statut à l'UICN a été réalisée. En ce qui concerne l'habitat naturel, la faune associée aux DCP est principalement constituée d'espèces classées comme " associés aux récifs " et "pélagiques océaniques" (respectivement 38% et 27%). Les 35% restants sont des espèces classées benthopélagiques et pélagiques côtières. Sur la base du nombre d'individus capturés durant la calée, 54% des espèces ont été observées avec qu'un individu par calée. 31 % sont des espèces qui nagent en petits groupes et seulement 15% des espèces observées nagent en formant de grands groupes autour des DCP (comme les thons majeurs et les petits thonidés). En ce qui concerne le statut de conservation attribué par l'UICN, 76% des taxons sont dans une situation de faible préoccupation, 16% des taxons n'ont pas été évalués, 4% des taxons manquent de données et seulement 4% des taxons sont considérés comme vulnérables. Ces espèces vulnérables correspondent à deux espèces de marlins (le makaire blanc de l'Atlantique: *Kajikia albida* et le makaire bleu de l'Atlantique: *Makaira nigricans*), un thon (le thon obèse: *Thunnus obesus*), un poisson-lune (*Mola mola*) et deux poissons arbalète (*Balistes punctatus* et *Balistes capriscus*). Au cours des 19 ans de la période analysée, les indices n'ont pas montré de tendance au cours du temps (cas de l'indice de richesse), ou de petites différences (indice de similitude MDS, courbes de dominance, indice de Shannon). Cependant, les informations et les résultats fournis dans la présente étude doivent être pris avec beaucoup de prudence car l'équilibre dans le plan d'échantillonnage et les objectifs dans la collecte des observations à bord n'ont pas été les mêmes tout au long de la période d'étude. Par conséquent, ces différences peuvent être aussi bien expliquées par des changements dans les stratégies de pêche sur les DCPd au cours du temps que par des différences méthodologiques entre les programmes d'observations scientifiques anciens et actuels. En gardant cette limitation à l'esprit, il n'y a aucune preuve d'impact significatif de la pêche sur DCPd sur la communauté des poissons osseux associés aux thonidés.

Un autre aspect important est le dommage potentiel des DCPd perdus sur les écosystèmes côtiers vulnérables. À partir des données de trajectoires des DCP déployés par les senneurs français sur la période 2008-2017, il a été mis en évidence que le nombre de bouées déployées a continué d'augmenter de façon spectaculaire ces dernières années, notamment dans l'océan Indien. Il convient de noter que le pourcentage des DCPd déployés qui finissent par échouer a augmenté jusqu'en 2013, mais reste étonnamment stable ou même légèrement en baisse après 2013. Les cartes de localisation des échouages identifient clairement les « hotspots » côtiers, tels que les côtes de l'Afrique de l'Ouest (Guinée-Sierra Leone et au Cameroun-Gabon), le Brésil et les Caraïbes pour l'océan Atlantique, et la Somalie, les Maldives, le Sri Lanka et les Seychelles pour l'Indien Océan. En reprenant à l'envers les trajectoires à partir des lieux d'échouage, des cartes

identifiant les zones pour lesquelles les bouées traversant une zone ont une forte probabilité d'échouer au cours des 3 mois suivants ont été produites. Pour mettre en évidence l'impact potentiel de l'échouage des DCPd dans les zones vulnérables, la même approche de retour en arrière de la trajectoire a également été menée exclusivement sur les bouées qui échouent dans les récifs coralliens. Dans le cas de l'océan Indien, il a été clairement montré que les zones à risque en termes de probabilité d'échouage changent avec les saisons et dépendent des régimes de mousson.

Afin de mieux définir une fermeture efficace de la zone temporelle DCPd pour protéger les juvéniles de thon obèse dans l'océan Atlantique, une étude a été menée pour détecter les hotspots de capture de petits thons obèse. Les captures totales de DCP par 1 ° carré * mois pour les flottes de senneurs opérant dans l'Atlantique Est ont été reconstituées à partir des données de capture / effort de la tâche II de l'ICCAT (par exemple, la flotte Européenne), ou extrapolées à la tâche I de l'ICCAT et réestimées par mois et 1 ° carré pour les autres flottes (par exemple, cas du Ghana où la tâche II par mode de pêche soumise à l'ICCAT est nettement inférieure à la tache I), il a également été supposé que pour chaque strate de 1 ° carré * mois explorée par les senneurs européens et la flotte ghanéenne, il était préférable d'utiliser l'échantillonnage effectué aux débarquements sur les calées faites sur les DCP européens que les données soumises au secrétariat de l'ICCAT afin de réestimer la quantité de juvéniles de thon obèse capturés sur DCP par la flotte ghanéenne. Les résultats de l'analyse spatio-temporelle ont montré que les principales captures de DCPd de thon obèse juvénile sont observées de septembre à janvier. Suite à cela, une analyse des indicateurs d'association spatiale globale et locale de Moran a permis d'identifier des hotspots de septembre à janvier au centre de l'Atlantique puis de novembre à janvier dans le golfe de Guinée. Cette tendance saisonnière est en accord avec une analyse des captures mensuelles de petits thons obèse faites sur DCPd par les senneurs sur la période 2014-2018. Il n'y a aucune évidence d'un effet du moratoire sur DCPd sur un changement dans la proportion de thon obèse capturé dans des bancs libres. Il convient de rappeler que la principale espèce capturée en banc libre est l'albacore et que la plus grande capture mensuelle de thon obèse (juin-juillet) ne dépasse pas 10% du total des captures en banc libre.

Une analyse des activités des navires de soutien espagnols avant, pendant et après les deux mois de moratoire pour les trois moratoires établis par l'ICCAT entre 2016 et 2018 a été réalisée afin d'explorer l'efficacité de l'aide à la pêche fournie par ces navires aux senneurs pendant ces périodes de réglementation. La schéma d'activité de ces navires d'appui pendant les fermetures sur DCP a différé considérablement entre 2016 et les deux autres années, peut-être en raison du fait que les recommandations 14-01, 15-01 et 16-01 ont affecté différentes zones. Il y a eu de légères baisses du nombre de DCP déployés et entretenus ou contrôlés par des navires d'assistance, ainsi que de légères augmentations du nombre de récupérations de DCP par rapport aux mois précédant et

suivant immédiatement la période de moratoire de janvier à février; bien que la série montre une grande variabilité tout au long de l'année. Un problème important lors de l'analyse des données sur DCP, provenant des livres de bord des DCP, est la difficulté de suivre chaque DCP sans les informations réelles sur la transmission des bouées; pour plusieurs raisons notamment l'absence d'information des activités sur ces DCP des baliseurs ne battant pavillon espagnol et des problèmes liés au codage et à l'enregistrement des DCP. En conséquence, le nombre de DCP déployés par des baliseurs et pêchés ultérieurement par un senneur était étonnamment faible. La combinaison des livres de bord des DCP des senneurs et des navires d'appui suggère que les DCP déployés en janvier et février hors des zones moratoires ne sont pas pêchés une fois la fermeture terminée dans ces zones. Au contraire, les DCP déployés en novembre-décembre peuvent dériver hors des zones régulées et être pêchés ensuite en janvier-février. Il semble cependant que l'impact des moratoires sur l'activité des baliseurs soit limité.

De plus, l'efficacité du moratoire de pêche actuel sur les DCP Rec [15-01] a été évaluée en utilisant les données de marquage de l'AOTTP (2016-2018) pour les juvéniles d'albacore et de thon obèse (longueur à la fourche <70 cm) par (1) comparaison du taux de recapture des juvéniles dans et en dehors du moratoire à l'aide du risque relatif de recapture, et par (2) la distance linéaire parcourue en mer en kilomètres, les directions cardinales et le temps en mer ont été calculés pour les individus marqués à l'intérieur du moratoire en 2017. Il a été montré que les taux de recapture lorsque des albacores juvéniles étaient marqués à l'extérieur de la zone du moratoire sont égaux à 18 fois le taux de recapture des thons qui ont été marqués à l'intérieur de la zone du moratoire (2017 et 2018 confondus). Cela suggère que le moratoire a été efficace pour protéger les juvéniles d'albacore. En raison du faible nombre d'observations de marquage-recapture, le résultat n'est toujours pas clair pour le thon obèse. Une étape supplémentaire consacrée à tester un effet de type frontière a montré que 50% des albacores marqués à l'intérieur du moratoire l'ont été à moins de 100 km de la limite nord du moratoire (latitude nord = 5 °). À partir de l'analyse du diagramme circulaire, nous avons montré que depuis le début de la période du moratoire, les albacores juvéniles ont été principalement recapturés dans l'est et l'ouest / nord-ouest avec des distances relativement longues couvertes (en tenant compte du temps de liberté de 1 à 2 mois considéré). Les données de capture-recapture de l'AOTTP offrent de nombreuses perspectives prometteuses pour comprendre pourquoi les juvéniles d'albacore et de thon obèse migrent préférentiellement dans certaines régions de l'océan Atlantique oriental.

Aujourd'hui, les gestionnaires des pêches ne sont pas seulement confrontés à l'exploitation durable des ressources de thon tropical mais aussi à la conservation des écosystèmes tout en procurant des revenus alimentaires et en préservant durablement les moyens de subsistance des pêcheurs. En conséquence, la gestion plurispécifique, l'atténuation des prises accessoires, la protection des écosystèmes vulnérables doivent être intégrées pour atteindre les objectifs écologiques et socio-

économiques. Parce que l'application des méthodes de recherche conventionnelles est souvent insuffisante pour soutenir une prise de décision efficace lorsque les décisions doivent être prises quel que soit le niveau de connaissances ou d'incertitude, nous proposons une ligne directrice pour la mise en œuvre d'une approche de gestion adaptative (MA) pour faciliter la prise de décision en termes de gestion des ressources des espèces hautement migratoires (HMS) dans une approche écosystémique des pêches.

Au lieu de se concentrer sur la gestion du thon tropical en utilisant l'évaluation de la stratégie de gestion (MSE) qui omet l'effet collatéral des pêcheries tropicales sur l'écosystème épipélagique, une MA pourrait offrir une approche alternative pour permettre des jugements de valeur sur la façon de contrôler une utilisation durable de la pêche sur DCP dans le cadre d'une approche écosystémique des pêches. Compte tenu du fait que l'AM est « l'apprentissage par la pratique », ce guide propose une méthodologie pour intégrer les opinions des différentes parties prenantes (scientifiques, pêcheurs, gestionnaires des pêches et représentants d'ONG) depuis la co-conception des objectifs communs et l'identification où les actions pourraient être appliquées, à l'évaluation des progrès résultant de la mise en œuvre des mesures de gestion. Le processus itératif de prise de décision de l'AM utilise des modèles informatiques (par exemple, des outils de simulation comme les systèmes multi-agents) paramétrés avec la connaissance des acteurs pour synthétiser et construire des stratégies de gestion alternatives afin de parvenir à un consensus sur la gestion des ressources naturelles. La confrontation du modèle avec les circonstances réelles conduit à le réviser et à le modifier progressivement afin de prendre en compte l'incertitude caractéristique des pêcheries de thons tropicaux. Selon le niveau d'information et de données disponibles, la mise en œuvre d'une AM peut s'appuyer sur des modèles opératoires, plus simples que pour la MSE, qui s'appuient sur une fonction d'optimisation. L'AM peut être validée par des méthodes statistiques pour évaluer si la mesure de régulation répond aux objectifs fixés par les parties prenantes.

4.3. Resumen Ejecutivo

El Contrato Específico nº9 "Catch, Effort, and Ecosystem impacts of tropical tuna fisheries" (CECOFAD2) de SAFEWATERS2 se realizó con el fin de (1) mejorar nuestra comprensión sobre el uso de Dispositivos Concentradores de Peces (DCPs) en las pesquerías de cerco de atún tropical y (2) evaluar el impacto de esta práctica pesquera en especies pelágicas asociadas y ecosistemas vulnerables.

En la actualidad no existen procedimientos adecuados para la estandarización de los índices de CPUE de cerqueros, y por ese motivo, la mayoría de las evaluaciones de las poblaciones de atún tropical en todo el mundo se basan en índices de CPUE de palangre que rara vez tienen en cuenta la implementación de nuevas

tecnologías en el proceso de estandarización y solo reflejan la biomasa de la proporción adulta de las poblaciones de atún. En consecuencia, una de las principales tareas definidas en CECOFAD2 fue proporcionar información sobre los posibles factores explicativos utilizados en el cálculo de los índices de abundancia estandarizados de CPUE para túnidos tropicales juveniles y adultos en DCPs y en banco libre de cerqueros europeos en los océanos Atlántico e Índico. Los datos de la información tecnológica no oficial relacionada con la pesca con DCP fueron recuperados durante los primeros 12 meses del proyecto a través del proyecto europeo de investigación complementaria (RECOLAPE). Todavía faltan datos importantes, como el vínculo entre los cerqueros individuales y los buques de apoyo para algunas flotas, pero ahora hay nueva información disponible sobre los cambios tecnológicos a lo largo del tiempo en relación a marcas y modelos de boyas con ecosonda.

Una de las variables que potencialmente podría afectar al tamaño del banco bajo el DCP y, en consecuencia, la tasa de captura, es la densidad de objetos flotantes ("FOB", es decir, que incluye los DCPs más los objetos naturales o artificiales). La estimación de la densidad de DCPs como proxy de la densidad de "FOBs" se ha considerado como un factor importante para este proyecto. Para la flota francesa, los cerqueros asociados a DCPs monitorearon todas las posiciones y trayectorias de GPS de boyas (es decir, pertenecientes a cualquier pabellón) para producir un mapa de densidad desde 2010. Para la flota española, la recuperación de datos estaba todavía en curso en el momento de esos primeros análisis durante 2018 y dicha recuperación se completó durante 2019. La parte restante de la densidad de boyas (es decir, aquellas sin trayectorias disponibles) de las pesquerías de cerqueros no europeas (por ejemplo, Ghana, Seychelles) aún necesita ser estimada.

Algunas boyas identificadas (ID) en los libros de registro de observadores y capitanes, para las cuales no se dispone de datos de trayectorias necesitan ser analizadas (p.e. algunas de banderas españolas y otras no europeas). Para ello, los identificadores de boyas registradas pueden utilizarse en modelos de Captura-Recaptura espacial para estimar la distribución espacial y temporal de los DCPs no identificados, la densidad del tiempo en el mar y la probabilidad de detección.

En estos modelos, se tiene en cuenta el esfuerzo de exploración variable. Los resultados preliminares obtenidos solo con actividades en boyas no rastreadas por los cerqueros franceses mostraron que este método puede ser útil para evaluar la densidad de las boyas utilizadas por otras flotas de cerqueros.

Además de la tecnología de pesca desarrollada por los cerqueros europeos, se ha llevado a cabo un análisis de las actividades pesqueras relacionadas con los DCPs por parte de la pesquería europea con caña que opera desde Dakar (Senegal). A principios de la década de 1990, esta flota con redes de caña ha implementado una nueva estrategia de pesca (es decir, el "banco- asociado a la embarcación") donde un buque de cebo vivo ha actuado como un objeto flotante para atraer

atunes, cambiando con el tiempo hacia el uso creciente de DCPs para agregar atunes tropicales con una zona de pesca concomitante más amplia en el Océano Atlántico Oriental. Dependiendo de la estación del año, cada grupo de barcos de cebo vivo puede usar hasta más de 300 boyas operativas. La captura total por grupo aumentó con el número de boyas operativas, pero la tasa de captura (captura por número de boyas) disminuyó inversamente.

La estandarización de la CPUE de cerqueros europeos se realizó con éxito para adultos de aleta amarilla en lances realizados a banco libre al nivel de escala establecido. Para tener en cuenta el hecho de que los atunes tropicales están estructurados espacialmente en bancos y en grupos de bancos y que, en consecuencia, cualquier cambio en la abundancia puede verse influenciado por el cambio en el número (o densidad) de bancos en el mar, por el cambio en el tamaño de banco o por ambos, desarrollamos una extensión del modelo Delta-log que toma la forma de tres submodelos de la siguiente manera: (1) un modelo Poisson GLMM que estandariza el número de lances positivos y nulos, por barco y unidad de tiempo y ubicación, (2) un modelo GLMM binomial que tiene en cuenta la proporción de lances positivos para adultos de aleta amarilla, (3) un modelo LMM log-normal para describir la captura condicional al lance positivo (es decir, el tamaño del banco). La CPUE estandarizada para bancos libres se definió como el producto del número de lances (positivos y nulos) por estratos espacio-temporales, la proporción de lances con adultos de aleta amarilla (> 10 kg) y la captura de adultos de aleta amarilla por lance positivo. La originalidad de este trabajo se basó en la inclusión de i) lances nulos, considerados como presencia de bancos de aleta amarilla, ii) días de pesca (es decir, días en los caladeros por los cuales el cerquero está pescando) sin lance, considerado como ausencia de lances a banco libre, y iii) tiempo de búsqueda en el mar por barco y día por cuadrícula de 1 ° * 1 ° para tener en cuenta la heterogeneidad en la exploración de las cuadrículas. Este nuevo enfoque de estandarización, por lo tanto, representa un avance significativo sobre los esfuerzos anteriores y el índice estandarizado se ha utilizado en la evaluación del stock de aleta amarilla en el Océano Atlántico y en el análisis de sensibilidad para el Océano Índico. La estandarización de CPUE para la pesca con DCP se ha limitado a un componente y todavía está en progreso debido a las dificultades para (1) discriminar la parte del esfuerzo de pesca dedicado a establecer el DCP que pertenece a cada barco (es decir, no detectado al azar) para la proporción de DCPs ajenos (es decir, encontrados al azar) y (2) para tener en cuenta variables no convencionales, como la asistencia prestada por los buques auxiliares a los cerqueros que han sido identificados como un componente claro del esfuerzo de pesca (es decir, ICCAT-Rec [16-01]). De la misma manera que para la estandarización de la CPUE en lances a banco libre, debe investigarse la integración de factores ambientales en el modelo, así como los métodos de clasificación espacial, con el objetivo de reducir la cantidad de tiempo empleado para el cálculo de grandes bases de datos (es decir, cómo contabilizar las dimensiones espaciales y temporales con un número moderado de

parámetros para estimar). Sin embargo, el progreso en la estandarización de la CPUE en DCPs logrado durante CECOFAD2 se beneficiará en el Contrato Específico en curso N ° 14.

Como alternativa a la CPUE en DCPs, durante CECOFAD2 se investigaron los índices directos de abundancia de atún mediante el uso de boyas con ecosondas conectadas a DCPs en la flota española. La estimación de la abundancia de especies de atunes y no atunes utilizando directamente los datos de biomasa acústica de las boyas acústicas requiere recopilar y procesar información heterogénea de la boya con ecosonda de diferentes marcas y modelos.

Por esta razón, el desarrollo de una base de datos consistente de boyas con ecosonda requirió la limpieza de los conjuntos de datos antes de estandarizar un índice de abundancia derivado de los datos de boya de ecosonda. Debido a que el factor de proporcionalidad entre el Índice de Abundancia derivado de boya (BAI) y la abundancia desconocida no es constante, las mediciones nominales de los registros de boya con ecosonda se estandarizaron utilizando un enfoque de modelo mixto lineal generalizado (GLMM) y se utilizó una distribución delta-lognormal para estimar BAI como el producto de la probabilidad de presencia de atún y la abundancia relativa media donde se detectó atún. El BAI derivado, que se supone representa el cambio a lo largo del tiempo de los atunes juveniles, se integró en los modelos de evaluación de stock de aleta amarilla de 2019 realizados por ICCAT e IOTC en 2019.

Los análisis del proceso continuo de asociación y disociación, así como el tiempo de residencia bajo DCPs, también se realizaron a partir de datos de ecosonda recopilados en cerqueros franceses. De este estudio se ha demostrado que los DCPs recién desplegados, equipados con una boya de Marine Instruments, son colonizados por las agregaciones de atún después de un promedio de 20.5 días en el Océano Atlántico. Los resultados también revelaron, por primera vez, que el tiempo de residencia continua de una agregación de atún alrededor de un solo DCP es de aproximadamente 9 días y que transcurre un promedio de 7 días entre la salida de la agregación y la posterior repoblación del DCP por otros atunes. La relación de la suma de todos los tiempos continuos de residencia de las agregaciones de atún medidas bajo un DCP a su tiempo total de en el agua después de la colonización se estimó en base a observaciones individuales de DCP. En promedio, se demostró que los DCPs estaban ocupados por la agregación de atún aproximadamente el 50% de su tiempo en el agua después de la colonización. Estas medidas pueden verse afectadas por variaciones estacionales. Sin embargo, debe tenerse en cuenta que para este modelo de boya (M3I), los rendimientos actuales de los algoritmos desarrollados para evaluar la presencia o ausencia de atún son satisfactorios, mientras que las estimaciones de biomasa están débilmente correlacionadas con las capturas realizadas en el mismo DCP. La misma conclusión se extrajo del estudio español BAI. La captura en la boya mostró una tendencia positiva con la biomasa estimada, pero el coeficiente de correlación es

bajo debido a la variabilidad de los datos y parece depender de la cantidad de captura de atún en el lance. Además, otros factores como los factores ambientales (por ejemplo, la temperatura de la superficie del mar), el área o la temporada podrían estar afectando a esta relación y su impacto en la biomasa de la boya y la relación de captura deben explorarse más a fondo.

Para mejorar el conocimiento del impacto ambiental de las pesquerías de atún tropical y desarrollar medidas de gestión del ecosistema que tengan en cuenta las consideraciones del ecosistema, exploramos los riesgos de la pesca con DCP en especies protegidas y en peligro de extinción, así como en hábitats vulnerables, y las posibles medidas reguladoras para reducir este impacto. Un análisis realizado a partir de los datos de un observador francés sobre el impacto potencial de la pesca con DCPS reveló que las capturas de tiburones sedosos (Carcharhinus falciformis) aparecieron principalmente localizadas alrededor de las costas de Gabón y Angola en el Océano Atlántico, mientras que su distribución parecía estar más extendida en todas las regiones de pesca en el Océano Indio. Paralelamente, se ha desarrollado un enfoque novedoso para derivar un índice de abundancia para los tiburones sedosos en el Océano Índico, basado en un modelo empírico que explica su dinámica de asociación en los DCPs. La serie temporal (2007-2018) de los índices de abundancia relativa a nivel mundial mostró una tendencia creciente con una magnitud que depende del área. Este aumento en la abundancia de tiburones podría ser el resultado de una combinación de factores que tuvieron lugar a partir de 2010 (por ejemplo, introducción de DCPs no enmallantes, AMP de Chagos, cambio de esfuerzo de pesca debido a la piratería, prohibición de la pesca de tiburones en Maldivas). Sin embargo, es importante tener en cuenta que este índice relativo refleja una tendencia y no es una estimación de la población, lo que significa que las tendencias al alza observadas no deben interpretarse como una indicación de una población sana.

Con el objetivo de evaluar el impacto potencial de la pesca con DCPs en peces óseos y otras especies marinas, se realizó un análisis comparativo del índice de biodiversidad, abundancia, curvas de dominancia y acumulación de especies a partir de los datos recopilados por el programa científico español ObServe. En la información recopilada para cada uno de los taxones (es decir, especie o familia), se realizó un análisis descriptivo de cada taxón, abundancia, tipo de hábitat, biología, distribución y comportamiento social y estado de la UICN. Con respecto al hábitat natural, la fauna asociada a los DCPs son principalmente especies clasificadas como hábitats "asociados a arrecifes" y "pelágicos oceánicos" (38% y 27%, respectivamente). El 35% restante son especies clasificadas como bentopelágicas y costeras pelágicas. Sobre la base del número de individuos capturados durante un lance, el 54% de las especies se observaron con un solo individuo. El 31% son especies que nadan en grupos pequeños y solo el 15% de las especies observadas nadan formando grupos grandes alrededor de los DCPs (como el atún y especies similares). Con respecto a la situación del estado de conservación de la UICN, el 76% de los taxones se encuentran en una situación

de baja preocupación, el 16% de los taxones no han sido evaluados, el 4% de los taxones carecen de datos y solo el 4% de los taxones son considerados vulnerables. Estas especies vulnerables corresponden a dos especies de marlines (la aguja blanca del Atlántico: Kajikia albida y la aguja azul del Atlántico: Makaira nigricans), un atún (el patudo: Thunnus obesus), un pez luna (Mola mola) y dos tipos de ballestas (Balistes punctatus y Balistes capriscus). Durante el período de 19 años analizado, los índices no mostraron tendencia a lo largo del tiempo (por ejemplo, índice de riqueza) o pequeñas diferencias (similitud MDS, curvas de dominancia, índice de Shannon). Sin embargo, la información y los resultados proporcionados en el presente estudio deben tomarse con gran precaución, ya que el equilibrio y la igualdad en el muestreo a bordo del observador no han sido los mismos durante todo el período de estudio. En consecuencia, estas diferencias podrían explicarse por cambios en las estrategias de pesca en los DCPs a lo largo del tiempo y/o por diferencias metodológicas entre los programas de observación antiguos y actuales. Con esta limitación en mente, no hay evidencia de un impacto significativo de la pesca con DCPs en la comunidad de peces óseos asociados a DCPs.

Otro aspecto importante es el daño potencial de los DFAD perdidos en ecosistemas costeros vulnerables. A partir de los datos de trayectoria de los DCPs desplegados por los cerqueros franceses durante el período 2008-2017, se evidenció que el número de boyas desplegadas ha seguido aumentando drásticamente en los últimos años, especialmente en el Océano Índico. Cabe señalar que el porcentaje de DCPs desplegados que terminan varados aumentó hasta 2013, pero sorprendentemente se mantiene estable o incluso disminuye ligeramente después de 2013. Los mapas de localizaciones de varamientos identifican claramente los puntos críticos costeros, como las costas de África (Guinea-Sierra Leona y Camerún-Gabón), Brasil y el Caribe, para el Océano Atlántico, Somalia, Maldivas, Sri Lanka y Seychelles, para el Océano Índico. Al partir de las ubicaciones de los varamientos, se han producido mapas que identifican las áreas para las cuales las boyas que cruzan un área tienen una alta probabilidad de varamiento en los próximos 3 meses. Para resaltar el impacto potencial de varamientos de DCPs en áreas vulnerables, el mismo enfoque de rastreo se ha llevado a cabo también exclusivamente en boyas que se dirigen a los arrecifes de coral. En el caso del Océano Índico, se demostró claramente que las áreas de riesgo en términos de probabilidad de varamiento cambian con las estaciones y dependen de los regímenes de los monzones.

Para una mejor definición de un efectivo cierre espacio-temporal para DCPs para proteger a los juveniles de patudo en el océano Atlántico, se realizó un estudio para detectar puntos críticos de captura de patudo pequeño. La captura total con DCPs por 1° por cuadrícula y mes para las flotas de cerco que operan en el Atlántico oriental se reconstituyó a partir de los datos de captura por unidad de esfuerzo de la tarea II de ICCAT (por ejemplo, flota de la UE), o se aumentó a la tarea I de ICCAT y se volvió a estimar por mes y 1° cuadrícula para las otras flotas (por

ejemplo, en el caso de Ghana, la tarea II por modo de pesca presentada a ICCAT es significativamente menor que la tarea I), también se supuso que por cada estrato de 1°cuadrícula por mes explorados por los cerqueros europeos y por la flota ghanesa, era mejor utilizar el muestreo realizado en lances europeos a DCPs en los desembarques que los datos presentados a la secretaría de ICCAT para reestimar la cantidad de patudos juveniles capturados en DCPs por la flota ghanesa. Los resultados del análisis espacio-temporal mostraron que las principales capturas en DCPs de patudo juvenil se observan de septiembre a enero. Después de esto, un análisis de los indicadores globales y locales de asociación espacial (usando el índice de Morán) permitió identificar puntos críticos de septiembre a enero en el centro del Océano Atlántico y luego de noviembre a enero en el Golfo de Guinea. Este patrón estacional estuvo de acuerdo con un análisis de las capturas mensuales de cerqueros pequeños de patudo en DCPs durante el período 2014-2018. No hay evidencia de un efecto de la moratoria para DCPS en un cambio en la proporción de patudo capturado en lances a banco libre. Cabe recordar que la principal especie capturada en lances a banco libre es el atún de aleta amarilla y que la mayor captura mensual de patudo (junio-julio) no excede el 10% de la captura total de la escuela libre.

Se realizó un análisis de las actividades de los buques de apoyo españoles antes, durante y después de los 2 meses de moratoria de las tres moratorias establecidas por ICCAT entre 2016 y 2018 para explorar la eficiencia de la asistencia brindada por estos buques a los cerqueros durante este periodo de regulación. El patrón de actividad de los buques durante los cierres a DCPs difirió significativamente entre 2016 y los otros dos años, posiblemente debido al hecho de que las recomendaciones 14-01, 15-01 y 16-01 afectaron a diferentes áreas. Hubo ligeras caídas en el número de DCPs desplegados y atendidos o controlados por buques auxiliares, así como pequeños aumentos en el número de recuperaciones de DCPs en comparación con los meses inmediatamente anteriores y posteriores al período de moratoria de enero a febrero; aunque la serie muestra una gran variabilidad durante todo el año. Un problema importante al analizar los datos de DCPs de los libros de registro de DCPS es la dificultad de rastrear DCPs únicos sin la información de transmisión de la boya real, debido a varias circunstancias; incluida la actividad de los buques con pabellón no español sobre estos DCPs y las cuestiones relacionadas con la codificación y el registro del DCP. Como consecuencia, el número de DCPs desplegados por buques de suministro y luego establecidos por un cerquero fue inesperadamente bajo. La combinación de los libros de registro de DCPs de los cerqueros y los buques de apoyo sugiere que los DCPs desplegados en enero y febrero fuera de las áreas cerradas no se pescan una vez que finaliza el cierre en estas áreas. Por el contrario, los DCPs desplegados en noviembre-diciembre pueden salir de las áreas cerradas y pescar en enero-febrero. Sin embargo, parece que el impacto de los cierres en la actividad de los buques de suministro es limitado.

Además, la eficiencia de la actual moratoria de pesca con DCP (Rec [15-01]) se evaluó utilizando datos de marcado del AOTTP (2016-2018) para juveniles de aleta amarilla y patudo (longitud de la horquilla <70 cm) mediante (1) la comparación de la tasa de recaptura de juveniles dentro y fuera de los estratos de la moratoria mediante el uso del riesgo relativo de recaptura, (2) la distancia más corta en kilómetros en el mar, las direcciones cardinales y el tiempo en el mar se calcularon para las personas marcadas dentro del área de la moratoria en 2017. Se mostró que las tasas de recaptura cuando los atunes de aleta amarilla juveniles fueron marcados fuera del área de la moratoria es igual a 18 veces la tasa de recaptura de los atunes que fueron marcados dentro del área de la moratoria (2017 y 2018 confundidos). Esto sugiere que la moratoria ha sido efectiva para proteger a los juveniles de aleta amarilla. Debido al bajo número de observaciones de liberación-recaptura, el resultado aún no está claro para los patudos. Un paso adicional dedicado a probar un efecto frontera mostró que el 50% del atún aleta amarilla marcado dentro de la moratoria se marcó dentro de los 100 km del extremo norte de la moratoria (Latitud Norte = 5°). Del análisis del diagrama circular, mostramos que desde el comienzo del período de moratoria, el atún juvenil de aleta amarilla se recapturó principalmente en el este y oeste/noroeste con distancias relativamente largas cubiertas (teniendo en cuenta el tiempo de libertad de 1 a 2 meses considerado). Los datos de liberación-recaptura del AOTTP ofrecen muchas perspectivas prometedoras para comprender por qué los juveniles de aleta amarilla y patudo migran en algunas partes preferentemente en el Océano Atlántico Oriental.

Hoy en día, los gestores de pesquerías de túnidos no solo se enfrentan a la explotación sostenible de los recursos de atún tropical, sino también a la conservación de los ecosistemas, al tiempo que proporcionan ingresos alimentarios y salvaguardan los medios de vida de los pescadores de manera sostenible. Como consecuencia, la gestión de múltiples especies, la mitigación de la captura incidental y la protección de los ecosistemas vulnerables deben integrarse para lograr objetivos ecológicos y socioeconómicos. Con frecuencia, los métodos de investigación convencionales se han mostrado insuficientes para apoyar decisiones efectivas en un escenario de incertidumbre. Para estos casos proponemos una guía para implementar un enfoque de gestión adaptativa (GA) para facilitar la gestión de recursos de especies altamente migratorias (EAM) y para facilitar un enfoque ecosistémico de la pesca.

En lugar de enfocarse en el manejo del atún tropical mediante el uso de la Evaluación de la Estrategia de Manejo (EEM) que omite el efecto colateral de las pesquerías tropicales en el ecosistema epipelágico, un proceso de GA ofrece un enfoque alternativo para permitir valorar la mejor manera de controlar un uso sostenible de la pesquería-con-DCP dentro del marco de un enfoque ecosistémico. Basado en el hecho de que AM está "aprendiendo sobre la marcha", la directriz propone una metodología para integrar las opiniones de diferentes partes interesadas (científicos, pescadores, funcionarios gubernamentales y

representantes de ONG) desde el co-diseño de objetivos e indicaciones comunes donde las acciones podrían aplicarse a la evaluación del progreso resultante de la implementación de medidas de gestión. El proceso de toma de decisiones iterativo de AM utiliza modelos informáticos (p. Ej., Herramientas de simulación como sistemas de múltiples agentes) parametrizados con el conocimiento de las partes interesadas para sintetizar y construir estrategias de gestión alternativas para alcanzar un consenso para la gestión de los recursos naturales. La confrontación del modelo con circunstancias reales lleva a revisarlo y reconstruirlo, teniendo en cuenta gradualmente las características de incertidumbre de las pesquerías de atún tropical. Dependiendo del nivel de información y datos disponibles, la implementación de GA puede basarse en modelos operativos más simples que en EEM, utilizando una función óptima. La GA puede validarse mediante métodos estadísticos para evaluar si la medida de regulación responde a los objetivos fijados por los interesados.

5 Activities by Working Package

5.1 WP1 - Contribution to fishing mortality of new fishing technologies implemented by tuna PS fisheries

5.1.1. Objectives

The objectives of this task include a reviewing of conventional data and unofficial technological information coming from different sources, a review of methods used to estimate the fishing effort directly related to dFADs uses, and the integration of unofficial information in the standardization of the CPUEs.

5.1.2. Sub-task 1.1. Review methods to cross check PS data coming from different sources (logbooks, observers' reports)

This task reviewed all types of information (i.e., conventional and unofficial data) considered useful for assessing the impact of dFAD fishing on all identified tropical tunas and associated pelagic species, including utilizing raw data on tropical tunas and associated pelagic species caught by dFADs collected in the frame of RECOLAPE (WP.4). In line with this, we summarize below the data collection and processing for the dFAD, the Vessel Monitoring System VMS and the observers' data.

dFAD data

The basic cleaning and analysis of French dFAD trajectory data followed the overall procedure described in Maufroy et al. (2015). For the period 2006-2015, a first set of position data concerning both Marine Instruments (MI, which is the manufacturer of the vast majority of buoys currently used by the French fleet) and non-Marine Instrument buoys was obtained directly from three French fishing companies (CFTO, Saupiquet and Sapmer). Then, from 2010 to 2018 a second set of position data and acoustic information was obtained directly from MI (**Figures 5.1.1 and 5.1.2**). Aberrant position data (i.e., impossible positions such as at the geographic poles or pairs of identical positions due to poor GPS capture) were removed before analysis. Where multiple positions for a single buoy time stamp (i.e. same time and day GPS position) which can occur due to time stamp truncation) were given, an average was calculated to produce a single position for every buoy-time stamp. French dFAD trajectories were then classified either at-sea or onboard using a random forest model (*sensu* Maufroy et al., 2015).

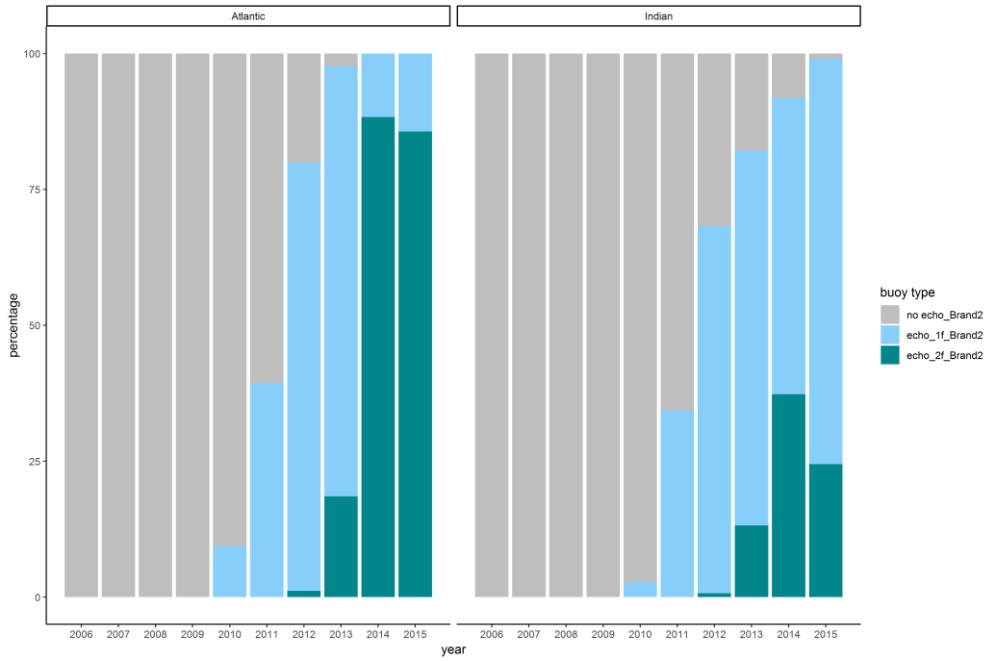

Figure 5.1.1. Percentage of buoy type utilized by the French Tuna fishing fleet between 2006 and 2015. All data has been taken from the French Tuna Associations position database for the Atlantic Ocean (left panel) and Indian Ocean (right panel). Brand 2 refers to Marine Instruments (MI). The list of the buoy type categories is constituted by various buoy models (this figure is an output of the RECOLAPE project)

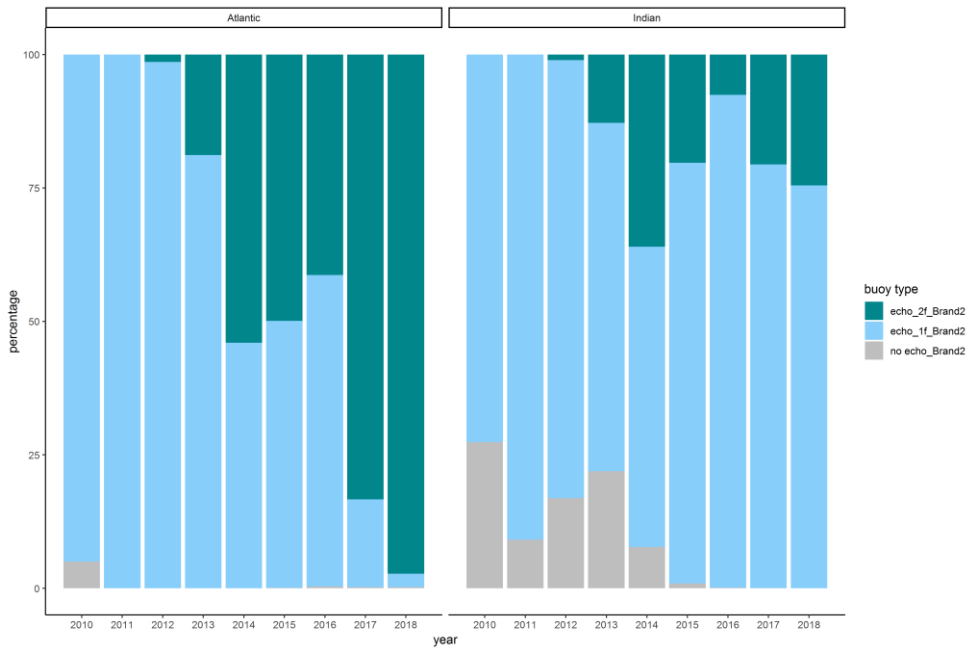

Figure 5.1.2. Percentage of buoy type utilized by the French Tuna fishing fleet between 2010 and 2018. All data has been taken from the French Tuna Associations acoustic database for the Atlantic Ocean (left panel) and Indian Ocean (right panel). Brand 2 refers to MI. The list of the buoy type categories is constituted by various buoy models (this figure is an output of the RECOLAPE project.

Spanish flag and associated flag buoy positions available for the study, (i.e., partial recovery of buoy data conducted in 2018) was completed in 2019 in the frame of RECOLAPE[4] Project. Such data was sourced from three buoy brands in the Atlantic and Indian Ocean, covering the period 2010 to 2018. Buoys used by ANABAC (i.e., Atunsa and Echebastar companies) and OPAGAC fleet (all companies) were utilized; MI brand buoys deployed within 2010-2012 were unable to be used, as their data could not be exported due a technical issue in the recovery process (**Figure 5.1.3**; see also Grande et al, 2019). From 2013, information from 85% of PS vessels in the Atlantic and 90% of PS vessels in the Indian Ocean was recovered.

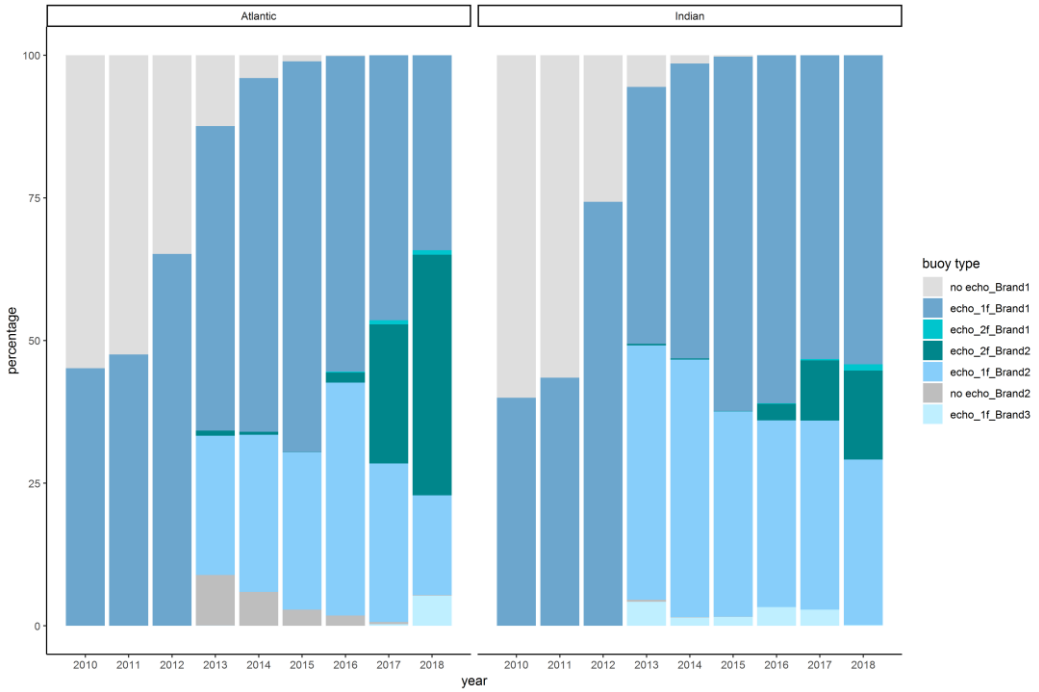

Figure 5.1.3. Percentage of buoy type and year constituting the raw Spanish Tuna Associations´ position database for the Atlantic and Indian Ocean from 2010-2018. The list of the buoy type categories is constituted by various buoy models (Brand 1 refers to Satlink, Brand 2 to MI and Brand 3 to Zunibal). Note that for the period 2010 to 2012 Brand 2 individual buoy positions could not be obtained (this figure is an output of the RECOLAPE project).

In CECOFAD 2, during analyses within 2018, all raw buoy data was filtered to exclude records on land, on board and those from deactivated buoys (which were labeled 'NA'), following the method described in Santiago et al. (2017). In 2019, in the frame of RECOLAPE Project the filtering protocol was improved within filtering of erroneous location data, data related to failures in satellite

[4] FRAMEWORK CONTRACT – MARE/2016/22 "Strengthening regional cooperation in the area of fisheries data collection", Annex III "Biological data collection for fisheries on highly migratory species"

communication and location data acquisition, buoys identified present on land (using a high-resolution shoreline from GSHHG4 buffered with 0.05° shapefile), and buoy data which had recorded on-board positions (defined in Grande et al. 2019, **Table 5.1.1**). For all filtering of on-board data, a random forest (RF) classification approach was developed from information from the Zunibal buoys, which have the capability to identify true positions at sea through a conductivity sensor. The sensor measures the ionic content between two electrodes and determines, through a simple algorithm, whether the buoy is in the water. The predictors variables used in the RF analysis were: distance between two points (km), velocity (km/h), change in velocity (km/h), acceleration (km/h2), azimuth (degree), change in azimuth (degree) and time since the first and last observation of the corresponding buoy trajectory (days) (**Figure 5.1.4**, see Orue et al., 2019 for further details). Within CECOFAD 2 this new filtering protocol was applied to the updated Spanish raw database.

The classification model utilized within this project and developed as part of CECOFAD2 is an improvement upon that developed by Maufroy et al. (2015). This model is based on a larger calibration dataset (roughly twice the size of the original) and includes additional predictor variables related to the temporal stability of speed and temperature immediately before and after each point classified. Analyses suggest that this improved model reduces classification error by approximately 50% than within previous models.

FILTER	Description
F1. Isolated	Isolated Position (>48 hours from another position estimated speed above > 35 knots relative next/previous position)
F2. Duplicated	Duplicated data (all fields are the same)
F3. Land	Data on land
F4. Ubiquity	Data entry having from the same date/time differe positions
F5. Not classified	Position not in the land and not classified by the sea/on board algorithm
F6. Onboard	Buoys on board
F7. Water	Buoys at sea. Operational buoys: Active buoy that transmitting a signal and is drifting in the sea (definiti from RECOLAPE)

Table 5.1.1. Filters defined for pre-processing raw position data (the filtering protocol is an output of RECOLAPE the project).

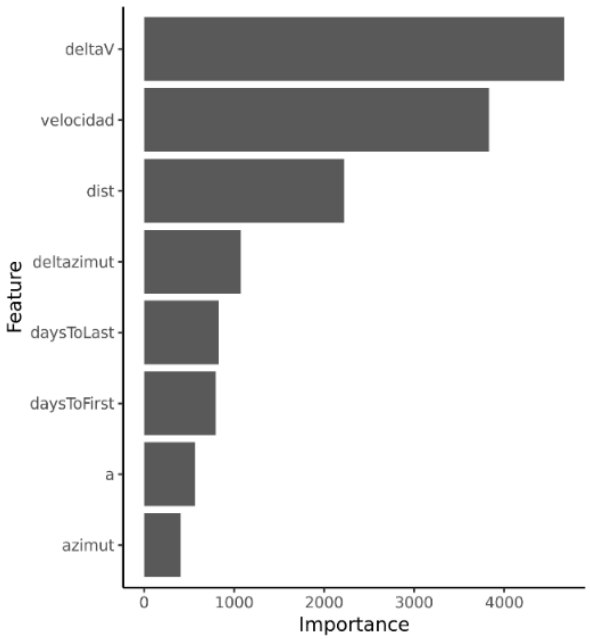

Figure 5.1.4. Variable Importance of the Random Forest Model. Name "deltaV" is the change in velocity, "velocidad" is the velocity, "dist" is the spatial distance between two points, "deltaazimut"is the change in azimuth, "daysToLast" is the time since the last observation, "daysToFirst" is the time since the first observation, "a" is the acceleration and "azimuth" is the azimuth. The average validation indices for sensitivity (i.e., 0.99), specificity (i.e., 0.89), Kappa (i.e, 0.87) and Area Under the Curve (AUC) (i.e, 0.94) were estimated to evaluate the performance effectiveness and efficiency of the RF classification (Orue et al., 2019).

In the Spanish buoys one position per day per buoy was available. In the case of French buoys all positions recorded by the buoy during the day were available. To estimate a position at midnight GMT every day for both the Spanish and French buoys, water trajectories for all buoys determined by the classification algorithm were linearly interpolated. These daily positions were aggregated on an 1°x1° longitude-latitude grid to generate a daily raster map of the number of dFADs per grid cell. These daily maps were then aggregated within each month, with the number dFADs per grid cell then divided by the number of days in the month to get an average dFAD density map for each month.

During 2018, for the Indian Ocean, French dFAD density maps were combined with Spanish dFAD density estimates. To correct for the partial coverage of Spanish data (from about 30% during 2010 to over 70% during 2017), total Spanish buoy densities were extrapolated from available data by dividing the initial Spanish dFAD density values in each grid cell-month strata by the fraction data coverage for the corresponding month (i.e., the number of vessels sharing the information and availability of information by buoy model) assuming the same deployment strategy for all Spanish vessels. Basic comparative analyses were then carried out, including generating time series of the relative proportion of French versus Spanish buoys, while also computing monthly linear regressions between spatial density maps of the Spanish and French fleets (Katara et al., 2018).

With this initial dFAD data set (i.e., data gathered during 2018) the estimated proportion of French buoys among total European Union (EU) buoys varied considerably from month to month. Estimates of French buoys ranged from 25% to 40% between 2010 and 2012, dropping to between 10% to 25% in 2013 and 2014, and then steadily increasing between 2015 and 2017 from 15% to 35% (Katara et al., 2018). The proportion of French buoys to the total of EU buoys was higher than previous analyses suggested (Maufroy et al., 2017), potentially indicating that the extrapolation procedure used on Spanish data may not be producing accurate results, particularly towards the beginning of the time series (2010 to 2013). Monthly linear regressions between French and Spanish density maps indicated strong seasonal variability in the strength of the relationship between the two (peaking in summer and fall), with the overall correspondence between the maps increasing over time, reaching an adjusted R^2 of ~0.7 for the summer months between 2015 and 2018 (Katara et al., 2018).

During 2019, due to advances made in the data recovery process, the 2018 year was covered, extending the total series of dFAD buoy data to 2018. Thanks to the improvement made on the Spanish data recovery, extrapolation of the Spanish data set only was conducted in the 2010-2012 period (estimating of MI buoys which could not be recovered). This updated dFAD density maps have been integrated for the PS FAD fishery CPUE standardization during 2019 that has been conducted in the frames of the CECOFAD 2 project (sub task 1.3).

Vessel Monitoring System (VMS) data

Basic treatment of French VMS data consisted of two major changes. These were the removal of aberrant positions at the geographic poles, as well as reducing multiple position entries for a single boat-time stamp combination to a single position, by randomly choosing one of the multiple observations (these events were rare and there were generally no more than two such repeats and positions were close or identical). French VMS data were divided into fishing trips based on data recorded in captain logbooks. There were very few anomalous VMS data, predominantly consisting of a mix of data from multiple boats (e.g., as identified by repeated large jumps between two seemingly normal boat trajectories). While waiting for clarification on these issues, these anomalous fishing trips, as well as trips where a vessel speed exceeded 15 m/s for long distances (PS speeds do not typically exceed 15 m/s), were eliminated before conducting further analyses.

Observer data

In order to quantify French PS dFAD deployments, visit and recovery activities, logbook and observer data on dFAD buoy operations were assembled and matched with dFAD trajectory data based on numerical identifiers recorded in each of the three datasets. Observer data required cleaning before being used for this purpose.

First, only data from the four most reliable observer programs were selected[5]. Second, only observer data with a numerical buoy identifier were examined as all others could not be reliably matched to dFAD trajectory data. Finally, large discrepancies between observer and logbook boat position information were noted, and the correct position was assessed based on minimum distance to VMS data from the boat corresponding to the observer/logbook data on the day of the observation. These large discrepancies generally appeared to be due to data entry errors (e.g., inversing the sign of the latitude or longitude, or switching longitude with latitude and vice-versa). In addition, observer data were used to obtain information of bycatch species taken by each fishing mode (i.e., free school and floating objects)[6].

Links with other projects

One of the objectives of the data recovery of non-official information was to improve the list of candidate variables for the standardization of the CPUE series. As recommended by CECOFAD 1 and from the 2016[7] and 2017[8] European working groups on PS CPUE standardization, held at IEO-Fuengirola and at AZTI-Pasaia, respectively, the access to non-official data for standardizing the CPUE on FADs is fundamental. On the basis of the list of non-official information analyzed during an EU CPUE workshop held in IRD-Sete[9] in 2018 and based on the outputs of RECOLAPE[10], a list of potential explanatory variables was defined. The information identified and collected in the frame of the RECOLAPE project (WP.4), in this Task 1 of CECOFAD 2 has been validated and processed for its integration, detection of the ideal resolution and for exploring new indices to be integrated in the model in

[5] DCF Senne (IRD), DCF Senne (TAAF), Moratoire ICCAT 2013-present (IRD) and OCUP.
[6] Data Collection Observer program (DCF) from 2003 to present with the 5 % of coverage of Atlantic and Indian fleet.
"Good Practices (BBPP)" programs from 2012 to present with around 90 % of coverage of Atlantic fleet.
"Fauna Asociada programs" from 1995 to 1996 (Atlantic only).
"Patudo Observer programs" from 1996 to 1999 (Atlantic only)
[7] Gaertner D., Katara I, Chassot E. (2016) Workshop for the development of indices of abundance for the EU tropical tuna purse seine Fishery. IEO Fuengirola, 19-22 July 2016; Handout, 17 pp.
[8] Gaertner D., Katara I, Billet N, Fonteneau A, Lopez J, Murua H, Daniel P. (2017). Workshop for the development of Skipjack indices of abundance for the EU tropical tuna purse seine fishery operating in the Indian Ocean. AZTI Pasaia, 17-21 July 2017; Handout, 17 pp.
[9] See Annex 3 Report of the Workshop for the development of Yellowfin indices of abundance for the EU tropical tuna purse seine fishery operating in the Indian Ocean 3-6 September 2018 IRD-UMR MARBEC, Sète (France)
[10] Census of the candidate variables, identification of the data source, and gathering the useful information needed to correct raw CPUE series from different sources: data provided by the fishing industry (e.g., echosounder data) and traditional data (collected in a routine basis under DCF such as the catch per set or catch per searching time).

Task 1.3. of CECOFAD 2. With these consideration in mind, a joint meeting between SC14 and SC9 (CECOFAD2) on PS CPUE standardization was conducted at AZTI Pasaia in 2019 (see intermediate meeting section).

Consequently, the institutes, in collaboration with the tuna owner companies (ORTHONGEL, OPAGAC and ANABAC), have worked on the recovery and integration of this information. This information will be used in the CPUE standardization process for the PS, FAD and free school fishery, planned during 2020 and in future analyses under IOTC Yellowfin work plan agreed in 2018 Scientific Committee meeting.

It should be mentioned that to avoid overlap between EU projects, the sub-task related to the improvement of some definitions related to FAD-fishing has been conducted in the frame of the RECOLAPE project. Because many EU scientists are participating in both projects, these definitions can be considered as the product of both projects (Grande et al., 2018a, b).

5.1.3. Sub-task 1.2. Review the methodologies used to estimate the fishing effort directly related to dFADs use

The use of spatially-explicit capture-recapture models based on Bayesian methodology to obtain spatio-temporal strata-specific estimates of dFADs.

Since the early 1990s, massive use of man-made (dFADs) or natural floating objects (log)[11] gradually equipped with GPS-buoys and used to aggregate tropical tunas, have strongly modified global PS fisheries. This has introduced major changes in the efficiency and selectivity of PSs, as well as raised concerns regarding increased bycatch (i.e., the catch of non-target species, either retained and sold on local markets or discarded at sea) of protected and non-commercial species. There are also concerns of increased juvenile catches and possible influence of the use of floating objects (FOB) on fish migration and potential impacts on the physiological condition of different fish species. In order to determine how fishing associated with the use of FOB can be used in a sustainable way, as well as to integrate this type of information in the CPUE standardization process, the total density of FOBs needs to be known.

The first step in determining the total density of FOBs used in fishing activities is to map the density of dFADs equipped with GPS-buoys and whose trajectories are available. For the French fleet, dFAD-associated PSs recorded all buoys GPS positions' on which they fished (French and others) and French trajectories' to produce a density map between 2010 and 2017. For the Spanish fleet, data recovery was still on-going at the time of the first analyses (during 2018), thus only a percentage of dFADs trajectories were available in 2018 for yellowfin tuna

11 See Tables 1 & 2, Annex 3 in ICCAT [Rec 16-01] for the detailed definitions of Floating objects (FOB), FAD and log.

(YFT) CPUE standardization in the Indian Ocean (Katara et al., 2018). The density of buoys for which trajectories are not available, i.e. buoys from other fisheries still needs to be estimated. The most recent methodology to estimate total density is a raising procedure based on a Bayesian estimation of the distribution of the relative proportion of observed GPS buoys for each nationality and the relative proportion of GPS buoy-equipped floating objects that are dFADs (Maufroy et al., 2015). The methodology limits are an a priori flat distribution of the data (i.e., a flat prior assuming an equal probability of the data) in Bayesian analyses and the variation in exploration effort that is not taken into account.

Using buoy IDs recorded in fine-scale operational data of observer and captain logbooks, identified buoys without available trajectories can be considered as animals. For these buoys a Spatial Capture-Recapture (SCR) model can then be applied to estimate remaining dFAD spatial and temporal distribution, time-at-sea density and probability of detection. In an SCR model, varying exploration effort is taken into account (upper panels in **Figure 5.1.5)**. Indeed, SCR models make use of auxiliary data on capturing location to provide density estimates for animal populations. Previously, models have been developed primarily for fixed trap arrays, which define the observable locations of individuals (here floating objects equipped with GPS-buoys) by a set of discrete points. However, data used are commercial opportunistic data corresponding to unstructured spatial survey (Russell et al., 2012; Thompson et al., 2012; Royle et al., 2013) where sampling (vessels trajectories) produce a survey path not laid out a priori, but rather evolves opportunistically during the course of sampling depending on local fishing conditions. This violates the main assumptions of standard SCR that the line is placed a priori, independent of density and unrelated to detectability. Thus, SCR models for search-encounter data (i.e., for detections of recognizable individuals in continuous space in unstructured spatial survey) were needed. We transferred these models to fishery datasets in order to estimate non-tracked buoys density considering buoys as animals, 1*1 degree squares as traps and vessels with activities on non-tracked buoys as detectors. A square is considered active in a particular month when it has been sampled (i.e., when a vessel trajectory crossed this particular square, and inactive otherwise). This information is essential to correct the potential bias induced by different spatial and temporal exploration effort.

Only activities from voluntary contributions of French tuna vessels shipmasters and tuna fishery associations were used, as it was not possible to have access to the Spanish list of the buoys IDs used to calculate their partial buoys density. After merging French logbook and observer datasets, activities on buoys used in the analyses are only those of buoys for which IDs have been reported and for which we do not have trajectory data (hereafter called non-tracked buoys, NTB).

After omitting activities on tracked buoys, in order to account for differences in exploration effort, the 1° squares "sampled" by the vessels reporting activities on NTB (i.e., NTB-associated vessels) are also needed, as well as the associated exploration effort (i.e., the associated total amount of hours spent per square). French PSs have been equipped with VMS since the early 2000s as part of the monitoring, control, and surveillance (MCS) program of the EU. The GPS position of a vessel with activities on NTB is then recorded on an hourly basis, enabling construction of grids of sampled 1*1 degree square over their typical 4–6 week fishing trip. Due to the sensitive topic of vessel locations, this information was not available for the Spanish fleet, thus the dataset utilized comprised solely of French data. Preliminary results are presented below (**Figure 5.1.5**).

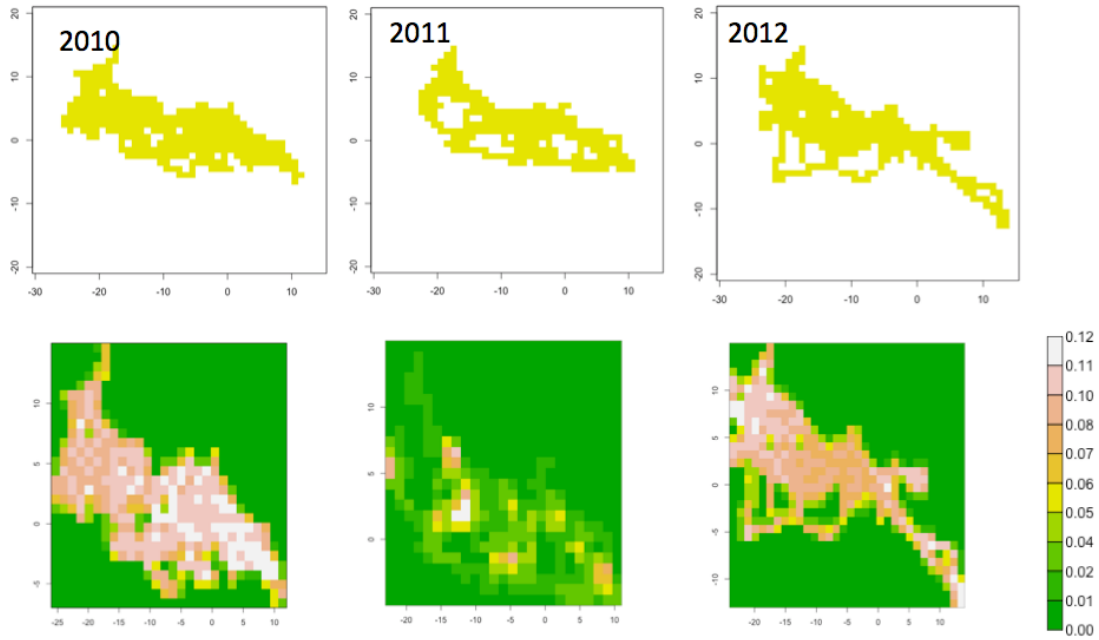

Figure 5.1.5 Density (per 100 km^2) of non-tracked buoys (lower panels) and their associated exploration effort (upper panels) for three different years in the Atlantic Ocean. Longitudes and latitudes are provided on the X and Y axes respectively.

Analysis of the dFAD activities for the European bait boat fleet operating off Senegal.

In the early 1990s, the European bait boat fleet operating from Dakar (Senegal) implemented a new fishing strategy (i.e., the "vessel associated-school"), where a baitboat acts as a floating object to attract tunas (Fonteneau and Diouf, 1994; Hallier and Delgado de Molina, 2000). This fishing strategy has changed over time, with a concomitant wider fishing grounds in the Eastern Atlantic Ocean, towards the increasing use of dFADs for aggregating tropical tunas (**Figure 5.1.6**). The current fishing strategy of bait boats mimics that of large industrial PSs, also

present in the same fishing ground. Since the mid-2000s, due to the increasing use of dFADs, the efficiency of this fleet has increased considerably, resulting in rising annual catches (Pascual et al., 2017). The dFADs deployed by this fleet are shared by groups of vessels working together. There is evidence of seasonality in the use of dFADs along the year, with the summer months being preferred for the use of these devices, reaching an average of 300 dFADs / month by group (Pascual et al., 2019).

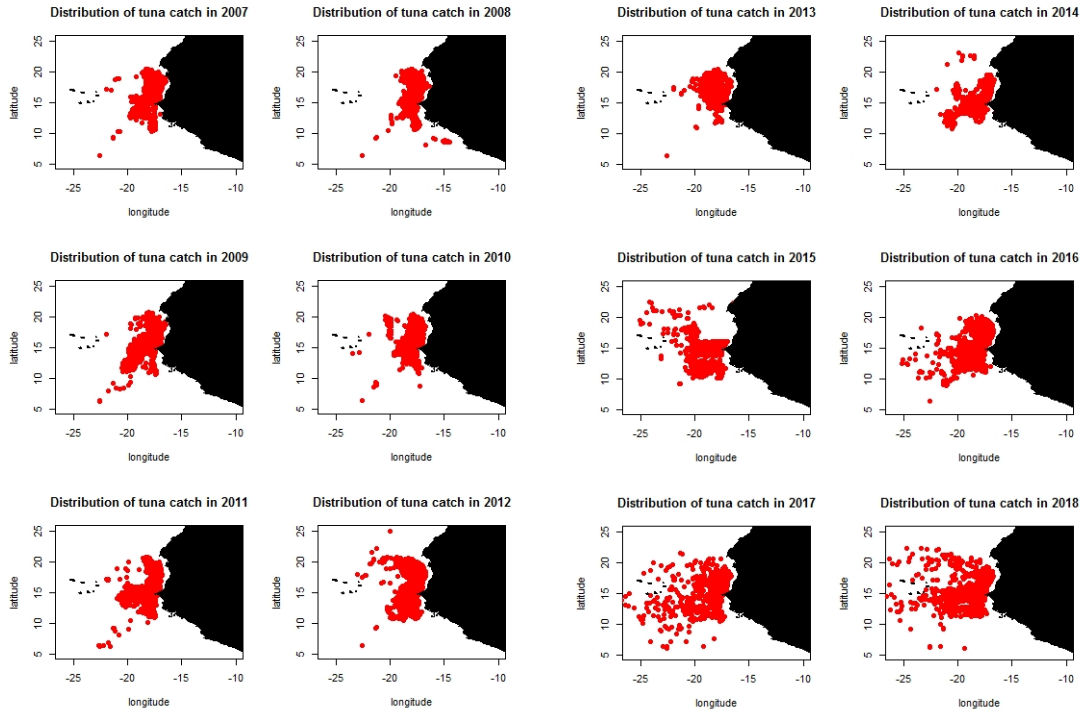

Figure 5.1.6. Fishing grounds of the European Baitboats operating from Dakar between 2007-2018

Catches, days at sea and fishing days are obtained through the logbooks of each baitboat. With the aim to analyze the trends over time of the catch rates, different indices were computed as follows:

- Catches: Total catch per group, month by year.
- CPUE: catches / days of fishing.
- CPUE2: catches / Nº buoy.
- CPUE3: captures / effort 1.
- CPUE4: captures / effort 2.
- Effort 1: Nº buoys / days at sea
- Effort 2: Nº buoys / fishing days

The information from dFADs is received in a standardized format, presenting the following information:

1. Name of vessel: Eight European bait boat vessels operating from Dakar
2. Buoy number: code number with one to four digits by identification.
3. ISN: alphanumeric code on the type of buoy and number of buoy (ahem: T7 +, T8E, T8x, Te8 all of Zunibal type with satellite connection and echosounder.
4. Date data: day, hour, minute and second of current buoy status.
5. Position data: latitude and longitude by buoy.

If the buoy is not transmitting or is not operational for the vessel, the information of fields (4) and (5) is recorded as "not transmitting", which indicates that the buoy has been lost. Data cleaning consisted of removing or filtering repeated records for the total count.

The analysis of the continuous monitoring of the identification codes of buoys used per month and vessels shows that 3 groups of vessels shared operations on dFADs "Group 2": composed by 3 vessels, "Group 3": by 3 vessels and "Group 4": by 2 vessels.

Catches and the number of operational buoys used by each group identified are presented in figures **5.1.7** and **5.1.8.**, respectively. The second and third quarters of the year are the most important months in terms of catches, while the number of dFADs used increased during summer.

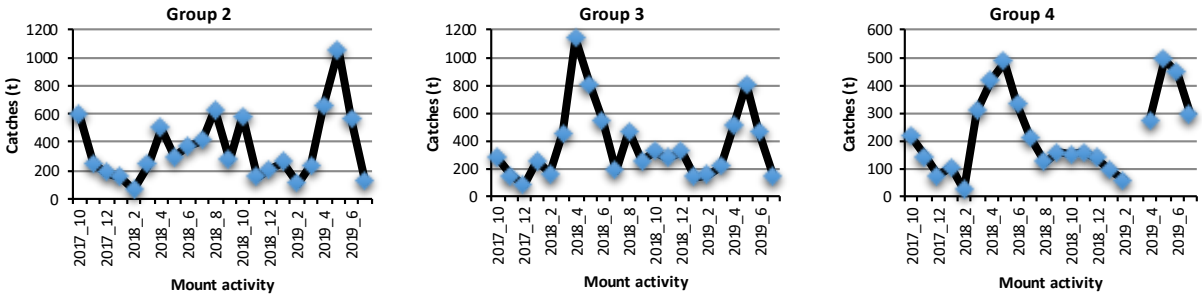

Figure 5.1.7. Monthly catches by group over the period studied.

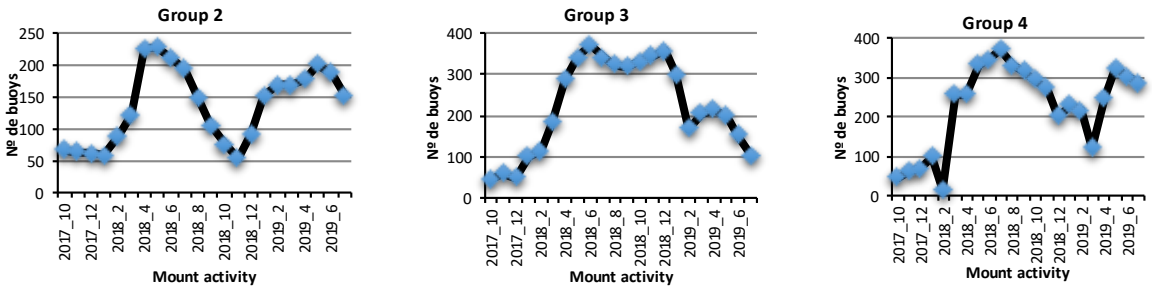

Figure 5.1.8 Number of operational buoys used by month for each group over the period studied

It must be noted that the number of operational buoys are very similar between the different groups of baitboats. As expected, the catches of every group increased when the number of operational buoys (i.e., buoy at sea switch on and transmitting) increased (**Figure 5.1.9**).

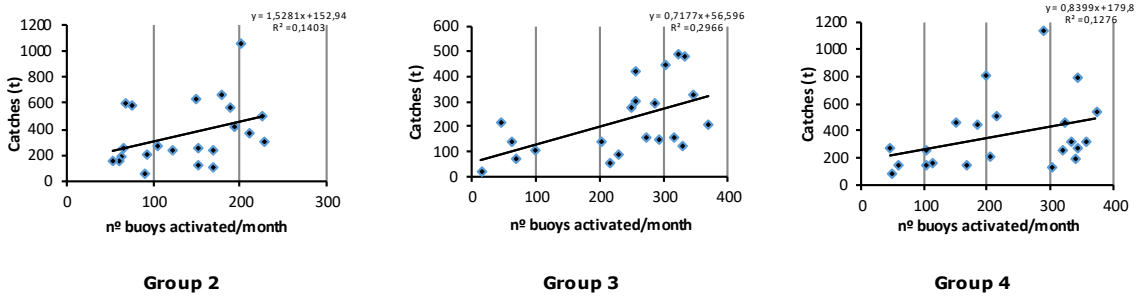

Figure 5.1.9. Relationship between the catch and the number of operational buoys by month and groups of bait boats

The CPUE index, expressed in catch (t) per fishing days, was positively correlated with the number of operational buoys (Pearson R: Group 2 = 0.62; Group 3 = 0.39; Group 4 = 0.54) (**Figure 5.1.10**). In contrast, the "CPUE 2" (catch / No. of operational buoys) decreased when the number of operational buoys increased (Group 2 : -0.35; Group 3 = -0.47; Group 4 = -0.52) (**Figure 5.1.11**).

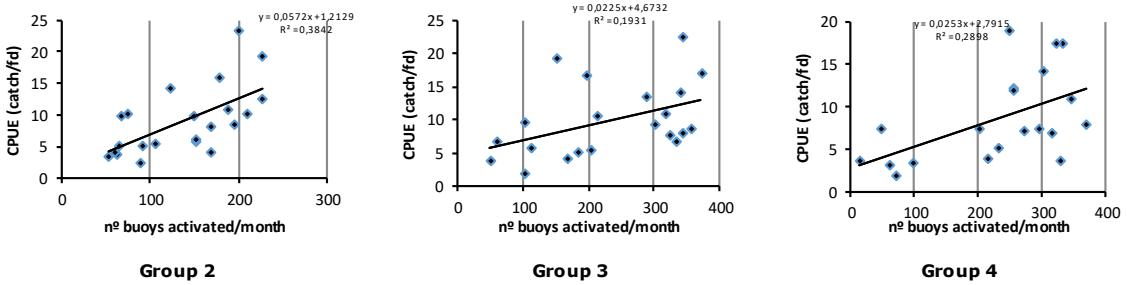

Figure 5.1.10. Relationships CPUE (catch (t) per fishing days) - Nº of operational buoys by month and groups of baitboats

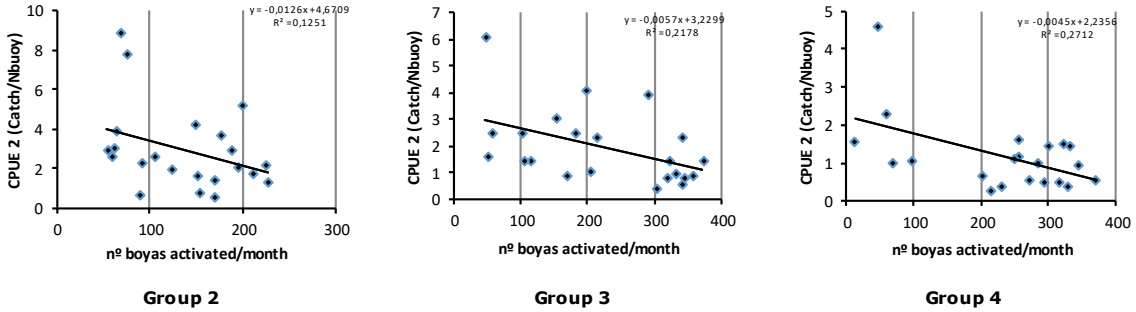

Figure 5.1.11. Relationships CPUE2 (catch / No. of operational buoys) - Nº of operational buoys by month and groups of baitboats

There was no evidence of a relationship between "the number of days at sea" or "the number of fishing days" and the number of operational buoys (**Figures 5.1.12** and **5.1.13**). A greater number of buoys does not imply more fishing days or sea days per month.

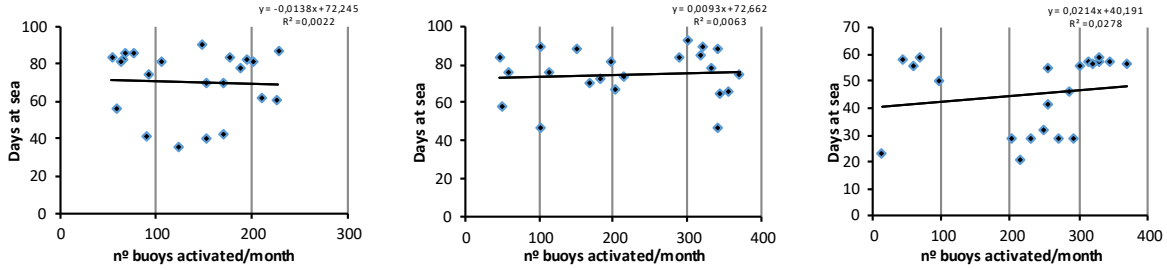

Figure 5.1.12. Relationship between the number of days at sea - Nº of operational buoys by month and groups.

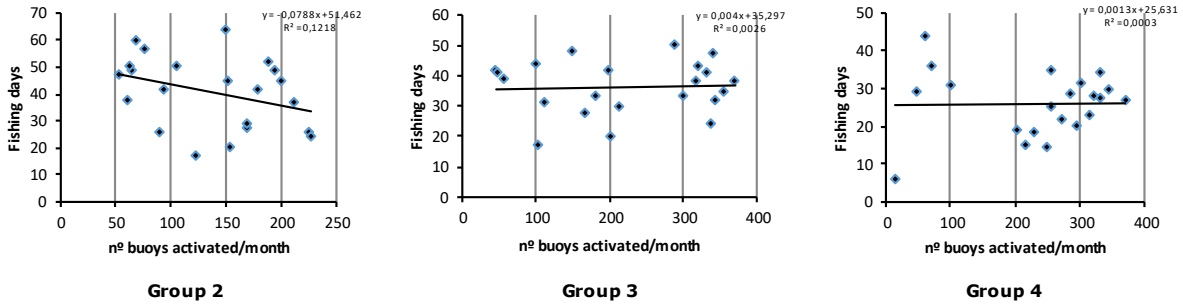

Figure 5.1.13. Relationships between the number of fishing days - Nº of operational buoys by month and groups

According to Fonteneau and Diouf, (1994), in the nineties the baitboat fishery changed its traditional bait boat fishing strategy, using the baitboat as a FAD. Currently, this fishery has increased its productivity by deploying dFADS and sharing more than 250 dFADS by groups of up to three boats throughout the year. A greater number of dFADs at sea produce a clear increase in monthly catches for each group of baitboats analyzed. With more than 200 operational buoys per group, more than 500 t of tunas were caught.

A greater number of dFADs at sea produces an increase in the yield per fishing days (CPUE). The use of more than 200 dFADs in the sea per month produces a catch between 15 t and 20 t by fishing days. It should be mentioned however that a greater number of dFADs at sea produces a decrease in yield by dFADs (e.g., CPUE 2). That means that individual yield is reduced with an increase in the number of dFADs at sea. The highest yields for each dFAD and month (values between 2 t to 6 t of tuna catch) occurred with an amount of 50 to 100 dFADs by month. These results suggest that using more than 200 dFADs by month per group reduced the productivity of each dFAD, to values between 1 t to 2.5 t by month.

5.1.4 Sub-task 1.3. Integration of unofficial information, collected with the collaboration of ship owners and PS fishing associations, in the standardization of CPUEs

PS CPUE standardization on free schools.

The time series of EU PS fleet catches per unit effort (CPUE) of large YFT (>10 kg) from the Atlantic Ocean and in the Indian Ocean were standardized using an extension of the Delta-lognormal GLMM. The rational for this was to account for the fact that tropical tunas are spatially structured, comprising schools and clusters of schools, and that in consequence any change in abundance may be influenced by the number (or density) of schools and/or the size of the school. With these considerations in mind, with the aim to depict the trend in abundance for adult YFT caught in free schools (FSC), three sub-models have been considered:

- Poisson GLMM that standardizes the number of positive and null sets, by vessel and unit of time and location;
- Binomial GLMM that takes into account the fraction of positive sets with large YFT; and
- Lognormal LMM to describe the catch conditional to positive set (e.g., the size of the school).

Standardized CPUE for FSC was thus defined as the product of the number of sets (positive and null) by spatio-temporal strata, the proportion of sets with large YFT (>10 kg) and the catch of large YFT per positive set. The originality of this work relied on the inclusion of i) null sets, considered as presence of schools of YFT, ii) fishing days without set, considered as absence of FSC, and iii) time spent by 1*1° centroid cell by boat by day (see below for more information), to constrain detectability, i.e. to take into account the exploration heterogeneity in these 1*1° cells. This new standardization approach, therefore, represents a significant advance over previous efforts, though there are a number of avenues for future progress. It should be noted that distances between successive sets null-FSC/next-FSC for a boat is not significantly different from all other combinations. That means that there is no need of buffer avoiding to count the same school several times.

To detect strata without sets, all activities recorded in French and Spanish logbooks were used for the periods 1993-2018 in the Atlantic Ocean and 1991-2017 (2018 removed due to quotas) in the Indian Ocean. In addition, several criteria were applied to select the most accurate data:

- Areas defined by all grid cells where large YFT (i.e., commercial categories 2 and 3) were fished for at least 5 years over a period of no less than 15 years, to avoid areas that are not routinely fished;
- Vessels with more activity than the 5% of the left hand distribution based on the cumulative number of days per boat (all activities confounded);
- Entire days with no activity with problematic operations;

- All sets per boat and day were aggregated and attributed to the centroid of these set activities. The single-boat searching time by day (searching centroid) was then calculated in the centroid cell as the number of hours of daylight (sun set time – sun rise time) –(number of sets done by the same boat the same day*median of setting time); and
- Total number of sets per day per boat was filtered and days with unrealistic data were removed

In the case of the Atlantic Ocean, due to collinearity issues (i.e., correlation between predictor variables explaining some of the same variance in the dependent variable, which in turn reduces their statistical significance), only representative cells of large YFT habitat were used, i.e., 1*1 degree cells with at least 20% of YFT category 2 & 3 as well as 5*5 degrees cells occupied more than 50% (**Figure 5.1.14**).

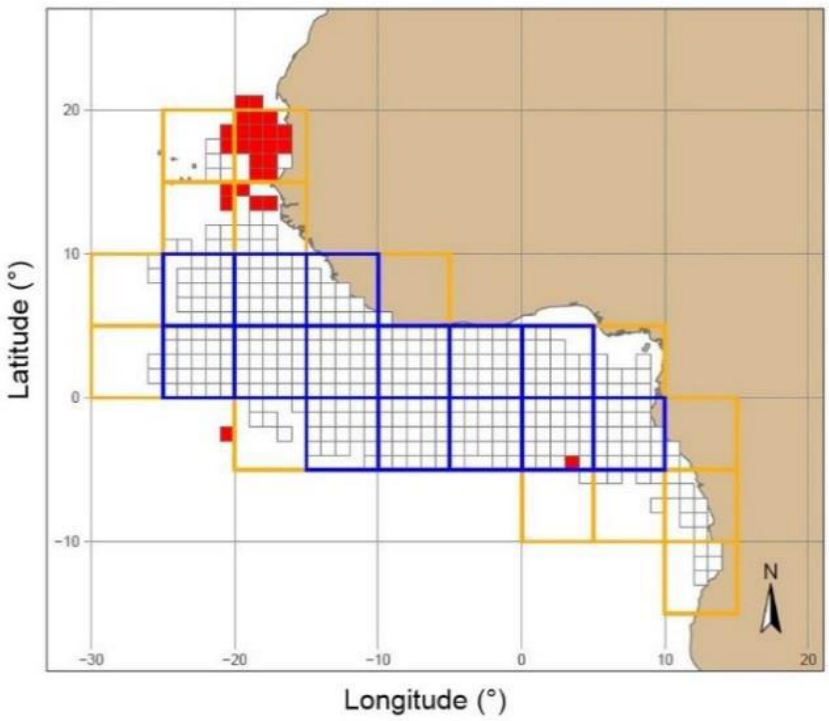

Figure 5.1.14. Atlantic study area with removed 1*1° cells (red) without at least 20% of YFT category 2 & 3 and 5*5° cells occupied less than 50% (yellow). 5*5 cells occupied more than 50% are shown in blue.

Due to the specific conditions found in each ocean, different candidate variables were explored (see **Table 5.1.2** for the Atlantic Ocean and **Table 5.1.3** for the Indian Ocean).

Variable	Description
Fleet country	France; Spain
Numbat	Unique vessel identifier
Vessel storage capacity	In m3
Cwp55 grid cell	Reference grid of the fishing area at a 5ºx5º resolution
Number of sets on FOBs	Resolution monthly per cell
Number of positive sets	Number of positive sets per boat per day per centroid
Year	Year at which the fishing set took place
Quarter	Quarter of years
Age of vessel	Year – Year of vessel service
Economic Exclusive Zone	Identifiers of EEZs and the offshore area
Fishing access	EU fishing agreement in the different EEZs
Searching centroid	In h - Single-boat searching time in hours calculated as (sun set time – sun rise time) –(number of set*median of setting time)

Table 5.1.2. Candidate variables for the CPUE standardization model of large YFT on free schools in the Atlantic Ocean.

Variable	Description
Fleet country	France; Spain
Numbat	Unique vessel identifier
Vessel storage capacity	In m3
Cwp55 grid cell	Reference grid of the fishing area at a 5ºx5º resolution
Number of sets on FOBs	Monthly resolution per grid cell
Number of positive set	Number of positive sets per boat per day per centroid
Year	Year at which the fishing set took place
Quarter	Quarter of years
Age of vessel	Year – Year of vessel service
Searching centroid	In h - Single-boat searching time in hours calculated as (sun set time – sun rise time) –(number of set*median of setting time)
Piracy	Presence/absence of piracy per cell
Gulland's index of fishing effort concentration	Measure the extent to which a fleet has concentrated its fishing effort in areas with higher than average catch rate

Table 5.1.3. Candidate variables for the CPUE standardization model of large YFT on free schools in the Indian Ocean.

With regards to the CPUE series of Indian Ocean YFT in free schools, the potential effect of the piracy (**Figure 5.1.15**), or environmental factors likely more involved with catchability than with real changes in stock abundance (Gulland Index; **Figure 5.1.16**) were considered. In comparison, selected areas in the Atlantic Ocean were covered by EU fishing agreements, though this covariate was not considered.

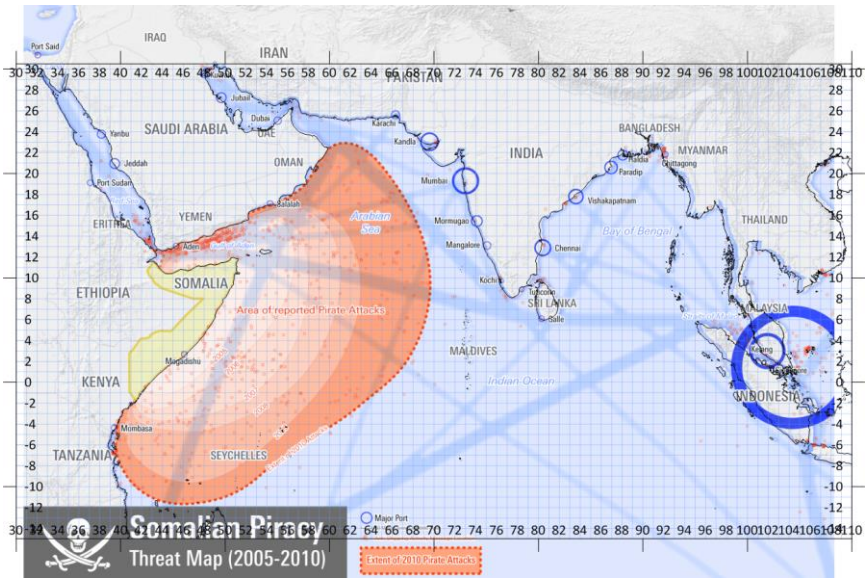

Figure 5.1.15. Areas affected by the piracy in the Eastern Indian Ocean

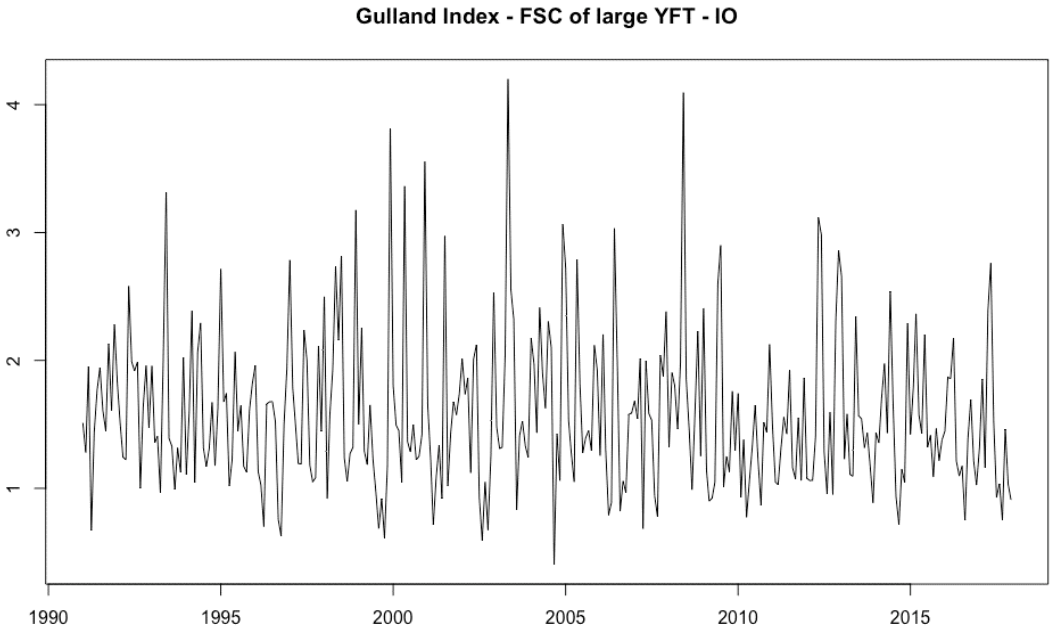

Figure 5.1.16. Gulland's Index (fishing effort concentration) calculated monthly in the Indian Ocean selected cells.

Due to the large number of candidates, a Lasso variable selection procedure was used for detection of the explanatory factors useful for the standardization of the CPUE.

Regarding the Atlantic Ocean, after the Lasso selection procedure three sub-models (i.e., components) were retained. We performed the Poisson GLMM where the full model included the following fixed effects: fleet country, age of the vessel, number of sets on floating objects (FOB, which includes natural logs and dFADs), vessel storage capacity, year, quarter and 5ºx5º grid cell. The number of FOB sets per trip was included as a proxy for vessels' fishing strategy changes across time due to increased dFAD number. The random structure within the model were fishing access and a vessel unique identifier. The time spent by searching centroid by day was calculated as (sun set time – sun rise time) – (number of set*median of setting time) and was used as an offset.

Component 1:

num_sets_fsc ~ fleet country + age of the vessel + num_sets_fob + vessel storage capacity + year + quarter + cwp55_group + (1|numbat) + (1|eez:fishing_access) + offset(searching_centroid)

The full model for the binomial GLMM (Component 2) and the lognormal LMM (Component 3) had the following fixed effects: fleet country, vessel storage capacity, year, quarter, 5ºx5º grid cell. The random structure of these models included a vessel unique identifier. The number of positive sets was used as an offset.

Component 2:

yft_pos ~ fleet country + vessel storage capacity + year + quarter + cwp55_group + (1 | numbat) + offset(nb of positive sets)

Component 3:

log_capture ~ fleet country + vessel storage capacity + year + quarter + cwp55_group + (1|numbat) + offset(nb of positive sets)

The combined standardized CPUE on free schools is presented in **Figure 5.1.17**. The standardization procedure corrected the increasing trend depicted by the nominal CPUE in the last five years. The result of this study has been accepted by the participants at the ICCAT yellowfin data preparatory meeting and integrated in the ICCAT yellowfin stock assessment (SA) conducted in Cote d'Ivoire in July 2019 (Guery et al., 2019a). The integration of this PS abundance index in the SA models substantially modified the perception of the status of the Atlantic YFT stock, which had been evaluated previously with the joint-longlines index only.

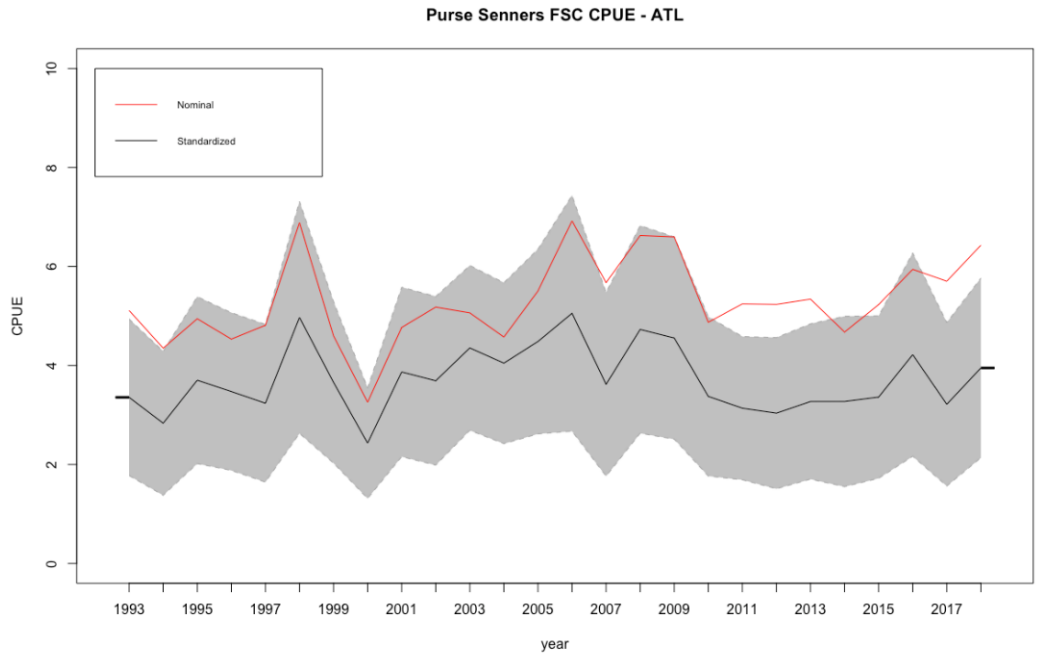

Figure 5.1.17. Standardized CPUE (t* number of free school sets on YFT / vessel and day at sea) for Atlantic YFT category 2 & 3 (black line), with 95% CIs (grey,) and compared to nominal CPUE (red) over the period 1993-2018.

In the case of the Indian Ocean yellowfin CPUE, after the Lasso selection procedure, three sub-models were retained. The full model of the Poisson GLMM included the following fixed effects: fleet country, age of the vessel, number of sets on floating objects (FOB, which includes natural logs and FADs), vessel storage capacity, year, quarter, Gulland index and Piracy. The number of FOB sets per trip was included as a proxy for vessels' fishing strategy changes across time due to the increase of dFADs. The random structure of the model includes a vessel unique identifier. The time spent by searching centroid by day was calculated as (sun set time – sun rise time) – (number of set*median of setting time) and was used as an offset.

Component 1:

num_sets_fsc ~ fleet country + age of the vessel + num_sets_fob + vessel storage capacity + year + quarter + gulland index + piracy + (1| numbat) + offset (searching_centroid)

The full model for the binomial GLMM (Component 2) and the lognormal LMM (Component 3) included the following fixed effects: fleet country, vessel storage capacity, year, quarter and Gulland index. The random structure of these models included a vessel unique identifier. The number of positive sets was used as an offset, as data were aggregated by boat, day and centroid cell.

Component 2:

yft_pos ~ fleet country + vessel storage capacity + year + quarter + gulland index + (1 | numbat) + offset(nb of positive sets)

Component 3:

log_capture ~ fleet country + vessel storage capacity + year + quarter + gulland index + (1|numbat) + offset(nb of positive sets)

The combined standardized CPUE of Indian Ocean large YFT on free schools is presented in **Figure 5.1.18**. The standardization procedure corrected the peak depicted by the nominal CPUE for the period 2003-2006. This peak is assumed to reflect mainly an increase in catchability, due to the presence of large prey abundance (e.g., *Natosquilla* spp.) in the Western Indian Ocean. The introduction of the Gulland Index (which indicates that the PSs were concentrated in rich areas) smoothed the peak. The presence of a smaller peak in the standardized CPUE for the years following the "golden years" could be associated with a better recruitment. The result of this study has been introduced in the sensitivity analysis during the IOTC WPTT meeting conducted in October 2019 (Guery et al, 2019a).

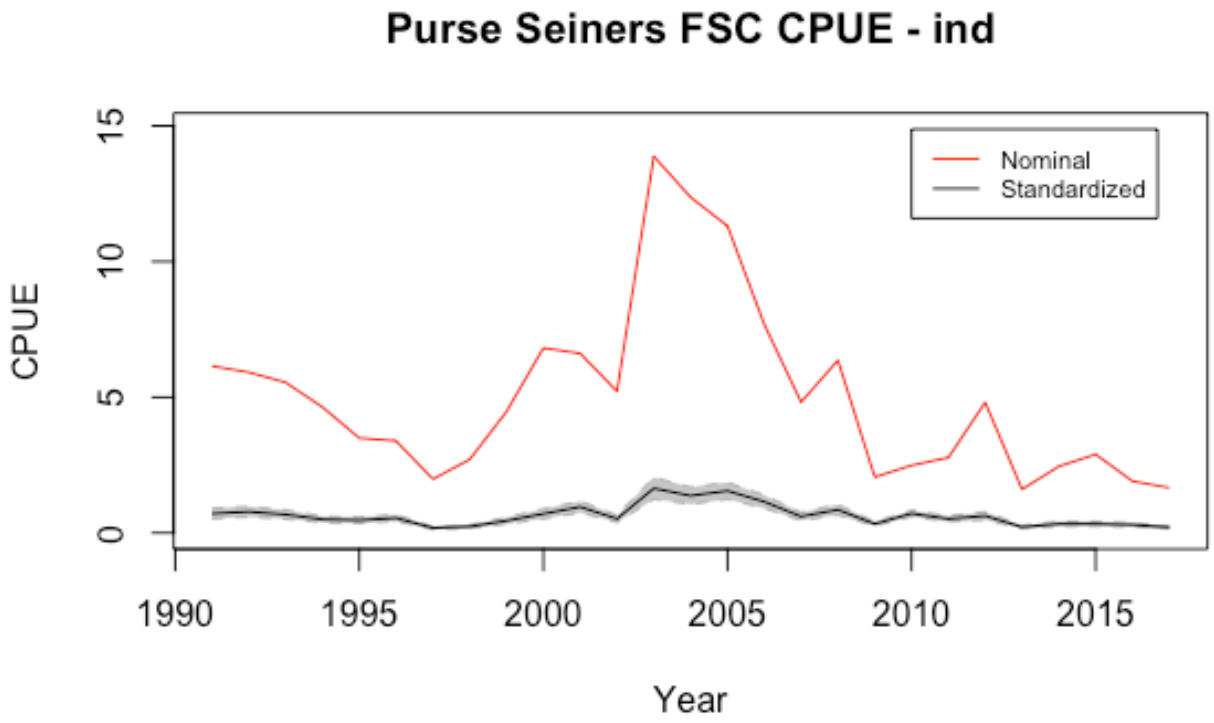

Figure 5.1.18. Standardized CPUE (t* number of free school sets on YFT / vessel and day at sea) for Indian Ocean yellowfin tuna category 2 & 3 (black line), with 95% CIs (grey,) and compared to nominal CPUE (red), over the period 1991-2017.

PS CPUE standardization on dFADs.

The time series of EU PS fleet catches per unit effort (CPUE) of juvenile YFT (<10 kg) from the Indian Ocean was standardized using the lognormal component of the Delta-lognormal GLMM. The rational for this was as a first attempt to depict the trend in abundance for juvenile YFT caught under dFADs. A lognormal LMM was thus used to describe the catch conditional to positive set (e.g., the size of the school). To detect strata without sets, all activities recorded in French and Spanish logbooks were used for the period 1991-2017 (2018 removed due to quotas) in the Indian Ocean. In addition, the same criteria as used for the CPUE standardization on FSC were applied to select the most accurate data:

- Areas defined by all grid cells where small YFT (i.e., commercial categories 1) were fished for at least 5 years over a period of no less than 15 years, to avoid areas that are not routinely fished;
- Vessels with more activities than the 5% of the left hand distribution based on the cumulative number of days per boat (all activities confounded);
- Entire days with no activity with problematic operations;
- All sets per boat and day aggregated and attributed to the centroid of these set activities; and
- Total number of sets per day per boat were filtered and days with unrealistic data removed

Due to time coverage availability, two different time periods (1991-2017 and 2010-2017) were considered and different set of candidates variables explored (**Table 5.1.4**). See details in the Free school CPUE standardization section.

Chlorophyll-a (Chl-a) concentration derived from MODIS (O'Reilly *et al*., 1998) over the period January 1991 to December 2017 was examined. High Chl-a values indicate areas with high productivity and potentially high density of micronekton organisms may be preyed upon by YFT. For instance, the record catches of yellowfin in 2004-2005 were associated with anomalously high levels of Chl-a (Marsac 2008, Fonteneau *et al*., 2008) and an increase in the density of the stomatopod *Natosquilla investigatoris* found in abundance in YFT stomachs (Potier *et al*. 2004). At a monthly timescale, grid cells with high levels of Chl-a can thus be indicative of foraging aggregations of YFT and thus increased catchability.

Variable	Description	Time period
Fleet country	France; Spain	1991-2017 and 2010-2017
Numbat	Unique vessel identifier	1991-2017 and 2010-2017
Vessel storage capacity	In m^3	1991-2017 and 2010-2017
Cwp55 grid cell	Reference grid of the fishing area at a 5ºx5º resolution	1991-2017 and 2010-2017
Number of positive sets	Number of positive sets per boat per day per centroid	1991-2017 and 2010-2017
Year	Year at which the fishing set took place	1991-2017 and 2010-2017
Quarter	Quarter of years	1991-2017 and 2010-2017
Gulland's index of fishing effort concentration	Measure the extent to which a fleet has concentrated its fishing effort in areas with higher than average catch rate	1991-2017 and 2010-2017
dFAD density	Density per 1*1° cells of French and Spanish dFADs (with and without echsounders) from trajectories data	2010-2017

Table 5.1.4. Candidate variables for the CPUE standardization model of juvenile yellowfin under dFADs in the Indian Ocean.

For the French fleet, density of dFADs was calculated from trajectories of French-deployed buoys between 2010 and 2017. Buoy identifiers, found in observer data from the period 2010-2017 but absent of dFAD trajectory data were used to estimate the fraction of coverage of French buoy trajectory data (i.e., the fraction of all French buoy trajectories that are found in our trajectory dataset) by year and ocean. The inversion of this fraction coverage was used as a raising factor to correct dFAD density estimates for missing data. For the Spanish fleet, the density of dFADs deployed from the Spanish fleet was calculated utilizing buoy trajectories from March 2013 to December 2018. Due to missing data on MI buoy brand between 2010 and February 2013, this unknown fraction during 2010-2013 was estimated from available data by multiplying the satlink Spanish dFAD density values in each grid cell-month strata by the MI to Satlink density ratio during 2013, except for January and February 2013 for which the average of 2013 (Mar-Dec) was used. This process was conducted as follows:

(1) Dr=Ds+Ds*Dratio, where Dr is the raised density for each grid and month, Ds is the density accounted for satlink buoys from March 2013 to December 2013 by month and grid (known) and Dratio is the density ratio estimated from March 2013 to December 2013 by month and grid, Dratio=Dm/Ds, where Dm is the density accounted for marine instruments from March 2013 to December 2013 by month and grid,

(2) then (2), in cases in which a ratio was not available for a given grid in a month (e.g. January and February) a mean ratio was applied. Trajectories data from one fishing company were still missing at the moment of the

analysis. This dFAD density variable calculated from the Spanish fleet deployments represents an improvement in Spanish data collection compared to previous works where this information was lacking.

For the period 1991-2017, after the Lasso selection procedure, the full model for the lognormal LMM included the following fixed effects: fleet country, vessel storage capacity, year, quarter and Gulland index. The random structure of these models included a vessel unique identifier. The number of positive sets was used as an offset, as data were aggregated by boat, day and centroid cell:

log_capture ~ fleet country + vessel storage capacity + year + quarter + Gulland index + cwp55 + (1|numbat) + offset(nb of positive sets)

For the period 1991-2017, the standardized CPUE of Indian Ocean juvenile YFT under dFADs is presented in **Figure 5.1.19**. All the variables included in the model significantly influenced the capture of small YFT caught under dFADs. For example, the latter was correlated positively to the Gulland Index (coefficient = 0.062, p-value < 0.0001).

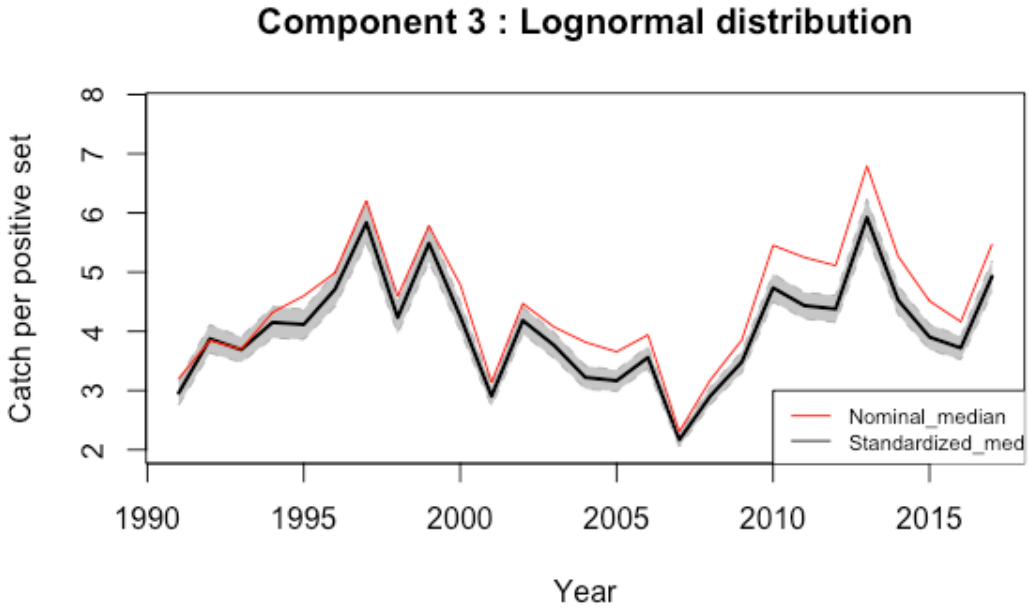

Figure 5.1.19. Standardized CPUE (t/positive set) for dFADs sets of Indian Ocean yellowfin tuna category 1 (black line), with 95% CIs (grey,) and compared to nominal CPUE (red) for the period 1991-2017, on an annual basis.

For the period 2010-2017, after the Lasso selection procedure, the full model for the lognormal LMM included the following fixed effects: fleet country, vessel storage capacity, year, quarter, Gulland index and the density of EU dFADs. The random structure of these models included a vessel unique identifier. The number of positive sets was used as an offset, as data were aggregated by boat, day and centroid cell:

log_capture ~ fleet country + vessel storage capacity + year + quarter + Gulland index + EU dFADs density + (1|numbat) + offset(nb of positive sets)

For the period 2010-2017, the standardized CPUE of Indian Ocean juvenile yellowfin under dFADs is presented in **Figure 5.1.20.** All the variables included in the model significantly influenced the capture of small YFT caught under dFADs. For example, the latter was slightly and negatively correlated and to dFADs density (coefficient = - 0.035, p-value < 0.0001), whereas positively to the Gulland Index (coefficient = 0.054, p-value < 0.0001).

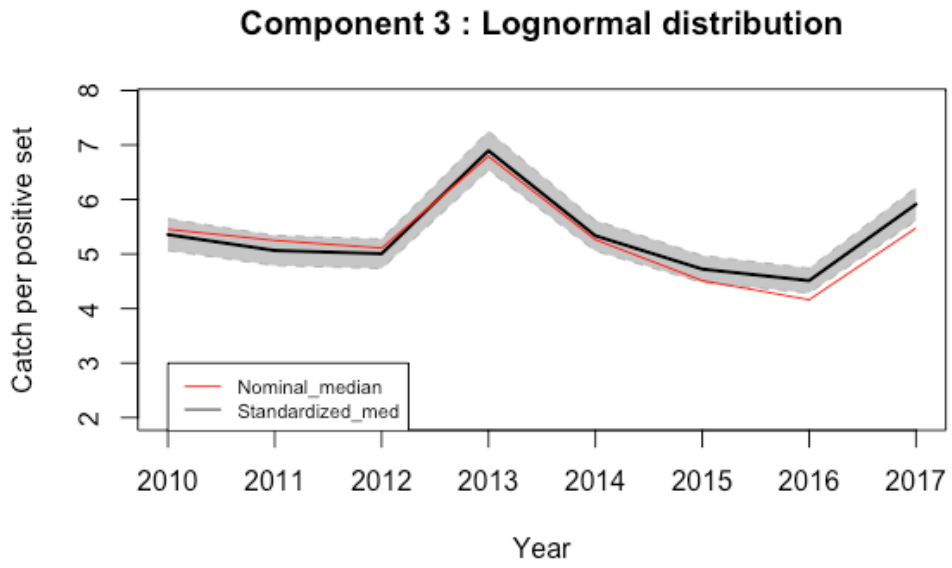

Figure 5.1.20. Standardized CPUE (t/positive set) for dFADs sets of Indian Ocean yellowfin tuna category 1 (black line), with 95% CIs (grey,) and compared to nominal CPUE (red) for the period 2010-2017 on an annual basis. Notice that for this shorter time period, the available potential explanatory factors differed from the entire time series (1991-2017).

5.1.5 Difficulties encountered, and future work expected

It must be noted that the total catch and the species composition derived from sale notes may be biased (Duparc et al, 2018) and consequently have not been considered accurate for the analyses on CPUE conducted within the framework of CECOFAD2. One of the major weakness of the study on the standardization of the CPUE series on dFADs is the difficulty to obtain information on the link between each support vessel (European as well as non-European) and their associated purse seiners from the European tuna companies. At the time of the Spatial Capture-Recapture (SCR) study not all the Spanish information on buoys was available but nowadays the data base has been completed so in the future the estimate will focus only to the remaining density of buoys for vessels not in EU tuna fishery associations (**Table 5.1.5**).

EU PS associations	Study year of CECOFAD 2 project	Time period covered by Buoy Brand		
		MI	Satlink	Zunibal
ORTHONGHEL (all companies)	2018	2006-2017	not used	not used
	2019	2006-2018	not used	not used
	2020	2006-2019	not used	not used
OPAGAC (all companies)	2018	2013-2017	2010-2017	2010-2017
	2019	2013-2018	2010-2018	2010-2018
	2020	2010-2019	2010-2019	2010-2019
ANABAC (all companies)	2018	not available	not available	not available
ANABAC (Echebastar and Atunsa)*	2019	2013-2018	2010-2018	2010-2018
ANABAC (all companies)	2020	2010-2019	2010-2019	2010-2019

**PEVASA not available during 2019*

Table 5.1.5. Data on buoys available at the end of the CECOFAD2 project.

As expressed in ICCAT-Rec [16-01][12], it makes sense to assume that the full or partial assistance of a support vessel is a factor impacting the fishing efficiency of an individual purse seiner. With regards to future work expected for standardizing dFAD CPUEs, it should be noted that further investigations are ongoing in the frame of the Specific Contract n°14 of Safewaters 2. This work is taking into account differences in dFAD detection (e.g. , depending on whether the dFAD belongs to the purse seiner or not), application of the 3 components Delta-lognormal GLMM, comparison with multispecies catch-ratios approach (e.g., Carruthers 2017) and inclusion of the environmental variables.

It must also be mentioned that the CPUE abundance index on dFAD, as well as the direct abundance estimator from echosounder buoy (see next section of the report), characterizes only changes over time of the population which is aggregated under dFADs. It is unclear if this index depicts the trend for the overall stock (i.e., the aggregated component plus the free school component). Combining the standardized indices of abundance of the 2 components of a stock, specifically for skipjack for which the life stages are caught at the same time by both fishing modes, should be considered.

[12] ICCAT-Rec[16-01] noted that "*FURTHER NOTING* that the activities of supply vessels and the use of FADs are an integral part of the fishing effort exerted by the purse seine fleet"

5.2. WP 2 - Direct abundance indices from echosounder buoys

5.2.1. Objectives

With the aim to obtain reliable acoustic abundance estimates from echosounder buoys, additional analyses on the accuracy and precision of biomass estimates must be conducted at the buoy/brand level. Therefore, within Task 2 the temporal and spatial dynamics of tuna under an individual buoy and within a network of FOBs (i.e., a group of FOBs located in the same area and assumed to interact in aggregating individual fish) will be analyzed and modelling approaches will be used to derive direct abundance at different spatial scales.

5.2.2. Sub-task 2.1. Estimate of the accuracy and precision of biomass estimates at the echosounder buoy scale

Within this section we examine different approaches in the exploration of acoustic data, with estimation of alternative abundance indices conducted. To undertake this work historic information from echosounder buoys in the Atlantic and Indian Oceans were gathered (2010-2018) under the RECOLAPE project. While IRD works only with MI buoys, AZTI works (recently) with MI, but also Satlink buoys. Both brands have different buoy models. Within this work we have utilized data from four Satlink echosounder models (DS+ (angle = 32º, frequency = 190.5 kHz); DSL+ (angle = 32º, frequency = 190.5 kHz); ISL+ (angle =32º, frequency = 190.5 kHz); and ISD+ (angle = 32º, frequency = 200 kHz; angle = 32º, frequency = 38 kHz). This work has also used data from four MI echosounder models (M3I (angle = 36º, frequency = 50 KHz); M4I (angle = 42º, frequency = 50 kHz; angle = 17°, frequency = 120 kHz; angle = 10°, frequency = 200 kHz); and M3i+ (angle = 36º, frequency=50 kHz; angle = 8º, frequency = 200 kHz).

Satlink buoys provide biomass estimates throughout 11 layers, up to a depth of 115 meters, while MI buoys provide biomass estimate throughout 50 layers, up to a depth of 150 meters. This difference in layers and depth of biomass estimates allows further examination of how this changes biomass estimates between brands, and therefore will contribute to improving the accuracy and precision of estimates. Based on the experience gained in RECOLAPE, and previous studies (Lopez et al., 2016; Baidai et al., 2018), new methodologies are constantly being applied to further explore and improve algorithms for biomass estimates. In addition, AZTI has been collating historic acoustic information from different sources into a common database (**Figure 5.2.1**); for this online Linux mounted programs and database managers are essential.

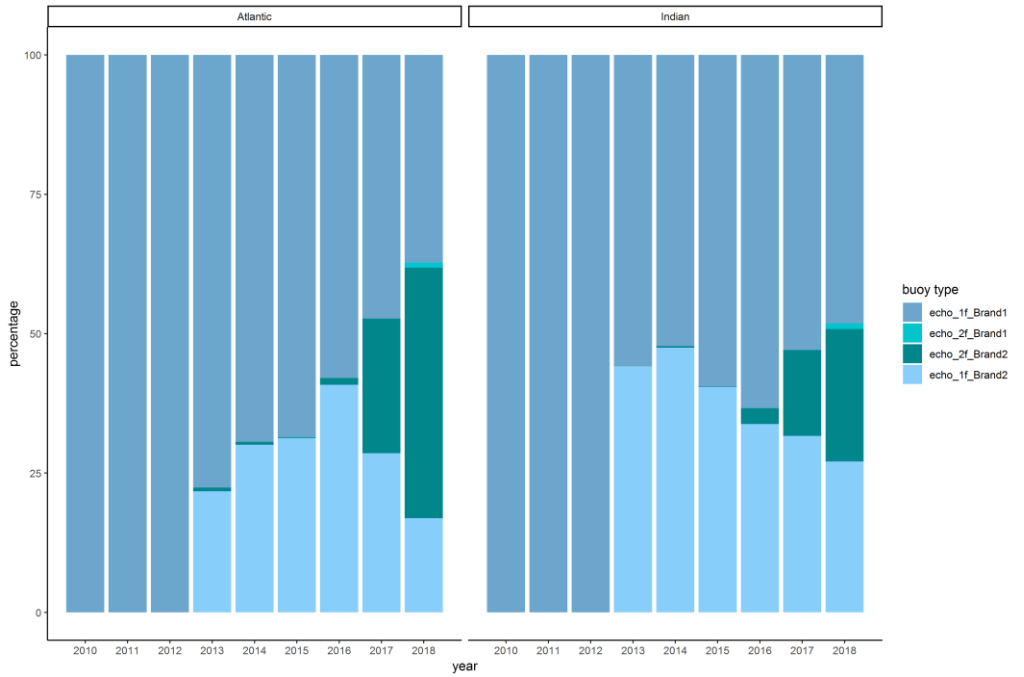

Figure 5.2.1. Percentage of buoy by type and year constituting the raw Spanish Tuna Associations´ acoustic database for the Atlantic and Indian Ocean from 2010-2018. The list of the buoy type categories is constituted by various buoy models. Note that for the period 2010 to 2012 acoustic information on Brand 2 could not be obtained (from RECOLAPE).

The number of acoustic records registered by a buoy depends on the sampling configuration of each buoy model. Acoustic data from MI and Satlink buoys are not recorded in the same units; MI provides an intensity value (0-7 or 0-15 scaled acoustic energy indices), while Satlink provides biomass data in tons. Therefore, a data standardization approach was performed as follows: sampling angles (M3I=36º; M4I=42º; M3I+=36º; DSL+=32º; ISL+=32º) and detection ranges (MI: 150 meters divided in 50 layers of 3 meters; Satlink: 115 meters divided in 10 layers of 11.2 meters and discarding the first 3 meters) are taken into account to sample the same volume of water and to minimize differences between frequencies (MI: 50 kHz; Satlink: 190.5 kHz). This ensures same depth ranges are set for both data sources (MI and Satlink); the vertical structure is shown in **Figure 5.2.2.**

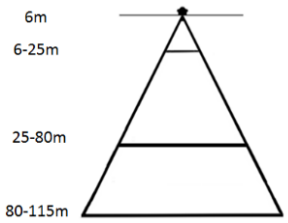

Figure 5.2.2. Depth ranges used at the water volume sampled by buoys.

In order to integrate information coming from different buoy models within and between buoy companies we propose a standardization approach for setting all data sources at equivalent acoustic units and sampling volume. The flow chart shown in the **Figure 5.2.3** displays all steps outlined in this approach.

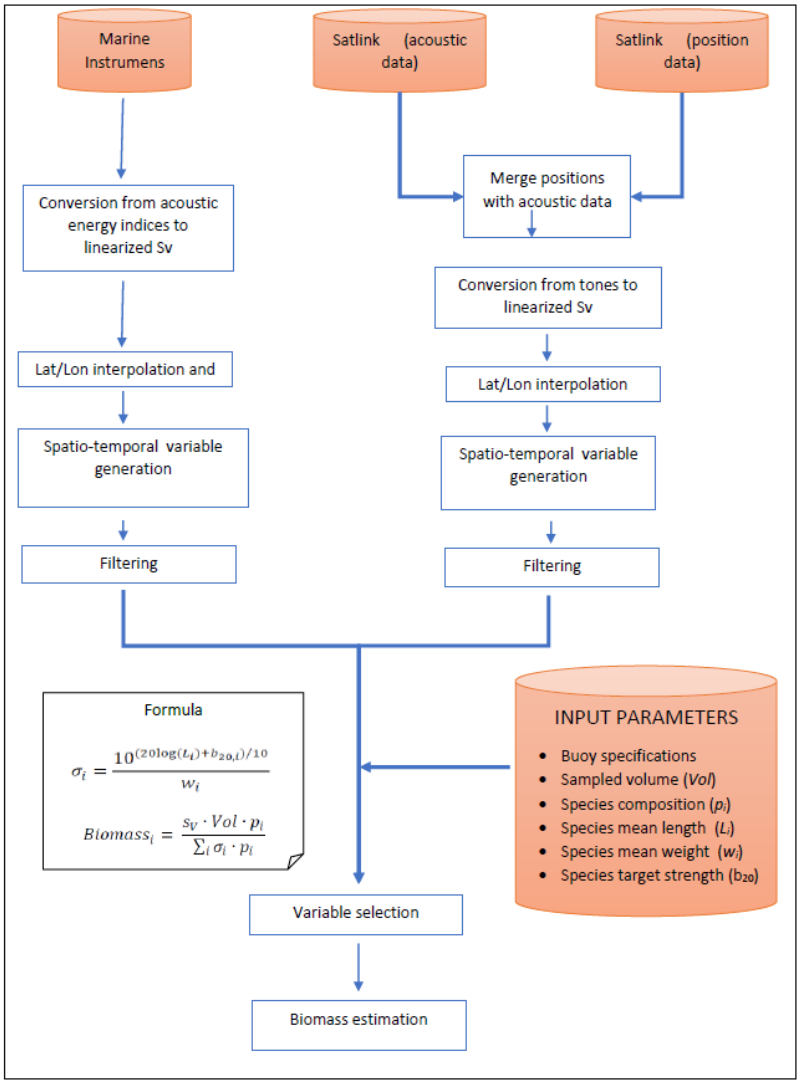

Figure 5.2.3. Flow chart of the standardization steps.

Merge positions with acoustic data (only Satlink) - The very first step is the inclusion of latitude and longitude values in the acoustic Satlink database, which is provided without geolocation. A unique latitude/ longitude value is available for the acoustic data recorded in a given day, but each acoustic register has the real stored time. Consequently, the position for each acoustic record is interpolated based on this stored time.

Conversion from acoustic energy indices to linearized Sv (MI); Conversion from tons to linearized Sv (Satlink) - In relation to harmonization of acoustic parameters used to calculate the biomass, Satlink uses a target strength ~ length relation calculated from typical density of one main tropical tuna species to provide biomass in tons. In a first step biomass data from Satlink is converted to volume backscatter (Sv) in decibels, reversing their formula for the biomass computation (Equation 1). In contrast, MI utilizes a 0-7 or 0-15 scaled presence indice, which are converted to decibels using conversion tables provided by the manufacturer. Biomass is then recomputed using standard abundance estimations equations (Simmonds & MacLennan, 2005):

$$\text{(Equation 1) } Biomass_i = \frac{s_V \cdot Vol \cdot p_i}{\sum_i \sigma_i \cdot p_i}$$

where *Vol* is the sampled volume and p_i and σ_i are the proportion and linearized target strength of each species *i*, respectively. Species proportions in weight and mean fish lengths are extracted from ICCAT or IOTC (depending on the ocean) Task 2 data of the EU fleet.

Since acoustic data does not completely correspond with species distribution and mean fish length data (from EU Task 2), a strategy to assign species composition and fish length data to acoustic data was designed. This encompassed three strata, which were defined to aggregate mean species composition and mean fish length from each strata. The first strata encompassed: 1º * 1º grid, year and month. The second strata was designed to fill uncovered acoustic data from the first strata, utilizing 1º * 1º grid and year quarter. The third strata was used to provide all remaining uncovered acoustic data, taking data from year quarter and large regions. Large regions were defined for both the Atlantic and Indian Oceans: five large regions in the Atlantic Ocean (Region 1: longitude < 35W and latitude > 25N; Region 2: longitude > 35W and latitude > 10N; Region 3: longitude < 35W and latitude <= 25N; Region 4: longitude > 35W and latitude <= 10N; and Region 5: latitude < 10S) and four large regions in the Indian Ocean (Region 1: longitude < 70E and latitude > 10N; Region 2: longitude < 70E and latitude < 10N; Region 3: longitude > 70E and latitude > 10N; and Region 4: latitude < 10S).

Conversion from fish lengths to weights was accomplished using weight-length relationships from ICCAT and IOTC conversion factors. Then, the following TS-length relationships were used to obtain linearized target strength per kilogram:

$$\text{(Equation 2) } \sigma_i = \frac{10^{(20\log(L_i)+b_{20,i})/10}}{w_i}$$

where w_i is the mean weight of each species.

Analyzed buoy brands use 190 kHz and 50 kHz operating frequencies, consequently b20 values measured and estimated with 200 kHz and 38 kHz scientific echosounders were used, respectively. For the 200 kHz frequency, b20

values for skipjack tuna (SKJ) and bigeye tuna (BET) were taken from Boyra et al. (2018) and YFT values from Oshima (2008). On the other hand, for the 38 kHz frequency, b20 values for SKJ were taken from Boyra et al. (2018), while BET values were taken from Boyra et al. (2018) and YFT values from Bertrand et al. (1999) and Oshima (2008). The latest published values for SKJ and BET were used, while studies for YFT are scarce therefore the most accurate values were acquired from scientific bibliography (**Table 5.2.1**); as new TS-Length relationships are analyzed they will be integrated into the methodology. Optimum deep layers for bycatch was taken as 6-25m (from Baidai et al. 2018), while optimum deep layers for tuna aggregation were taken as 26 - 115 m (Moreno et al., 2007; Lopez et al., 2016; Orue et al., 2019a). Biomass below 25 m depth was gathered in two separate layers in this first approach, i.e., 25-80 and 80-115 (Moreno et al., 2007; Lopez et al., 2016).

Preliminary results of re-estimated biomass from raw data showed that the mean of different buoy types have less variability than the maximums (**Table 5.2.2**).

Depth Range	**6-25m**	**26-115m**		
Species	Bycatch	Skipjack	Bigeye	Yellowfin
TS (b20) for MI				
TS (b20) for SAT	68.7	-70.5	-72	-72
Mean Fish Length (cm)	30	Mean by strata*	Mean by strata*	Mean by strata*
Species distribution (%)	100	% by strata*	% by strata*	% by strata*

** "by strata" means that species composition (pi) and mean length (Li) are estimated per spatio-temporal strata (data from ICCAT or IOTC resources): Stratum 1: 1x1 degree grid, year, month; Stratum 2: 1x1 º grid, trimester; Stratum 3: Large regions, trimester.*

Table 5.2.1. Depth range, species, target strength (TS), mean fish length and species distribution, all expressed as %, used in this study.

Model	**Min**	**Max**	**Mean**	**Median**
DSL+	0	38.7	0.462	0.09
ISL+	0	48.7	0.827	0.29
M3+	0	117	0.542	0.11
M3I	0	81.2	0.462	0.12

Table 5.2.2. Mean, maximum, minimum and median of the estimated biomass by buoy model of raw data (all data available without applying any filter)

With the aim of better understanding the performance of the different buoy brands and to discuss the capacity of these buoys to estimate the biomass beneath them, the estimated biomass in a given buoy were crossed with the catch associated with that buoy. To accomplish this, unique dFAD sets in which the buoy ID was recorded were first selected. Within this data all acoustic data recorded 48 h before the set and occurring between 4-8 h in the morning (in which tuna seem more positively associated with dFADs) were selected. As tuna aggregations are dynamic, sets also occurring close to this time range of the day were selected as representative of the acoustic signal measured.

Recorded catch of each dFAD will be related to multiple acoustic soundings. Therefore, to provide the most robust estimator by avoiding eventual outlier values in biomass estimates (and therefore the optimum percentile values) 50 to 99 percentile were tested, per each model and ocean (**Figure 5.2.4**).

In total, 12,916 catches on dFADs collected by observers were crossed with acoustic soundings following the criteria defined above. Only catches in which the buoy was properly identified and occurring in the 2010-2018 period from 4h to 10h AM were selected, with all other data discarded to avoid possible sources of statistical noise.

To assess the relationship between acoustic estimates of tuna biomass (SKJ, YFT, BET) and catch data (tons) linear regressions across each buoy brand are provided (**Figure 5.2.5**). For each model and ocean the most appropriate percentile value was applied based on the sensitivity analyses.

Results overall showed that despite high variability, regressions were predominantly statistically significant and with a weak positive trend, showing that biomass estimates from buoy data are positively related to catch rates. There were a low number of matches between buoys and catches for M3+, but this buoy model relatively uncommon in the Spanish fleet, and therefore there is the likelihood that such patterns are associated with low levels of data.

In this first assessment of the correlation between buoy estimates of biomass and catch, the variance explained is low. Indeed, based on interviews with skippers, the correlation between catch and acoustic estimates seems not to be linear; in order to define their fishing strategy skippers as a whole do not only rely on buoy estimates, but also consider other factors including the area that the dFAD has been drifting through, the season, and the regional environmental conditions. These potentially important factors may have an effect on buoy behavior and therefore accuracy in providing acoustic estimates. Therefore, in order to further evaluate the relationship between catch and acoustic estimates subsequent analysis need to be carried out, including the effect of environmental parameters, depth of the sounding for volume estimation and biomass, or new species composition by strata (e.g., outputs of the new T3). Also new time:day windows for selecting the best appropriate acoustic sounding, as well as alternative vertical stratification of tuna, which can be affected by the depth of the thermocline, should be explored. Additionally, the impact of bycatch-tuna ratio and effect of bycatch species in the acoustic sounding should be assessed.

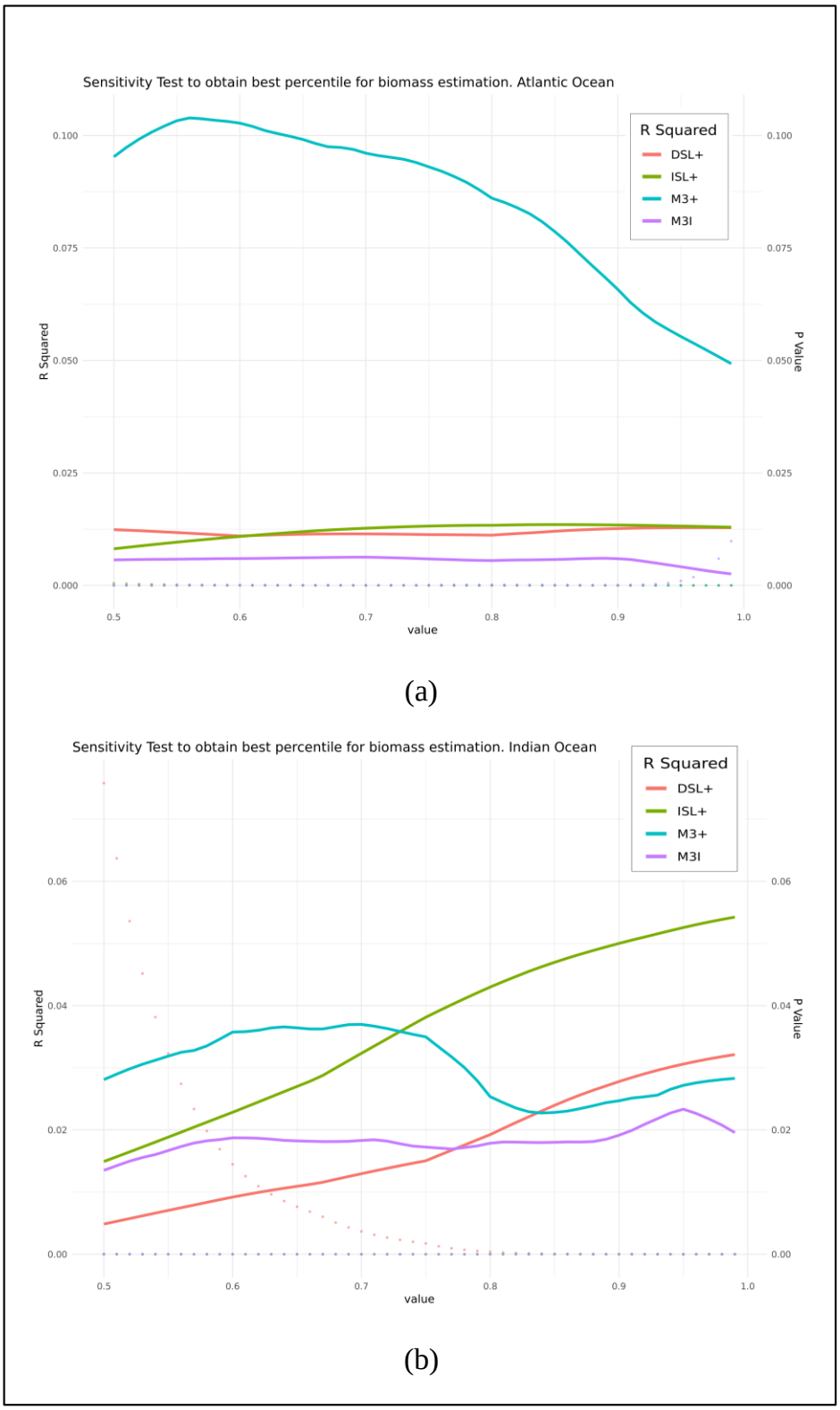

Figure 5.2.4. Sensitivity tests for the Atlantic (a) and Indian Ocean (b).

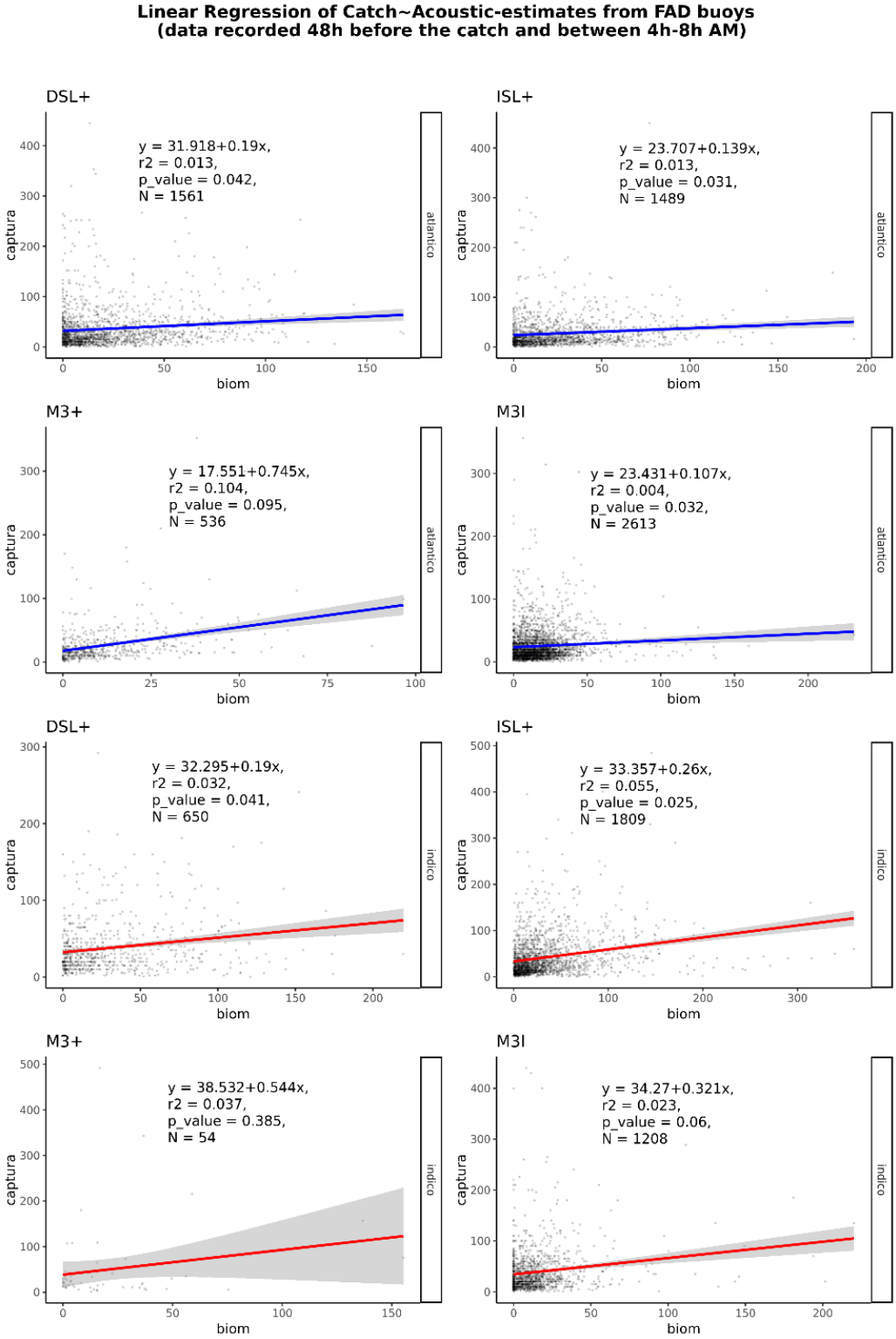

Figure 5.2.5. Fitted regression coefficients, r squared values, p values and N values for each model and ocean.

There has been recent work by IRD to develop a dedicated algorithm to improve the accuracy and precision of biomass estimates obtained from the M3I buoys (MI). These buoys are used predominantly by the French PS fleet in the Atlantic and Indian oceans and constitute the majority of the 2010-2017 buoy database. This model of buoy is equipped with echosounders that sample the water column at a frequency of 50 KHz and a beam angle of 42°. The raw sampling values from these buoys are then converted into scores ranging from 0 to 7, representing (predominantly for visual interpretation) the amount of biomass present per 3-meter depth layer. The recorded values are also converted by an internal buoy algorithm into an index of fish biomass under the dFAD.

A preliminary analysis based on the comparison of the biomass index provided by the buoy and the actual catches performed on the same aggregations, was carried out to estimate the reliability of the index produced from converting the internal buoy algorithm. For scientific studies, it is commonly admitted that a set done at less than 1 mile distance of a dFAD is considered as a dFAD set. However in the present study we selected the observations for which one hour before the set the buoy was at a distance less than 4 miles (i.e., assuming a drifting speed lowest than 4 nm, this means that 1mn before the set the buoy should be about 100m around the set location). The dataset was obtained from cross-referencing catches from logbook and observer's database (IRD) in which the buoy ID was registered with their corresponding acoustic data recorded by the echosounder buoys, over the period from 2013 to 2017 (663 and 1639 catches data respectively in Atlantic and Indian Oceans). Results from both oceans showed that there was no significant correlation ($R^2 < 0.01$) between the biomass indices predicted by the buoy and the actual catch made on the same aggregation (i.e., school), highlighting the poor performance of this index (**Figure 5.2.6.**). The low accuracy of the buoy biomass index with the unavailability of the raw acoustic values sampled by the buoy (limiting the use of conventional echo-integration methods), has led us to develop an alternative approach for the exploitation of the data collected by the buoys.

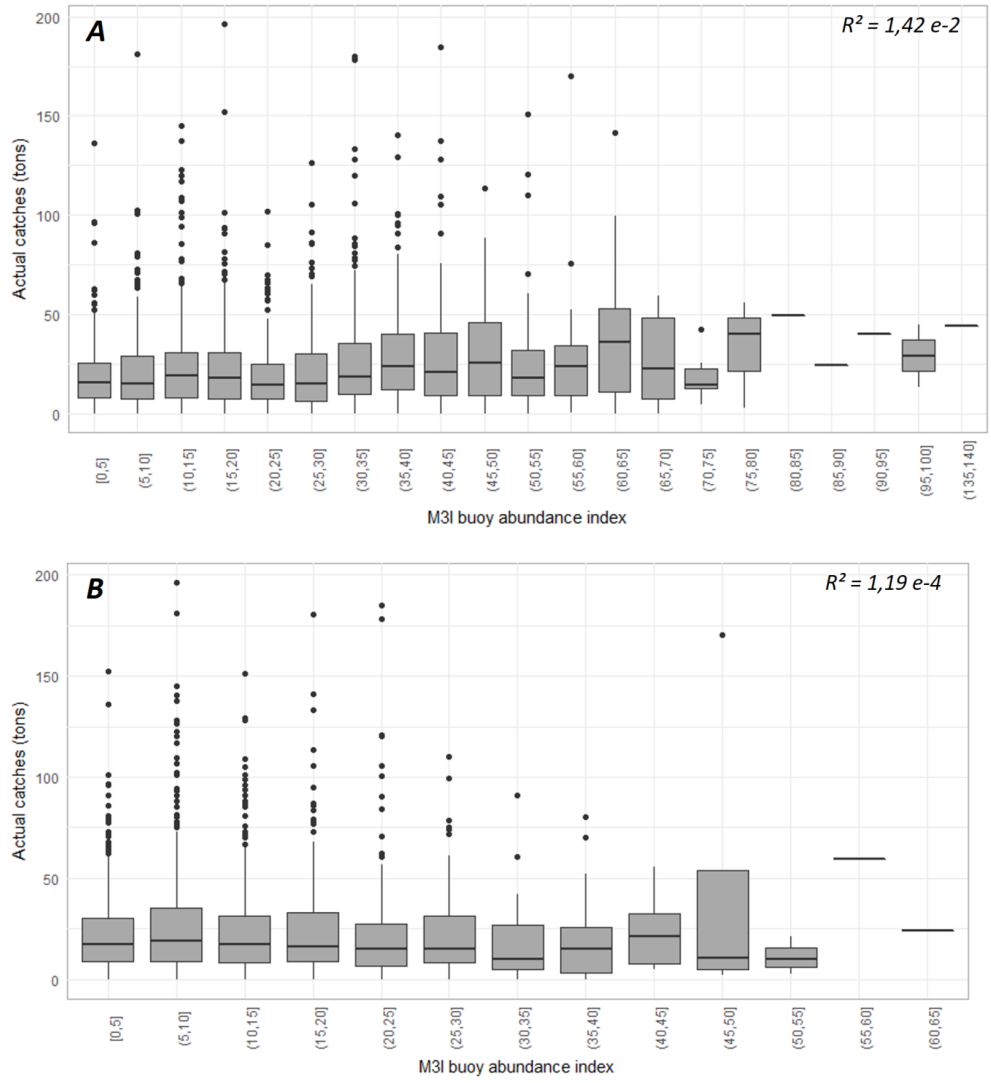

Figure 5.2.6. Reliability boxplot between buoy biomass index and actual catches on the same aggregations (A: maximum of the biomass indexes recorded the day before the set; B: average value of biomass indexes recorded the day before the set). R: Pearson correlation coefficient between actual catches and buoy biomass index.

The new approach we are providing to utilize data collected by the buoys is based on machine learning techniques (random forest; Breiman, 2001) and offers the advantage of being easily adaptable to other buoy models (Baidai et al., 2018). Its design can be assimilated to the analysis and interpretation developed by fishers during their own experience with the buoys. First, data pre-processing operations result in a synthetic sample summarizing the acoustic data recorded over 24 hours, through a matrix of 6 columns (one for each four hour interval), and six rows for different groups of layers, aggregated through cluster analyses. Then, random forest models, aimed at recognizing the characteristic acoustic patterns of different types of aggregation under FADs from these matrices, are built. The learning datasets are based on the cross-matching of the acoustic data

from buoys, with catches and activities on dFADs reported in logbooks and data from observers on board French tuna seiners between 2013 and 2018. They consist in processed acoustic data (matrices) recorded 24 hours prior to catch events (fishing sets), dFAD visits without set, and matrices obtained 5 days after new dFAD deployments. The rationale for considering these 5-day post-deployment periods is to account for the acoustic signal produced by non-tuna species, which are present under dFADs at the early colonization stages (Taquet, 2004; Nelson 2003; Moreno et al., 2007).

To show the utility of this alternative method, we constructed two different learning datasets: a binary dataset describing the presence or absence of tuna (i.e., "No tuna" and "Tuna"), and a multiclass dataset describing the size of the tuna aggregation. For the former, catch events were considered as presence of tuna aggregations, while deployments and visits of dFADs without sets were representative of tuna absence (see **Table 5.2.3**). For the multiclass classification, the tuna presence data obtained from the catch database was split into three classes: catch of less than 10 tons, catch between 10 and 25 tons, and catch above 25 tons, based on the sum of the reported catch of the three target tuna species (YFT, BET, SKJ; **Table 5.2.4**.).

The two learning datasets were used to train two types of classification algorithms: (1) a binary one describing the absence or presence of tuna, and (2) a multiclass classification considering different size classes of aggregations/schools under dFADs (i.e., no tuna, less than 10 tons, between 10 and 25 tons, more than 25 tons). Model training and evaluation were performed through a hold-out validation method repeated 10 times, considering each ocean separately. For the binary classification model, the random forests algorithm successfully discriminates the presence/absence of tuna, with an accuracy of 0.75 and 0.85 in the Atlantic and Indian oceans, respectively (**Table 5.2.5**).

Ocean	Catch data	Deployment data
Atlantic	888	968
Indian	10240	3431

Table 5.2.3: Structure of the learning dataset used in the presence-absence classification for the Atlantic and Indian Oceans.

Ocean	No tuna	< 10 tons	[10, 25 tons]	> 25 tons
Atlantic	888	397	303	268
Indian	10240	904	1288	1239

Table 5.2.4: Structure of the learning dataset used in the multiclass classification for the Atlantic and Indian Oceans.

Evaluation Metric	Atlantic	Indian
Accuracy	0.75 (0.02)	0.85 (0.01)
Kappa	0.51 (0.04)	0.70 (0.02)
Sensitivity	0.83 (0.02)	0.81 (0.01)
Specificity	0.67 (0.03)	0.90 (0.01)
Precision	0.73 (0.03)	0.88 (0.01)
F_1 score	0.75 (0.02)	0.85 (0.01)

Table 5.2.5: Summary of tuna presence/absence classification performances for the Atlantic and Indian Ocean: mean and standard deviation values (in bracket) of evaluation metrics.

For the binary classification model, the random forests algorithm successfully discriminates the presence/absence of tuna, with an accuracy of 0.75 and 0.85 in the Atlantic and Indian oceans, respectively (**Table 5.2.5**).

The multi-class classification model was less effective than the binary one (**Tables 5.2.6** and **7**). In the Atlantic Ocean, the highest proportion of misclassification was associated with the 10-25 tons category (0.22 in precision), whereas tuna schools below 10 tons, and above 25 tons, shared similar performances (precision of 0.32 and 0.28 respectively). Similarly, in the Indian Ocean, tuna schools over 25 tons and below 10 tons constituted the best-detected tuna aggregation size classes (precision of 0.44 and 0.42 respectively), while intermediate aggregation sizes (10-25 tons) were more poorly classified (precision of 0.35).

Evaluation Metric	Atlantic Ocean				
	No tuna	<10 tons	[10 , 25 tons]	> 25 tons	Average
Sensitivity	0.67 (0.03)	0.36 (0.05)	0.24 (0.08)	0.34 (0.06)	0.40
Specificity	0.82 (0.02)	0.80 (0.03)	0.84 (0.04)	0.85 (0.04)	0.83
Precision	0.77 (0.03)	0.32 (0.04)	0.22 (0.04)	0.28 (0.05)	0.40
Accuracy	0.67 (0.03)				
Kappa	0.82 (0.02)				

Table 5.2.6: Summary of multiclass classification performances for the Atlantic Ocean. Mean and standard deviation (in bracket) of evaluation metrics.

Evaluation Metric	Indian Ocean				
	No tuna	<10 tons	[10 , 25 tons]	> 25 tons	Average
Sensitivity	0.87 (0.03)	0.19 (0.01)	0.29 (0.02)	0.54 (0.04)	0.47
Specificity	0.80 (0.01)	0.91 (0.01)	0.82 (0.02)	0.77 (0.01)	0.82
Precision	0.59 (0.02)	0.42 (0.04)	0.35 (0.03)	0.44 (0.02)	0.45
Accuracy	0.87 (0.03)				
Kappa	0.80 (0.01)				

Table 5.2.7: Summary of multiclass classification performance for Indian Ocean. Means and standard deviations (in bracket) of evaluation metrics by classes.

Links with other projects

The RECOLAPE project in the WP4 provided an opportunity to gather acoustic information and describe the specification of acoustic data provided by each buoy model, define pre-processing protocols for acoustic data filtering, define common indices of uncertainty to evaluate the estimates on different buoy models, and estimate the uncertainty of the biomass estimate for different buoy model using these indices based on the algorithms that are currently available to estimate biomass. The data gathered in RECOLAPE, the protocols established, and the knowledge gained has allowed us to have historical data to be used in the Task 2 of CECOFAD 2 that has been pre-processed with the standardized protocols. In addition, in the frame of CECOFAD 2 the algorithms for biomass estimates have been improved and evaluated for the estimation of the presence of tuna and tuna biomass estimates (sub-task 2.1). Additionally, the echosounder data has been utilized in CECOFAD 2 for assessing aggregation dynamics (sub-task 2.2) and in the development of alternative indices of abundance (sub task 2.3).

5.2.3 Sub-task 2.2. Temporal and spatial dynamic of tuna under an individual buoy, and within a network of FOBs.

The dynamic association of tuna with dFADs can help tune the analysis of abundance indices from buoy data, while also contributing to the understanding of the mesoscale ecology and behavior of target and non-target species around dFADs (and in general around floating objects "FOB", natural or not). Different approaches are being adopted to explore the aggregative behavior of tuna and non-tuna species around dFADs by means of echosounder buoys.

AZTI is collaborating with Spanish PS fishing companies, which are predominantly using Satlink buoys to assess the aggregation processes of tuna and non-tuna species. this on-going work by AZTI uses information from 962 echosounder buoys attached to virgin (i.e., newly deployed) dFADs deployed in the Western Indian Ocean between 2012 and 2015 by the Spanish fleet (42,322 days observations). Generalized Additive Mixed Models, with a Gaussian error distribution and identity link function, were established to analyze the trend of biomass over 60 days associated with the virgin dFADs (Orue et al., 2019b). Buoy identification codes were included in the models as a random-effect term to address the dependency structure of the data (i.e., biomass abundance is collected repeatedly by the same buoy for each dFAD). The buoy information is crosschecked with dFAD and fishing logbooks to obtain the activity associated with the dFAD (i.e., deployment, fishing, visits, etc.) and location and time of the activity on the dFADs, with the aim to ensure that no fishing activity had occurred on the virgin dFAD. In addition, from the dFAD logbooks, the object characteristics (i.e., structure dimensions, depth of the underlying structure of the dFAD, materials, etc.) which could potentially influence the detection capabilities and aggregation process of tuna and non-tuna species, were obtained. Only newly deployed dFADs were considered in this study,

identified in dFAD logbooks and linked to our initial buoy database based on buoy identification code and date. Buoys that were deployed on natural objects were excluded from the study as these objects were previously in the water and their time at sea could not be accurately determined. Moreover, different seasons and areas are considered in the analysis to account for potential spatio-temporal patterns. This study aims to investigate the aggregation process of virgin (i.e., newly deployed) dFADs in the Western Indian Ocean using the biomass acoustic records provided by fishers' echosounder buoys.

The dFAD logbooks contained information on the depth and material used to construct the underwater part of the dFADs. According to the dFAD logbook, all the underwater parts of the dFADs were constructed with fishing nets, with the depths of the nets ranging from 10 to 60 meters. Deployments of the dFADs were grouped according to the four different regimes that affect the oceanography and production in the region: (i) winter monsoon from December to March, (ii) spring intermonsoon from April and May, (iii) summer monsoon from June to September, and (iv) autumn intermonsoon from October to November (Schott and McCreary, 2001). To account for potential spatial differences in the aggregation process we applied the models by areas. Regions were based on the ZET ("zones d'échantillonnages thonières") areas defined by Petit et al. (2000): (i) Somalia, (ii) NW Seychelles and (iii) SE Seychelles.

The first day of detection, defined as the first day the buoy emitted a non-zero signal for each species group, was investigated to detect significant changes in the aggregation process under the buoy. Mann-Whitney U tests were then used to examine whether there was a significant difference in detection days for tuna and non-tuna species, as well as by object depth category. Kruskal-Wallis H tests, followed by Dunn´s tests, were used for multiple comparisons and to elucidate whether the first detection day differed between seasons.

Generalized additive mixed models (GAMMs) (Wood, 2006), with a Gaussian error distribution and identity link function, were established to analyze the trend of biomass over 60 days associated with virgin dFADs. The independent variable (days at sea) was included as the main parameter to construct the smooth term of the GAMM. The argument "by" within the splines was included to account for potential differences among periods, area and dFAD depth categories in the models. This implementation resulted in one independent smooth function being fitted for each monsoon period by area and for each dFAD depth category. Similarly, buoy identification code was included in the model as a random effect, to address the dependency structure of the data (i.e., biomass abundance is collected repeatedly by the same buoy for each dFAD).

In order to avoid model overfitting, maximum degree of freedom (k) was limited to k = 4. Thus, the following notation was used to establish the final GAMM models:

Y~s(days at sea, k=4, by ="area"/"depth category") + random = ~(1|ID_dFAD)

Where Y is the biomass of a fish group (i.e., tuna and non-tuna), s represents a penalized thin plate regression spline type smoother for days at sea, k is the maximum degrees of freedom allowed for the smoothing function, and random = ~ (1 | ID_dFAD) is an *ad hoc* way of accounting for the autocorrelation structure of the data set in GAMMs.

Results show that in general, the average period for the arrival of fishes to the dFADs (i.e., first day that the echosounder detected biomass) was 12.2 ± 7.7 days. There were significant differences in the arrival time for tuna and non-tuna them (Mann-Whitney U test, U = 213980, $N1$ = 962, $N2$ = 962, $P < 0.001$). Tuna arrive to dFADs at 13.5 ± 8.4 days following deployment, whereas non-tuna species presence was recorded by 21.7 ± 15.1 days (**Figure 5.2.7, Table 5.2.8**).

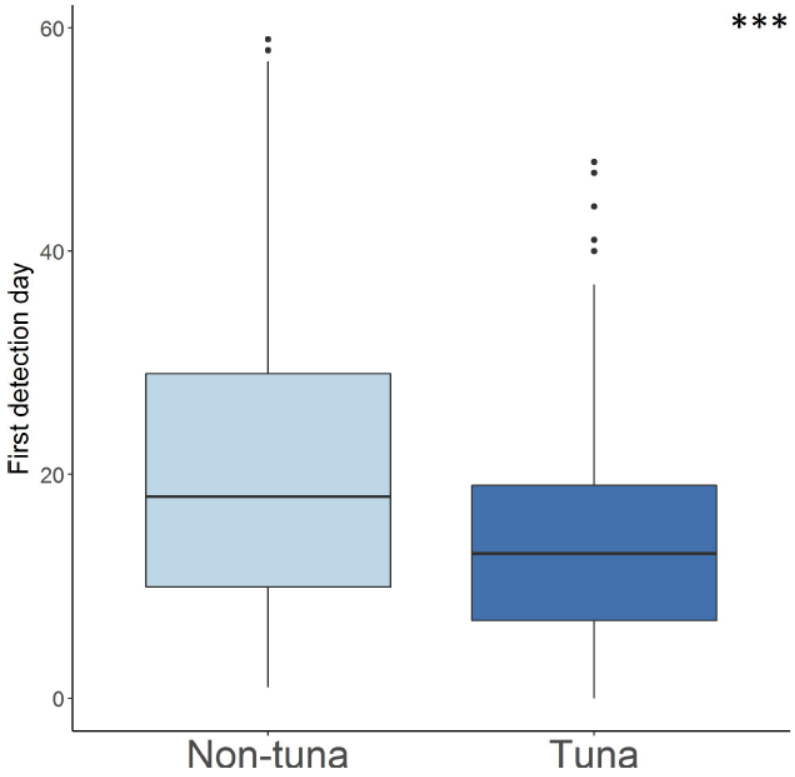

Figure 5.2.7. Box plot of first detection day of tuna and non-tuna species to the object. Asterisks indicate the significance levels of differences following Mann-Whitney U test (*p<0.05;**p<0.001;***p<0.001; NS not significant).

	n	Tuna (Mean±SD)	Non-Tuna (Mean±SD)
General	962	13.49±8.34	21.69±15.06
Depth < 20m	436	14.57±8.41	21.75±14.52
Depth > 20m	340	11.87±7.63	20.70±14.78
Winter moonson	304	12.26±8.08	19.92±14.50
Spring Intermonsoon	139	13.56±8.62	18.08±13.11
Summer monsoon	366	14.01±8.37	23.13±14.86
Autumn Intermonsoon	138	14.77±8.40	25.18±16.70

Table 5.2.8. Mean and standard deviation of first detection day of tuna and non-tuna species according to dFAD depth and season (n=number of samples)

The depth of the submerged section of the dFADs (e.g., netting) has species-specific effects on tuna but not non-tuna. For tuna, the netting that was deeper than 20m showed a shorter period till first detection than more shallow netting (Mann-Whitney U test, $P < 0.001$, $N1 = 436$, $N2 = 340$), while such patterns were not apparent for non-tuna species (Mann-Whitney U test, $P = 0.318$) (**Figure 5.2.8, Table 5.2.8**). The first detection day was also compared by monsoon period and species group (**Figure 5.2.9**). Tuna were detected before non-tuna species in all cases. Significant season-specific differences were found for the first tuna detection day (Kruskal-Wallis test, $P<0.05$). Dunns Test ($P <0.05$) confirmed that first detection is sooner during the winter monsoon than in summer monsoon and autumn intermonsoon periods. Non-tuna species also presented significant differences by periods (Kruskal-Wallis test, $H4 = 15.45$, $P<0.05$) and in this case, Dunns Test confirmed a significant difference ($P <0.05$) between winter monsoon and summer monsoon and autumn intermonsoon periods. Similarly, differences were found between spring intermonsoon period and summer monsoon and autumn intermonsoon periods.

The general models for biomass aggregation of tuna and non-tuna species at dFADs appear to be similar (**Figure 5.2.10**). In both cases a clear increase in biomass was detected until approximately day 30. The biomass reaches a peak earlier in the case of non-tuna species, around day 30, while for tuna the peak is reached around day 40. After this period, both tuna and non-tuna biomass remained steady.

When modeling the tuna biomass according to the depth category of the object (**Figure 5.2.11**) the GAMM showed that deep objects reach the biomass peak almost 10 days earlier than shallow objects. Also, deep objects showed a biomass decrease after the peak while, in shallow objects, biomass remains stable after reaching the maximum.

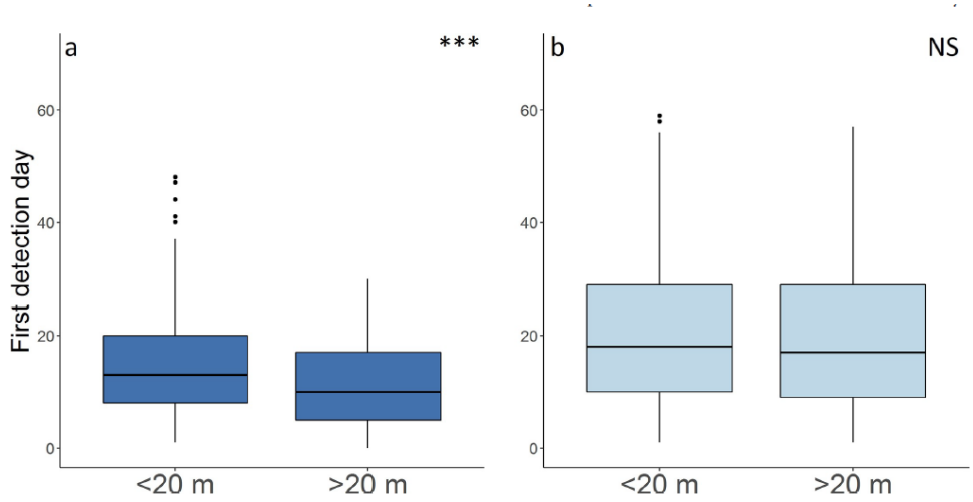

Figure 5.2.8. Boxplot of first detection day to the objects of (a) tuna and (b) non-tuna species for the different depth category of DFADs. Asterisks indicate the significance levels of differences following Mann-Whitney U test (*p<0.05;**p<0.001;***p<0.001; NS not significant).

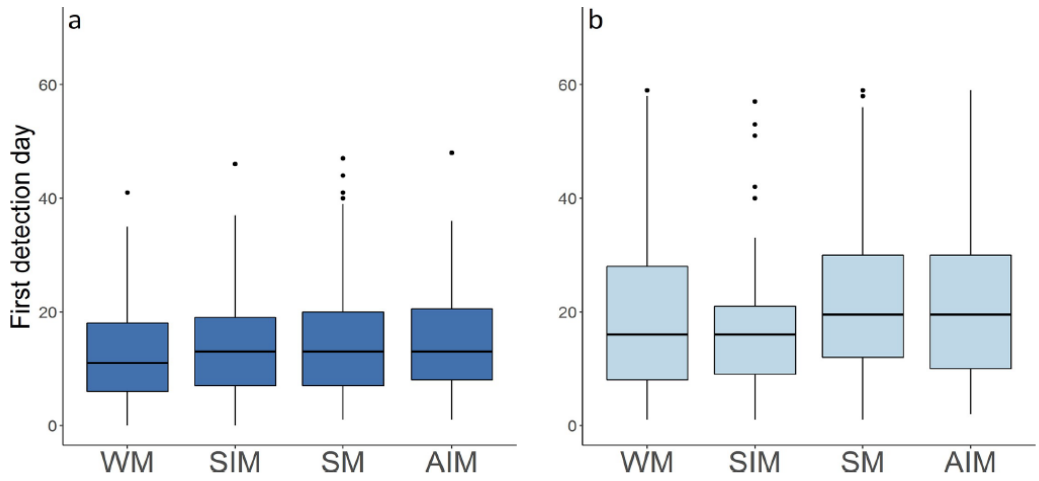

Figure 5.2.9. Boxplot of first detection day to the object of (a) tuna and (b) non-tuna species by monsoon period. WM= Winter monsoon, SIM = Spring intermonsoon, SM = Summer monsoon and AIM = Autumn intermonsoon.

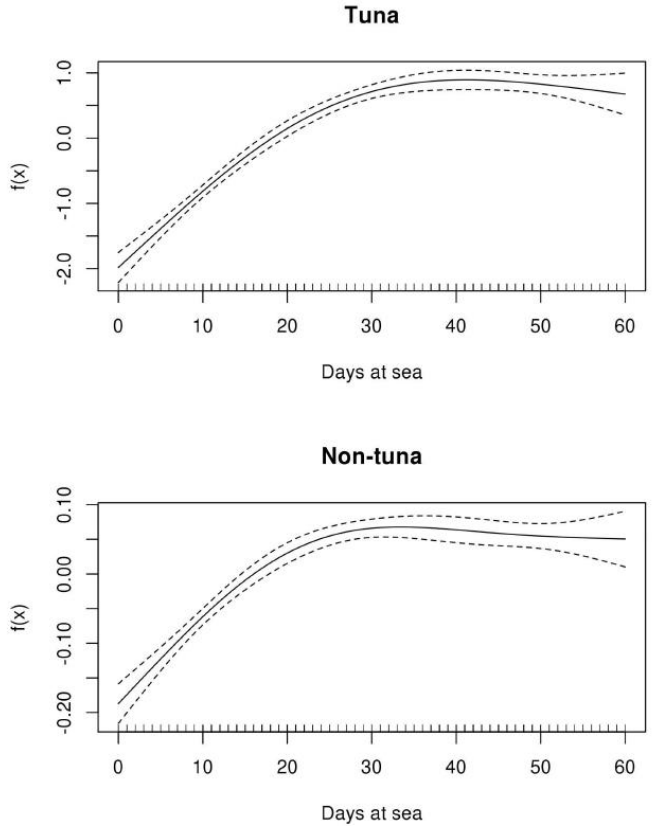

Figure 5.2.10. Functional shapes of the non-parametric relationship between biomass and days at sea with 95% confidence intervals (dashed lines), for tuna and non-tuna species

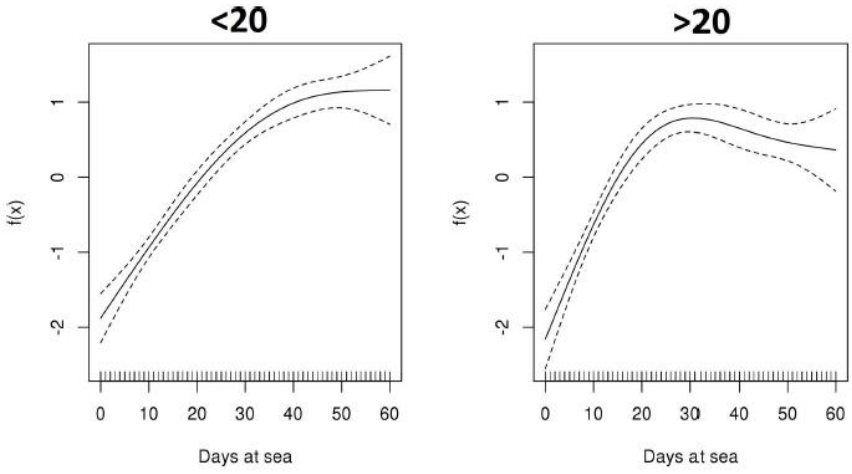

Figure 5.2.11. Functional shapes of the non-parametric relationship between tuna biomass and days at sea with 95% confidence intervals (dashed lines), according to the depth category of the object.

Figure 5.2.12 shows a clear tuna biomass increase in all periods. Although there is not a great difference in the aggregation process by areas within a specific monsoon season, especially during the summer monsoon and autumn intermonsoon, the biomass aggregation process in the SE Seychelles area is slightly different during the winter monsoon and spring intermonsoon. In these seasons, a continuous increasing trend is observed during the first month followed by a strong decrease from day 30 onwards in SE Seychelles. In the same area, from day 40 onwards while there is a small decrease during the winter monsoon, it stabilized during the autumn intermonsoon. In the case of Somalia and NW Seychelles, biomass trends are quite similar, with the exception of the spring intermonsoon, where NW Seychelles has a continuous increase while we find a biomass peak (i.e., day 25) in Somalia.

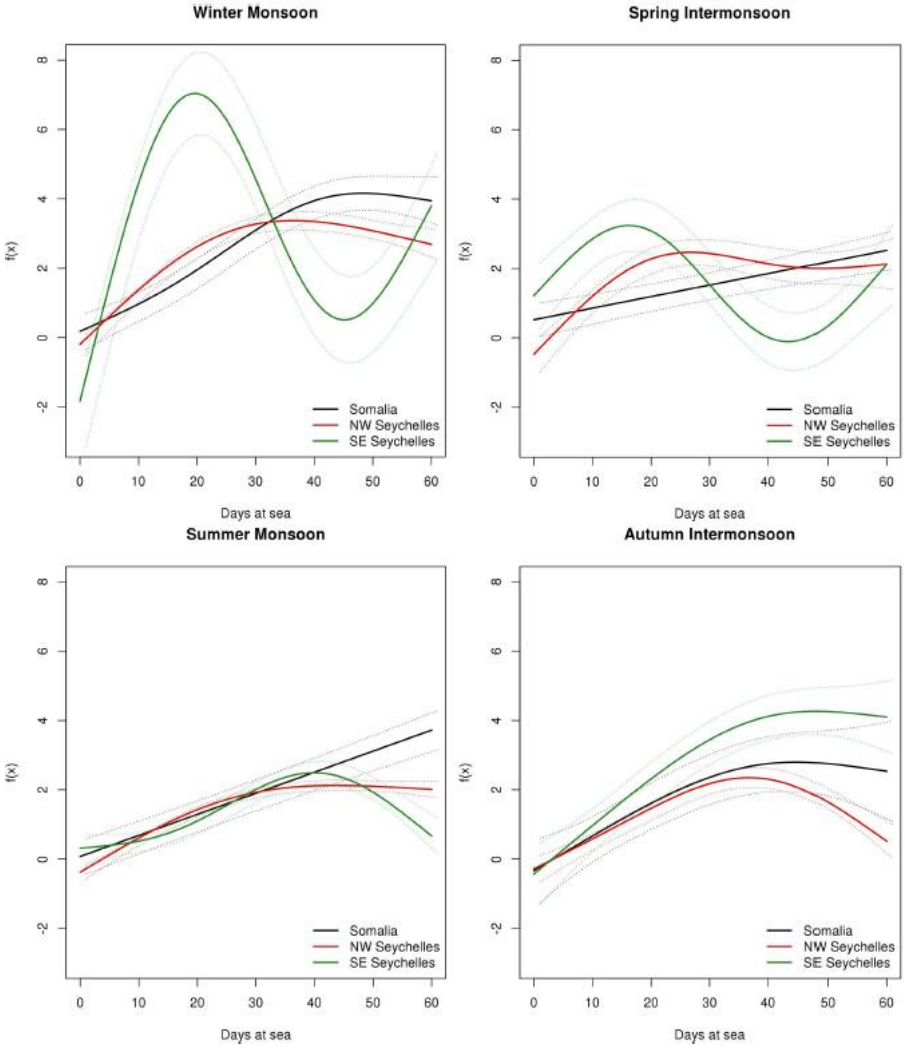

Figure 5.2.12. Functional shapes of the non-parametric relationship between tuna biomass and days at sea with 95% confidence intervals (dashed lines), for each period considered.

In addition, the biomass trend shows a small decrease in the Somalia area after the first month in all periods. In the case of NW Seychelles, a stabilization around day 40 is shown from October to March, while from April to September it shows an increasing trend during the 60 days.

For non-tuna species (**Figure 5.2.13**), models also shown an increasing biomass trend over the 60 days but one that is much smoother than in for tuna biomass estimates. In this case, SE Seychelles also shows the most different biomass aggregation trend than all other regions, with a biomass peak at 25 days during the winter monsoon. Somalia and NW Seychelles models show a constant linear increasing trend.

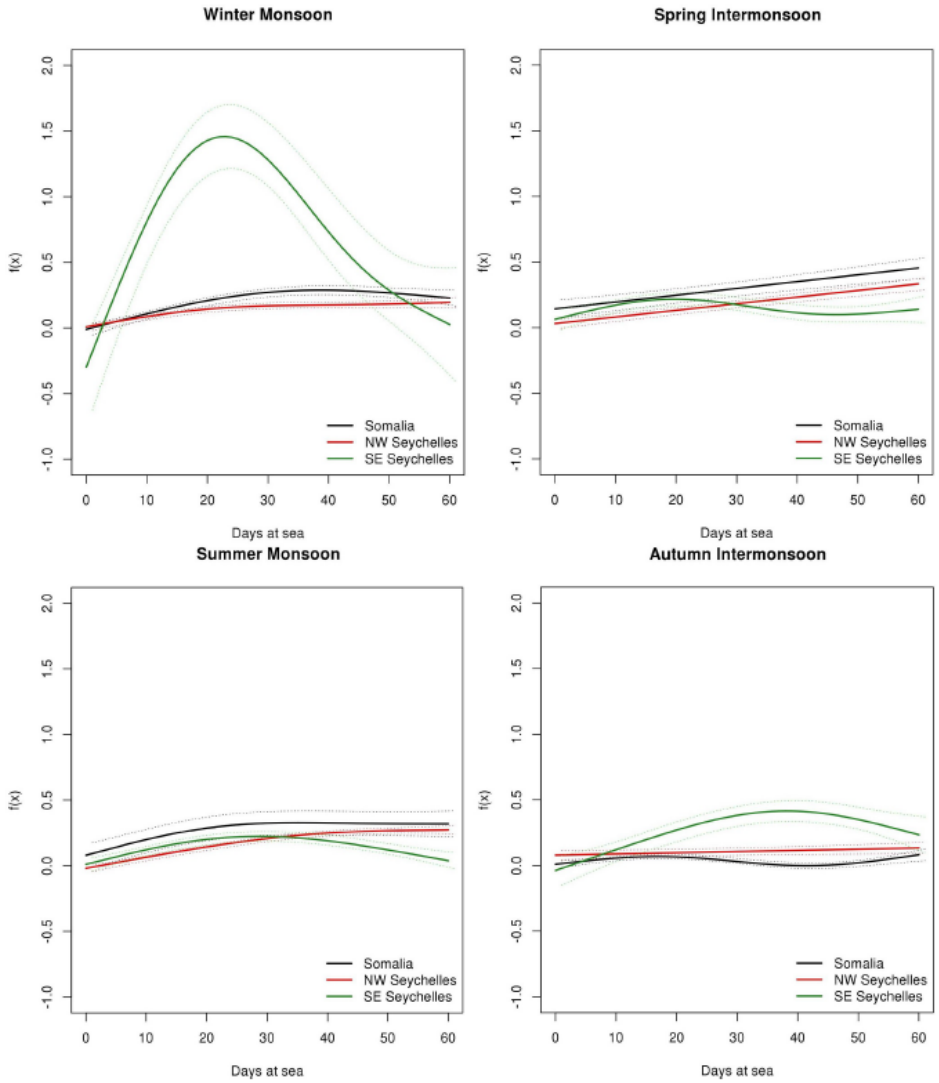

Figure 5.2.13. Functional shapes of the non-parametric relationship between non-tuna biomass and days at sea with 95% confidence intervals (dashed lines), for each period considered.

This study, using SATLINK buoys[13], contributes to a much better understanding of tuna and non-tuna aggregation mechanisms in relation to both dFAD structure and deployment seasons. In summary, the first detection day of fish at dFADs was approximately 1–2 weeks, but this differed significantly between tuna and non-tuna species. Although fishers consider that deeper dFADs may favor faster and larger fish aggregations (Murua et al., 2016), this aspect has never been investigated in detail in relation to the aggregation processes. The analysis showed a significant relationship between object depth and colonization of tuna, suggesting faster tuna colonization for deeper objects. For non-tuna species this relationship appeared not to be significant.

The Indian Ocean is characterized by strong environmental fluctuations associated with monsoon regimes and seasonal variability in fishing grounds and catch. Therefore, analyzing the aggregation process in different periods could help with designing spatio-temporal management measures for tuna fisheries. Within this project we found that aggregation dynamics differed between monsoon periods in both tuna and non-tuna species. These differences could be explained by changes in the biophysical environment associated with seasonality. However, social factors may also affect the aggregation process of tuna and non-tuna species at dFADs, such as the density and abundance of the local tuna population or dFADs. These research results will assist in working towards the sustainability of tuna fisheries, and may help to design optimal management measures for tuna and non-tuna species.

Similarly, the approaches developed by Baidai et al. (2018) were applied by IRD to analyze the colonization phase of tunas at dFADs, considering a subset of 393 dFADs newly deployed by the French fleet in the Atlantic Ocean from 2013 to 2018 (Baidai et al., 2019). The study focused on acoustic data collected on dFADs by the M3I buoy model. This approach is based on a preliminary processing of the acoustic data recorded during a full day (24 hours) of sampling, followed by a classification based on the random forest algorithm. Preliminary data processing consists of clustering the acoustic data sampled by the buoy over 6 temporal bins of 4-hours and 6 aggregated-depth layers, which summarize the daily acoustic information into a 6 × 6 matrix referred to as "daily acoustic matrix". The classification of tuna presence/absence was then carried out on a daily basis, using random forest algorithms trained from acoustic data recorded on dFAD deployments and visits without fishing sets (labelled as 'tuna absence') and positive fishing sets (labelled as 'tuna presence'). The strong performance in characterizing aggregations under dFADs (with overall accuracy of 75 and 85 %

[13] It should be also taken in mind that these results may be dependent on the buoy model used, as the estimates could vary depending on buoy model sensitivity given by the echosounder specifications.

respectively in the Atlantic and Indian Ocean, see Baidai et al., 2018), supported the use of this classification method.

Finally, a post-processing step to improve the predictions made by the classification models on the dFAD trajectories was applied. To this purpose, short-term predictions (isolated single days of presence or absence) were considered unlikely, were attributed to misclassification and corrected with the previous or next prediction value. This stage allowed the revision of 7.46 % of the initial predictions made by the classification model.

In the literature focused on FADs, Continuous Residence Time (CRT) is commonly referred to as the duration of residency of tagged tuna individuals at dFADs without day scale (>24h) absences (Ohta and Kakuma 2005, Capello et al. 2015). This metric was adapted at the scale of the aggregation to assess the residence times of tuna aggregations at dFADs. Accordingly, we considered aggregated Continuous Residence Time (aCRT) as the time during which tuna aggregations are continuously detected at the dFAD without day scale (>24h) absence. In a similar way, we also considered aggregated Continuous Absence Time (aCAT) as the continuous period of time that a dFAD spends without a tuna aggregation (**Error! Reference source not found.**). Values located immediately at the start (corresponding to colonization times) and the end of the trajectories (potentially truncated by the activity on the dFAD or the buoy), were excluded from the analysis. A total of 1130 aCATs and 1234 aCRTs were measured along the trajectories of the newly deployed dFADs

The average colonization time of a dFAD by tuna in the Atlantic Ocean was estimated at 20.5 days (SD 13.79). This metric was not sensitive to deployment locations of dFADs, as shown by the very close average values of colonization time between the Guinean current coast (GUIN) and the Eastern Tropical Atlantic (ETRA) provinces (mean 19.7 days, SD 15.2 and mean 21.05 days, SD 14.72, respectively; **Table 5.2.8**). In comparison, dFADs deployed from March to September were characterized by the lowest values of colonization time (mean 18.35 days, SD 14.97 and mean 18 days, SD 12.79 days, respectively for March-May and June-September seasons; **Table 5.2.9**). These values increase for dFADs deployed from October to December (mean 24.47 days SD 16.17 days) and peak during the January-February season (mean 31.14 days SD 24.94 days).

Deployment locations	Colonization time	aCAT	aCRT	Proportion of occupation time
ETRA	21.05 (14.72)	7.11 (8.67)	9.32 (13.01)	57.28 (22.95)
GUIN	19.65 (15.15)	8.26 (11.09)	8.86 (14.12)	51.32 (23.75)

Table 5.2.8. Mean and standard deviation (into brackets) of aggregation metrics per deployment locations (ETRA: Eastern Tropical Atlantic; GUIN: Guinean Current Coast).

Deployment seasons	Colonization time	aCAT	aCRT	Proportion of occupation time
Jan-Fev	31.14 (24.94)	9.68 (12.14)	7.11 (10.89)	42.48 (23.52)
Mar-May	18.35 (14.97)	6.17 (6.92)	12.36 (17.26)	64.06 (21.58)
Jun-Sept	18 (12.79)	7.94 (10.28)	7.47 (9.41)	54.28 (22.23)
Oct-Dec	24.47 (16.17)	5.56 (6.15)	8.65 (9.95)	60.19 (20.72)

Table 5.2.9. Mean and standard deviation (into brackets) of aggregation metrics per deployment seasons Deployment seasons

The results also revealed, for the first time, that the residence time of a tuna aggregation around a single dFAD is about 9 days and that dFADs spend on average 7 days without tuna. Thus, dFADs appear to be occupied by tuna aggregation about 50 % of their soaking time. These metrics can be affected by seasonal variations.

5.2.4 Sub-task 2.3. Modelling approach to derive direct indices of abundance at different intermediate spatial scales from local to regional scales depending on the needs

Echosounder buoys inform fishers remotely in real-time about the accurate geolocation of the dFAD and the presence and abundance of fish aggregations underneath them. Apart from its unquestionable impact in the conception of a reliable CPUE index from the tropical PS tuna fisheries fishing on dFADs, echosounder buoys also have the potential of being a privileged observation platform to evaluate abundances of tunas and accompanying species using catch-independent data. Current echosounder buoys provide a single acoustic value without discriminating species or size composition of the fish underneath the dFAD. Therefore, it has been necessary to combine the echosounder buoys data with fishery data, species composition and average size, to obtain a specific indicator of fish biomass. This work presents a novel index of abundance of juvenile YFT in the Atlantic Ocean and Indian Ocean, derived from echosounder buoys.

Acoustic data, provided by the company Satlink and Spanish fishing companies belonging to ANABAC and OPAGAC, cover the period from January 2010 to December 2018 in the Atlantic and Indian Oceans. Buoys are equipped with a sounder, which operates at a frequency of 190.5 kHz with a power of 100 W. The range extends from 3 to 115 m, with a transducer blanking zone running from 0 to 3 m. At an angle of 32°, the cone of observation under the buoy has a diameter of 78.6 m at a depth of 115 m. The echosounder provides acoustic information in 10 different vertical layers, each with a resolution of 11.2 m. During the period analyzed, three different buoy models have been used by the fleet: DS+, DSL+

and ISL+. These three buoy models work with a similar beam angle, frequency and power, and with the (above discussed) vertical stratification. DSL+ and DS+ obtain three acoustic records per day (before dawn, at dawn and after dawn) in the default mode. ISL+ has the capacity to sample throughout the day every 15 minutes, transmitting the signal if the value recorded for a 24 hours period is larger than the previous record.

The information on buoy position and acoustic information is received in two different data-sets with the following fields:

Data-set on buoy positions

Date: Date of the last position of the day

Time: Hour (GMT)

Buoy code: Unique identification number of the buoy, given by the model code (D+, DS+, DL+, DSL+, ISL+, ISD+ followed by 5-6 digits.

Latitude: Latitude of the last position of the day (in decimals)

Longitude: Longitude of the last position of the day (in decimals)

Velocity: v calculated from the distance/time between the last position of the day and the last position of the previous day.

Notes: Empty column

Data-set on acoustic records

Name: Unique identification number of the buoy, given by the model code (D+, DS+, DL+, DSL+, ISL+, ISD+ followed by 5-6 digits.

OwnerName: Name of the buoy owner assigned to a unique PS vessel

MD: Message descriptor (160, 161 and 162 for position data, without sounder data, and 163, 168, 169 and 174 for sounder data)

StoredTime: Date (dd/mm/yyyy) and hour (H:MM) of the echosounder record

Latitude, Longitude: Not provided (this information is provided in the position data-set)

Bat: Not provided. (Charge level (in percentage). Except for the D+ and DS+ in voltage)

Temp: Temperature (Not provided)

Speed: Speed in knots (Not provided)

Drift: bearing in degrees (Not provided)

Layer1 - Layer10: Depth observation range extends from 3 to 115 m, which is split in ten homogeneous layers, each with a resolution of 11.2 m. The buoy has also a blanking zone (a data exclusion zone to eliminate the near-field effect of the transducer between 0 and 3 m). Thirty two pings are sent from the

transducer and an average of the backscattered acoustic response is computed and stored in the memory of the buoy. The manufacturers method converts raw acoustic backscatter into biomass in tons, using a depth layer echo-integration procedure structured exclusively on an algorithm based on the TS and weight of SKJ.

Sum: Sum of the biomass estimated at each layer

Max: Maximum biomass estimated at any layer

Mag1, Mag3, Mag5 and Mag7: Magnitudes corresponding to the counts of detected targets according to the TS of the detection peak.

To calculate the biomass aggregated under a dFAD from the acoustic signal, the method discussed in sub-task 2.1. and in Santiago (2019a, b) was applied. Following that, a data cleaning process was then applied which included the removal of records without acoustic information (records with only position, speed and velocity), outliers (invalid, impossible or extreme values) related to bad geolocation, time, or other general variables. In addition to the 'regular' exclusions due to these types of inconsistencies, the following considerations were also taken into account for accepting the data for the standardization analysis:

Vertical boundary between tuna and non-tuna species: acoustic information from the shallower layers, <25m, was not considered for the analysis. According to Lopez et al. (2017) and Robert et al. (2013), the vertical boundary between non-tuna species and tunas can be considered at about 25 m. Excluding the first layers, we try to eliminate noise from the non-tuna species associated with the FAD.

Bottom depth: Using high resolution bathymetry data (British Oceanographic Data Centre, UK, www.gebco.net), acoustic records from buoys located in areas with a bottom depth shallower than 200 m were excluded. The rational of this exclusion is to not incorporate acoustic records of dFADs that have drifted to coastal areas where tuna are less likely to be present.

Acoustic measurements at sea: Buoys are normally turned on before deployment, so some records may correspond to onboard buoys. To deal with this issue we developed a random forest model (see Orue et al., 2019a; Task 1.1) to classify the buoys both at sea and onboard, using information from Zunibal buoys. Zunibal buoys have the capability to identify between positions at sea or onboard, using a conductivity sensor. The sensor measures the current between two electrodes, and then through a simple algorithm determines whether the buoy is sitting in the water or not (i.e., onboard). Records classified as onboard were excluded.

Time of the day: Only those samples obtained around sunrise, between 4 a.m. and 8 a.m., were considered for the analysis. These samples are supposed to capture the echosounder biomass signals that better represent the abundance of fish under the dFADs, as this is the time when tuna is observed to be more closely aggregated around the dFADs (Brill et al., 1999; Josse et al., 1998; Moreno et al., 2007). For the specific case of comparing the acoustic data with abundance it is important that the echosounder measurements are received

when the signal is more representative of the biomass around the dFAD model (Orue et al., 2019a).

Days since deployment: The objective of this selection criteria was to consider those acoustic records that were more likely associated within the dFAD trajectory, termed "virgin segments". A virgin segment is defined as the segment of a buoy trajectory whose associated dFAD likely represents a new deployment which has been potentially colonized by tuna and not already fished. Orue et al. (2019b) concluded that tuna seemed to arrive at dFADs in 13.5 ± 8.4 days and, thus, we consider as virgin segments (i.e., when tuna has aggregated to a dFAD) those segments of trajectories from 20-35 days at sea. In order to identify and separate those segments and their acoustic samples, the overall trajectories of the entire life-time of each buoy were fractioned in smaller sequences, corresponding to periods where they could have been attached to different FADs. A new sequence of a buoy was considered to occur, and hence an attachment to a new FAD, when the difference between two consecutive observations of the same buoy was larger than 30 days. Each sequence was assigned with a "new trajectory code" that included the code of the buoy plus the consecutive number of the sequence of each buoy. A deployment/redeployment of a buoy was considered to occur when the "new trajectory code" appears for the first time in the database. Sequences with less than 30 observations were excluded from the analysis. Sequences having a time difference between any of the consecutive observations longer than 4 days during the first 35 days were also excluded.

Detection threshold: Acoustic records equal or less than 0.1 tons were considered zeros. This is a conservative preliminary value as further validation is needed to confirm this estimate.

The estimator of abundance BAI was defined as the 0.9 quantile of the integrated acoustic energy observations in each of the "virgin" sequences. A high quantile was chosen because large values are considered to be likely produced by tuna (as opposed to plankton or bycatch species). In this case we selected a high quantile instead of the maximum to try to provide a more robust estimator by avoiding eventual outlier values. Covariates included year-quarter (yyqq), and 5º*5º areas, fitted as categorical variables. Other variables were velocity of the buoy, dFAD densities and a set of environmental variables. These environmental variables were chosen for their potential effect on the horizontal-vertical distribution of tuna and their association to dFADs (i.e., dFAD density, mixed layer height, sea surface temperature, chlorophyll concentration and detected fronts in sea surface temperature and chlorophyll daily datasets, computed using the Belkin and O'Reilly method), or echosounder measurement quality (buoy velocity). These environmental variables were incorporated in the model as continuous variables. A proxy of 1º*1º and monthly dFAD densities were calculated as the average number of buoys over each month. This calculation was the summing of the total number of active buoys recorded per day over the entire month, divided by the total number of days within that month.

The environmental variables evaluated in the model were:

Ocean mixed layer thickness[14]: defined as the depth where the density increase compared to density at 10 m depth corresponds to a temperature decrease of 0.2°C in local surface conditions (θ10m, S10m, P0= 0 db, surface pressure).

Chlorophyll[15]: Mass concentration of Chl-a in sea water (depth = 0).

Sea Surface Temperature (SST)[16]:

SST and Chl-a fronts: Oceanographic front detection was performed using the "grec" package for R for each daily dataset, that provides algorithms for detection of spatial patterns from oceanographic data using image processing methods based on Gradient Recognition (Belkin & O'Reilly, 2009).

The model we propose is based in an assumption very similar to the fundamental relationship among CPUE and abundance widely used in quantitative fisheries analysis. In our case we built the index based on the assumption that the signal from the echosounder is proportional to the abundance of fish.

$$BAI_t = \varphi \, . B_t$$

where BAIt is the Buoy-derived Abundance Index and Bt is the abundance in time t (Santiago et al., 2016).

It is assumed that acoustic echo-integration is a linear process, i.e., proportional to the number of targets (Simmonds & MacLennan, 2005) and has been experimentally proven to be correct with some limitations (Røttingen, 1976). Therefore, acoustic data (echo-integration) is commonly taken as an estimator of abundance, and is applied to provide acoustic estimation of the abundance of many pelagic species (e.g., Hampton, 1996). So, does large biomass indicated by acoustic data consistently result in large catches when sets follow soon after? A recent study has found a positive significant correlation between echosounder

[14] Source: Copernicus Marine Environment Monitoring Service (http://marine.copernicus.eu); Product: GLOBAL_REANALYSIS_PHY_001_030; Update frequency: Yearly; Available time series: 04/12/1992 to 27/12/2018; Temporal resolution: daily mean; Horizontal resolution: 1/12 ° (equirectangular grid); Units: [m]

[15] Source: Copernicus Marine Environment Monitoring Service (http://marine.copernicus.eu); Product: GLOBAL_REANALYSIS_BIO_001_029; Available time series: 1993/01/01 up to 2018/12/31; Temporal resolution: daily mean; Horizontal resolution: 1/4 ° (equirectangular grid); Units: [mg.m-3]

[16] Source: Multi-scale Ultra-High-Resolution Sea Surface Temperature (https://mur.jpl.nasa.gov); Product: JPL_OUROCEAN-L4UHfnd-GLOB-G1SST; Available time series: 2010/01/01 up to present; Target delivery time: daily; Temporal resolution: daily mean; Horizontal resolution: Regular 0.01-degree grid; Units: Kelvin degrees.

acoustic energy and catches of tropical tuna around dFADs (Moreno, et al., 2019). The study was based on data collected in two surveys conducted onboard commercial PSs during regular fishing activity in the Atlantic and Pacific Oceans in the years 2014 and 2016. Simrad EK60 echosounders with split beam transducers at 38, 120 and 200 kHz were used to collect acoustic data. Generalized linear models were run between acoustic backscattering energy (NASC, Maclennan et al., 2002) and catches of the three main tuna species found on dFADs (SKJ, BET, YFT) providing positive significant relationships with total catches (in weight) as well as catches for each tuna species.

As with the catchability, in order to ensure that the coefficient of proportionality φ can be assumed to be constant (i.e., to control the effects other than those caused by changes in the abundance of the population) a standardization analysis should be performed aiming to remove factors other than changes in abundance of the population. This can be performed by standardizing nominal measurements of the echosounders using a GLMM approach. Considering the low proportion of zero values, the delta lognormal approach (Lo et al., 1992) was not considered. GLMM (log-normal error structured model) was applied to standardize the acoustic observations. A stepwise regression was applied to the model with all the explanatory variables and interactions in order to determine those that significantly contributed to explain the deviance of the model. For this, deviance analysis tables were created for the positive acoustic records. Final selection of explanatory factors was conditional to: a) the relative percentage of deviance explained by adding the factor in evaluation (normally factors that explained more than 5% were selected), and b) the Chi-square ($\chi 2$) significance test. Those factors that explained less than 5% of the variability of the model were not considered. Interactions of the temporal component (year-quarter) with the rest of the variables were also evaluated. If an interaction was statistically significant, it was then considered as a random interaction(s) within the final model (Maunder and Punt, 2004).

The selection of the final mixed model was based on the Akaike's Information Criterion (AIC), the Bayesian Information Criterion (BIC), and a Chi-square ($\chi 2$) test of the difference between the log-likelihood statistics of different model formulations. The year-quarter effect least square means (LSmeans) uses a weighted factor for the proportional observed margins in the input data, to account for the non-balance characteristics of the data. The LSMeans were bias-corrected for the logarithm transformation algorithms using Lo et al. (1992). All analyses were done using the lme4 package for R (Bates et al., 2015). In this analysis the biomass of YFT aggregated under a dFAD were obtained from the acoustic signal of the echosounder buoys. The aggregations of YFT associated with floating objects are mostly composed of small individuals (approximately 46cm FL). Therefore, the Buoy-derived Abundance Index (BAI) would represent an indicator of YFT juvenile, with the SL of 46cm corresponding to approximately 1 year of life.

The model in the Atlantic Ocean explained 39% of the total deviance, with the most significant explanatory factors being year-quarter, 5º*5º area, and the random interaction of year-quarter*area. No significant residual patterns were observed. The quarterly series of standardized BAI index shows a general decreasing trend at the beginning of the series, from 2010 to 2012; then a stabilization period at a low level from 2013 to 2015, followed by an increasing trend in 2017 and 2018 to levels of the beginning of the series (Figure 5.2.14). The CVs remain relatively stable (between 12-25%) during the whole time series. This index has been integrated for the first time in the Atlantic Ocean yellowfin assessment.

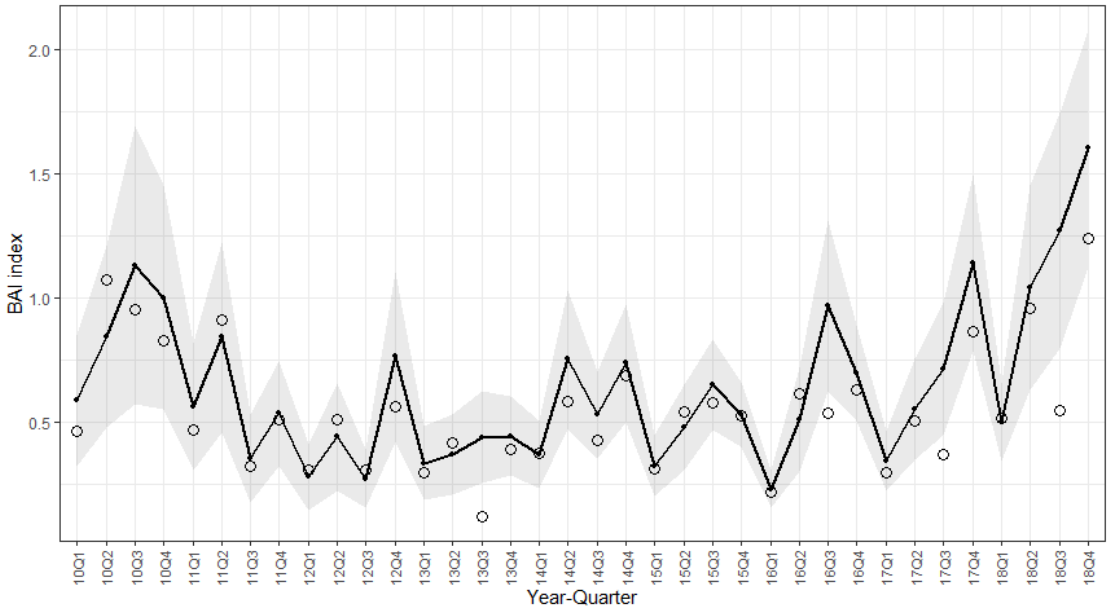

Figure 5.2.14. Time series of nominal (circles) and standardized (continuous line) Buoy-derived yellowfin juvenile abundance Index for the period 2010-2018. The 95% upper and lower confidence intervals of the standardized BAI index are shown.

In the case of the Indian Ocean, the model explained 24% of the total deviance, with the most significant explanatory factors being year-quarter, 5º*5º area and the ramdom interaction of year-quarter*area. No significant residual patterns were observed. The quarterly series of standardized BAI index shows that there is a relative stability over the period analyzed (**Figure 5.2.15**). However, three different stanzas can be clearly identified: a) an initial period, between the first quarter of 2010 and the third quarter of 2012, with an average BAI value of 2.67; b) a period of relatively higher values from the fourth quarter of 2012 to the fourth quarter of 2015 (BAI=4.22); and c) a final period of relatively lower values (BAI=1.88).

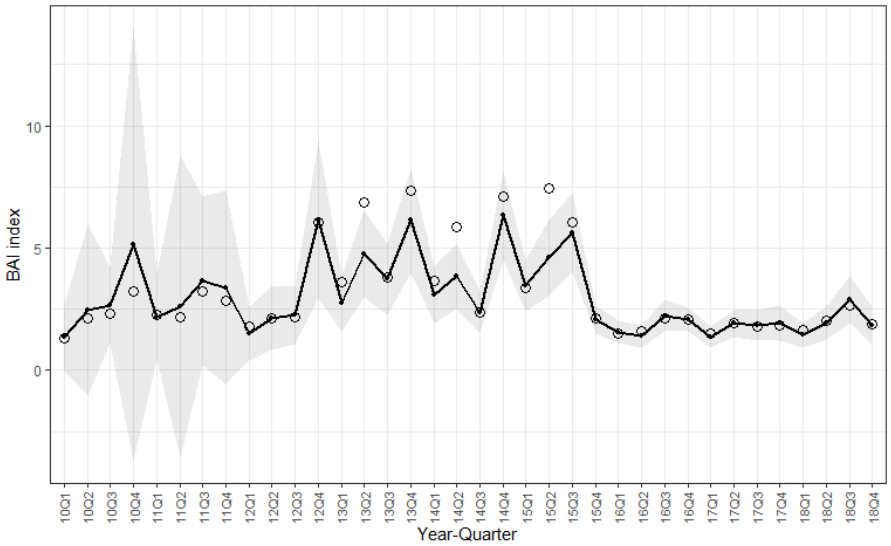

Figure 5.2.15. Time series of nominal (circles) and standardized (continuous line) Buoy-derived yellowfin juvenile Abundance Index for the period 2010-2018 in the Indian Ocean.

The 95% upper and lower confidence intervals of the standardized BAI index are shown (Figure 5.2.15). The first two periods showed a clear inter-quarter variability, while the later was relatively more stable. Coefficients of variation were higher at the beginning of the series (between 0.26 and 1.20 in 2010-2012), decreasing to values between 0.12 and 0.26 for the rest of the series.

5.2.5 Difficulties encountered, and future work expected

Work examining the accuracy of M3I buoy models (Baidai et al., 2018) demonstrated that, for this buoy model, current performances of the algorithms developed for assessing presence/absence of tuna are satisfactory, whereas the biomass estimates are weakly correlated with catches. As such, alternative approaches for the derivation of abundance indices, based on presence/absence data, are needed. Recent developments in this direction have recently been presented at ICCAT and IOTC (Baidai et al., 2019a, Baidai et al., 2019b). Indeed, the detection of tuna presence or absence under dFADs already offers unprecedented potential to understand aspects of the mechanisms underlying the dynamics of tuna aggregations under dFADs, as is the assessment of the colonization time, and factors influencing tuna aggregations or stability of the aggregations. This increased knowledge constitutes the first milestone towards the understanding of tuna dynamics underneath the dFADs.

To date echosounder buoys at sea provide a unique way of quantifying biomass values. When comparing it with the catch at the buoy, the relationship between the acoustic energy or the biomass estimated by the buoy is positive. However, the correlation between these factors was found to be low, and seems to be dependent on the set size. Also, other factors as environmental factors (i.e., sea surface temperature), area or season could be impacting the strength of this

relationship. Indeed, skipper follow the buoys and take decisions on fishing activities by monitoring the size of the aggregation underneath, while also taking into consideration buoy behavior between different regions. Therefore, we argue that the range of factors that may impact the relationship between estimated buoy biomass and the catch associated with the buoy should be further explored. In addition, the sampling unit of the set and data from the buoy may differ substantially and underlies the need for further sampling of both variables in future studies. Overall, further work should be conducted to evaluate the accuracy of biomass estimates by echosounder buoys. The catch data compiled in fishermen's logbooks constitute a broad source of information, which may provide a more consistent dataset than the observer database initially used in this work. We thus aim at exploiting this larger database in future analyses.

Buoys do not discriminate the species composition underneath the dFADs, as they provide a unique value. During this project, the species composition associated with the dFAD has been estimated using historical catch estimates by strata, which has been used to translate from total biomass underneath the dFAD to species specific biomass. This supposes that estimates of species composition are still vessel declaration dependent.

5.3. WP 3 – Impact of drifting FADs on the ecosystem

5.3.1. Objectives

In order to improve knowledge of the environmental impact of tropical tuna fisheries and develop ecosystem management measures accounting for ecosystem considerations, we explore here the impacts of dFAD fishing on protected and endangered species and vulnerable habitats, and the potential regulatory measures to reduce impacts. One of the major challenges faced by the tropical PS fishery is to reduce the impact of dFAD fishing on juveniles (i.e., FL < FL at 50% first maturity) of BET and YFT without substantial losses in terms of SKJ catch. For this reason, the effectiveness and feasibility of new potential time-area moratoriums on dFAD use will be explored and assessed in the context of the multispecies characteristic of the tropical tuna PS fishery.

5.3.2. Sub-task 3.1. Potential risks of FAD-fishing on protected and endangered species as well as on vulnerable habitats

Impact of dFAD fishing on sharks.

Special attention will be paid within this work to the potential impact of dFAD fishing on endangered species, especially a range of shark species. In this respect, the silky shark (Carcharhinus falciformis) has been considered as a priority in this project.

Silky shark analyses conducted on the French observer's database.

We first considered the number of silky sharks caught within a dFAD purse seine fishing set, based on the observers' data collected on-board French PSs. The distributions of the number of silky sharks caught per dFAD set were estimated on a monthly basis, both in the Atlantic (**Figure 5.3.1.**) and Indian oceans (**Figure 5.3.2.**). To this purpose, kernel densities of the number of reported sharks in each PS set for each ocean were estimated on a monthly basis. Statistical units were based upon these kernel densities, considering all data within the 95% quantile density contours.

This analysis revealed a contrasting picture between the two oceans: catches of silky sharks in the Atlantic Ocean appeared mostly localized around the Gabon and Angola coasts, in the Indian Ocean their distribution appeared more spread across all fishing regions (**Figure 5.3.3**).

Based on the analyzed data, we developed a novel approach to derive an abundance index for silky sharks, based on an empirical model that accounts for their association dynamics at dFADs (Diallo et al., 2018). The model parameters (probability of associating/departing from dFADs, dFAD density) were inferred from the distribution fits of silky sharks caught at dFADs and from observers' data reporting the number of random dFAD encounters in the study region. Using this data, a relative abundance index of silky sharks in the Indian Ocean was derived (Diallo et al., 2018).

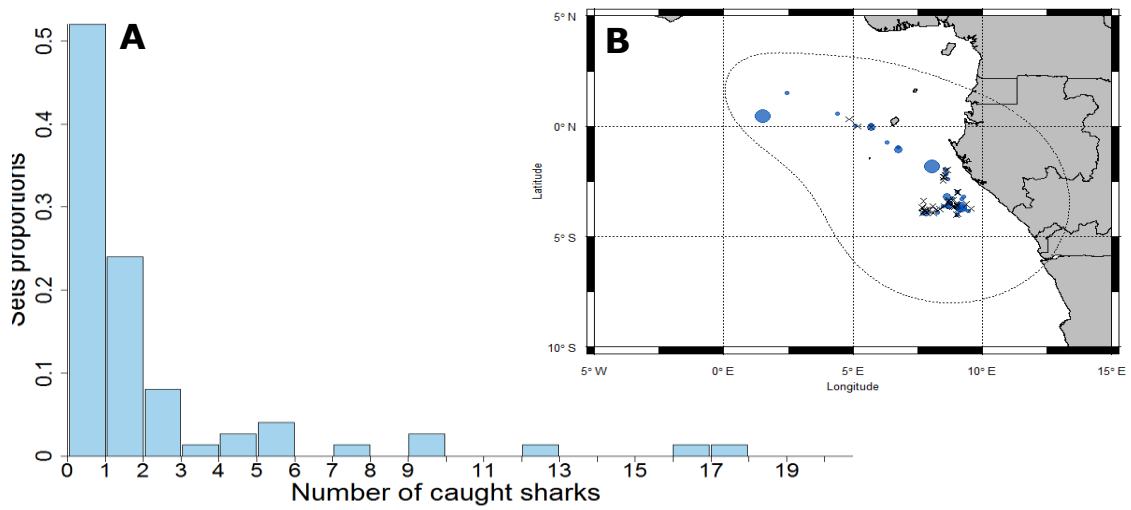

Figure 5.3.1. Example of observed sets for silky shark in the Atlantic Ocean. Panel A shows the catch events histogram of the observed sets off Gabon's coast in June 2016 presented in panel B. Crosses represent sets with no silky sharks and dots represent sets where sharks were caught (the size of the dot is proportional to the number of sharks individuals caught).

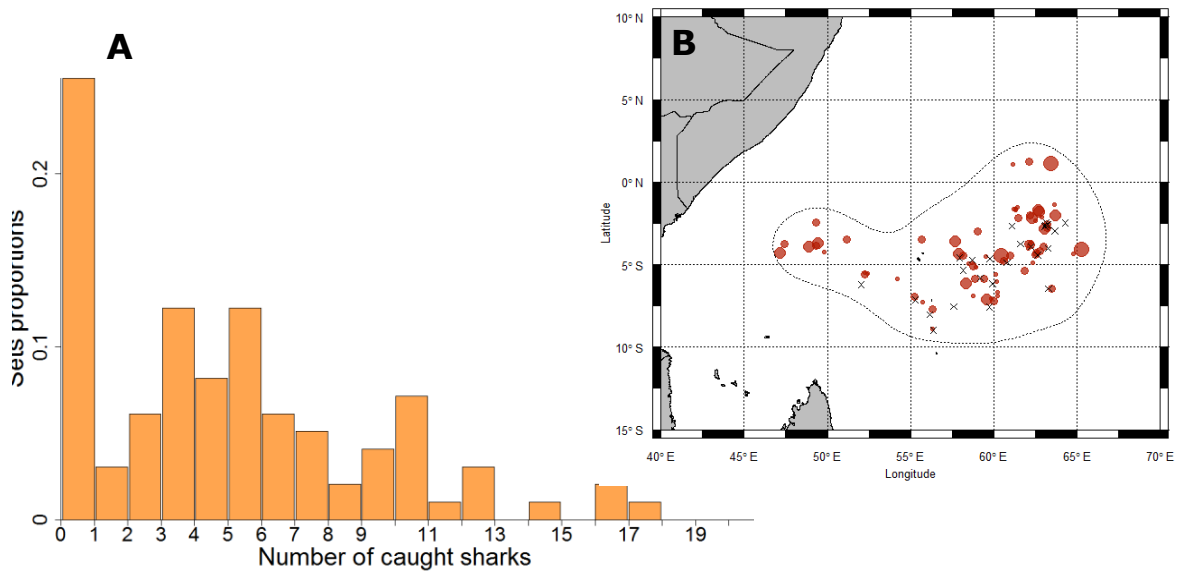

Figure 5.3.2. Example of observed sets for silky shark in the Indian Ocean. Panel A shows the catch events histogram of the observed sets off Somalia's coast in January 2016 presented in panel B. Crosses represent sets with no silky sharks and dots represent sets where sharks were caught (the size of the dot is proportional to the number of sharks individuals caught).

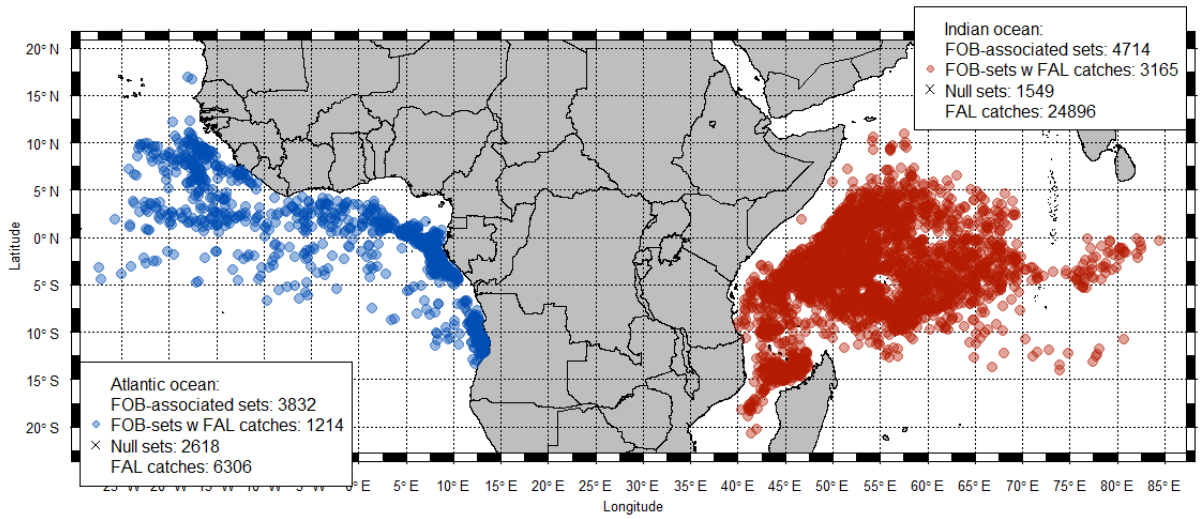

Figure 5.3.3. Distribution of silky shark catches of the French PSs between 2005 and 2017 in the Atlantic and Indian oceans.

Silky shark analyses conducted on the Spanish and French observer's database

An extended analysis focused on the derivation of an abundance index for silky sharks, as per Diallo et al. (2018), using a larger database, developed by Spanish and French observers' data (sourced from within a collaborative study involving IRD, IEO and AZTI). Compared to Diallo et al. (2018), twice as much data was available with a time series extending for more than a decade (**Figure 5.3.4.**). This study focused primarily on the Indian Ocean, between 2007 and 2018. From this work two study sites were chosen: Seychelles area and the Mozambique Channel (see **Figure 5.3.5.**).

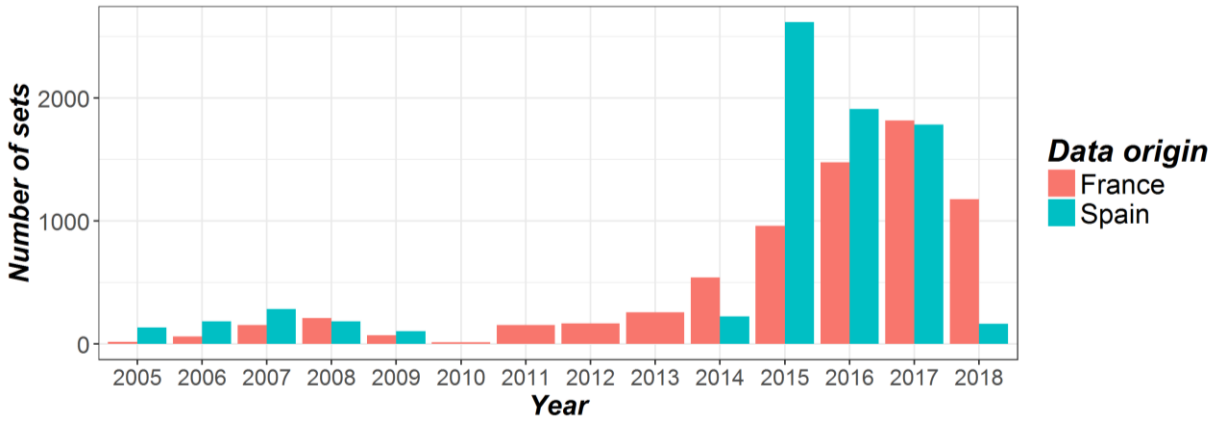

Figure 5.3.4. Histogram of the number of fishing sets realized by France and Spain in the observer's dataset.

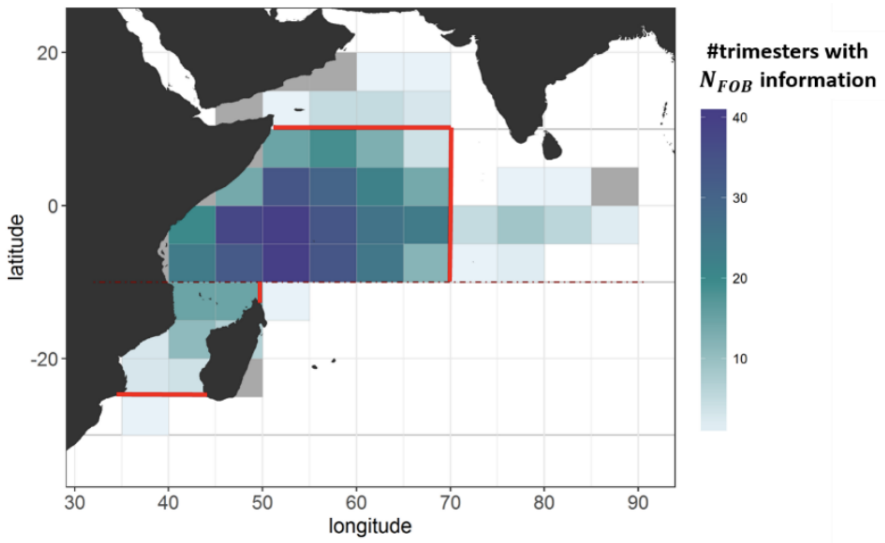

Figure 5.3.5. Delimitation of the study areas (red lines). Upper rectangle represents the Seychelles area and lower rectangle represents the Mozambique Channel area. The map also depicts the areas where the FOB-density index is available for the period of study.

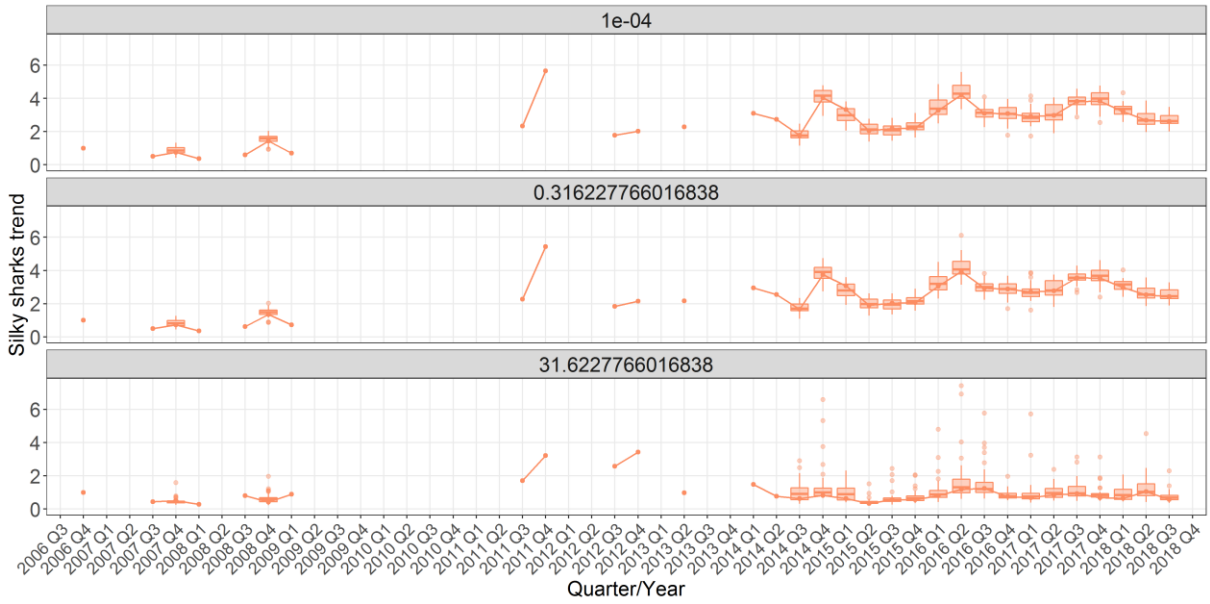

Figure 5.3.6. Silky shark abundance trend for the Seychelles area based on three different model scenarios characterized by different values for the parameter gamma (see Diallo et al., 2019). Boxplots represent index values derived from the bootstrapped samples.

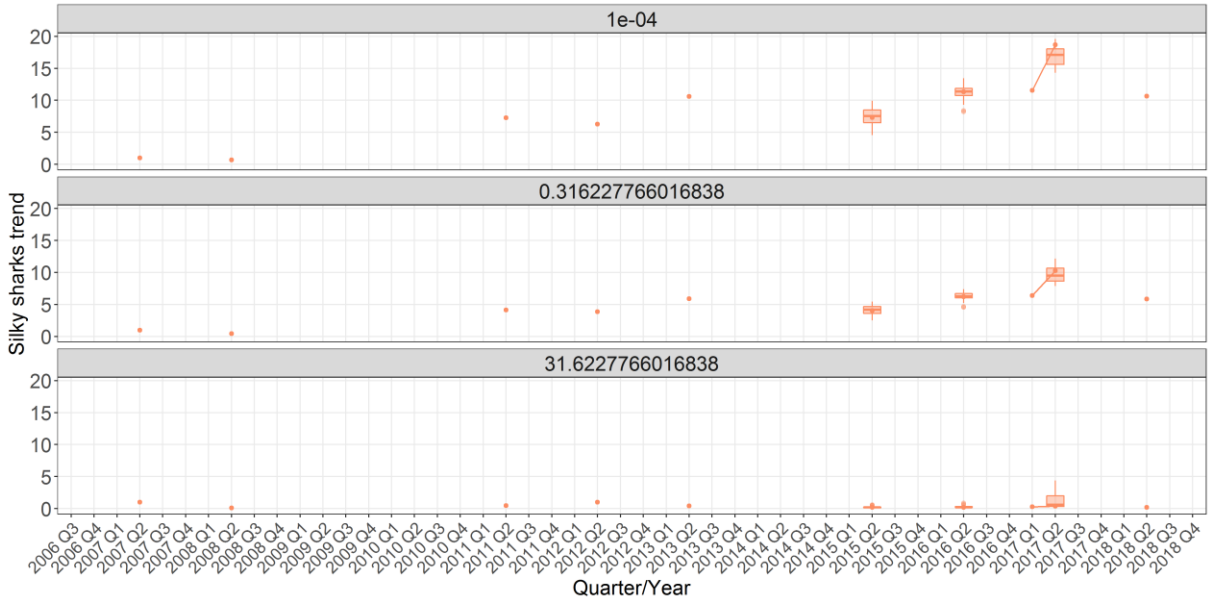

Figure 5.3.7. Silky shark abundance trend for the Mozambique Channel area based on three different model scenarios characterized by different values for the parameter gamma (see Diallo et al., 2019). Boxplots represent index values derived from the bootstrapped samples.

The fit to the distribution of the number of silky sharks caught at dFADs on a quarterly basis were then determined, in order to set the parameters of the empirical model and to derive the abundance index for silky sharks from the study regions (Diallo et al. 2019). As sample size varied significantly from one unit of time and space to another (**Figure 5.3.4.)**, bootstrap resampling was conducted in order to detect the effect of this sampling variability on the abundance index value.

The fitting analysis showed that a social model best described the experimental distributions (97% of cases, Diallo et al., 2019). A relative abundance index for silky sharks for each area/quarter was therefore derived, considering the first year as a reference year, with three different model scenarios developed (see **Figures 5.3.6.** and **5.3.7.**; Diallo et al. 2019).

The temporal series of the relative abundance indices globally (**Figures 5.3.6 and 5.3.7**) showed an increasing trend, with the magnitude of this increase depending on the region. Such an increase in shark abundance could be a result of a combination of factors that took place as from 2010 (e.g., introduction of non-entangling FADs, Chagos MPA, shift of fishing effort due to piracy, Maldivian shark fishing ban). It is important, though, to note that we are unaware of the state of silky shark population in the 2000ies, nor possess figures about the stock. Since we produced a relative abundance index, even with increasing trends, results should be taken with caution as we cannot conclude that they indicate a healthy population.

Impact of FAD-fishing on bony fishes and other marine species.

The impact analysis of a fishery or fishing method should cover many aspects of the marine ecosystem that are difficult to test. Finding changes in the biological community of an ecosystem may be one of the first signs of impact in the ecosystem impact studies. The fishing activity can reduce abundance, and alter the physiology and life history traits, which, in turn, affect the functional role of the species within the biological community. Fishing may also induce changes to open-ocean community trophodynamics, and reduce biodiversity and resilience in open-ocean ecosystems. The likelihood of ecosystem impacts occurring due to fishing is directly related to the fishing effort and is thus also expected to be increasing. Despite the increasing trends in fishing effort, ecological research into the impacts of fisheries on open-ocean environments has lagged behind coastal and deep-sea environments. The ecosystem-level impacts of fishing in offshore oceanic habitats are less well studied and inferences from studies of similar systems must pave the way for new research avenues (Ortuño & Dunn 2017).

Several hypotheses have been suggested to explain fish aggregation under floating objects, with many factors influencing fish behavior (Fonteneau, 1992; Hall, 1992; Kingsford, 1993). Amongst these factors, the most appealing are: fish congregate around dFADs looking for refuge from predators (Hunter and Mitchell, 1968; Feigenbaum et *al.,* 1989); fish may aggregate because more food is available under dFAD flotsam; the disturbance produced by the flotsam in the uniformity of the ocean may attract taxa (Hunter and Mitchell, 1968; Holland *et al.,* 1990). Assessing the impact of the PS fishery on the pelagic ecosystem is not an easy task. To undertake an assessment the total species involved or affected by this fishery must be understood, as well as understanding the structure and composition of the community before the fishery began. The main demographic

factors expected to be influenced by fishing are expected to be community diversity and abundance, as well as changes in the numerical dominance of certain species – the main objective of the current work was to test whether such factors were impacted by the present PS fishery associated with dFADs.

The methodology for data collection and processing is common to the Atlantic and Indian Oceans (Ariz et al, 2010), and involves three research organizations of the European Union: Research Institute for Development (IRD, France), Centro technological Marine and Food Research (AZTI-Tecnalia, Spain) and the Spanish Institute of Oceanography (IEO, Spain)[17].

A comparative analysis of biodiversity index, abundance, dominance curves and accumulation of species, throughout the study period was conducted[18]. The current analysis was restricted to the scientific Spanish Observer program on Spanish PS flagged vessels. On the information collected for each of the taxa, a descriptive analysis of each taxa, its abundance, the type of habitat available, the biology of the taxa, its distribution and any social behavior was examined. Bibliographic references of each taxa are provided in **Annex 4**, as well as the conservation status according to IUCN (2019), see **Annex 5**).

Habitat definitions used:

Coral reef fish or reef-associated: fish which live amongst or in close relation to coral reefs. Coral reefs form complex ecosystems with tremendous biodiversity.

Pelagic zone: of the open ocean, and can be further divided into regions by depth.

Epipelagic zone: From the surface down to around 200 m. This is the illuminated zone at the surface of the sea where enough light is available for photosynthesis.

Pelagic neritic zone is the relatively shallow part of the ocean above the drop-off of the, the neritic zone, also called coastal waters.

Pelagic oceanic zone: oceanic fish (also called Open Ocean or offshore fish) live in the waters that are not above the continental shelf.

Mesopelagic zone: From 200 m down to around 1000 m, also known as the middle pelagic or twilight zone, is the part of the pelagic zone that lies between the photic epipelagic and the aphotic bathypelagic zones.

Benthopelagic fish: fish that inhabit the water column just above the seabed, feeding on benthos and zooplankton. Most demersal fish are benthopelagic.

[17] Sample forms of the EU purse seiner observer program can be downloaded from the ICCAT website:
https://www.iccat.int/Documents/SCRS/Manual/CH4/Annex%201%20to%20Chapter%204.zip

[18] Clarke, K. R., Gorley, R. N. 2006. PRIMER v6: User Manual/Tutorial. PRIMER-E: Plymounth).

Demersal fish: fish that live and feed on or near the bottom of seas or lakes (demersal zone).

Bathypelagic zone: Below the mesopelagic zone it is pitch dark. This is the midnight or bathypelagic zone, extending from 1000 m to the bottom deep water benthic zone.

Catch and bycatch data from the PS observer program were extracted for dFADs sets and the period 1995 to 2018. In addition, biological information on each bony fish species recorded on a dFAD set by the observers is presented in an attached file (Excel file: "CECODFADII Checklist Habits Fauna Associated dFADs 2019 FINAL.xlsx").

With regards to the natural habitat of each taxa, the associated fauna may originate from a variety of habitats. Of the data collected, 27% of species were from "oceanic pelagic" habitats typical of this marine ecosystem, 38% of species were typical of a "reef-associated" habitat, while 17% of species were classed as "benthopelagic", with movements from the sea bed to the surface. A smaller proportion, 10%, were "pelagic coastal" species of neritic waters, while less than 5% of taxa were classified as bathypelagic, bathydemersal or "freshwater-brackish" species (**Figure 5.3.8**).

Information on social behavior is obtained based on the number of fish specimens observed during the dFADs set. Of these taxa, 54% appear alone (A), while 31% are taxa that swim in small groups (SG) and only 15% of the observed taxa swim forming large groups around the dFADs (BS), which include tuna and tuna like species (**Figure 5.3.9**).

The conservation status situation of each fish taxa according to the IUCN is presented. Of these taxa, 76% are in a low concern situation, 16% of taxa have not been evaluated, 4% of taxa lack data and only 4% of taxa are considered as vulnerable (**Figure 5.3.10**). The species that are deemed vulnerable were two billfish species within the family Istiophoridae (*Kajikia albida* and *Makaira nigricans*), bigeye tuna (family Scombridae) (*Thunnus obesus*), the sunfish (*Mola mola*), and two species from the family Balistidae (*Balistes punctatus* and *Balistes capriscus*) (**Figure 5.3.10**). The % composition of catches by number of specimens show that catches with one IUCN vulnerable specimen represent more than 60 % of the cases for billfish and mola mola, and more than 35 % for the balistid species (**Figure 5.3.11**).

Indices of abundance, richness and biodiversity of the community throughout the study period are presented (**Table 5.3.1**). The richness index ranged from a minimum of 1 species to a maximum of 16 species by set. The Margalef´s and Shannon´s biodiversity index ranged from 0.11 to a maximum of 3.6673 and 2.8842, respectively (**Table 5.3.1**).

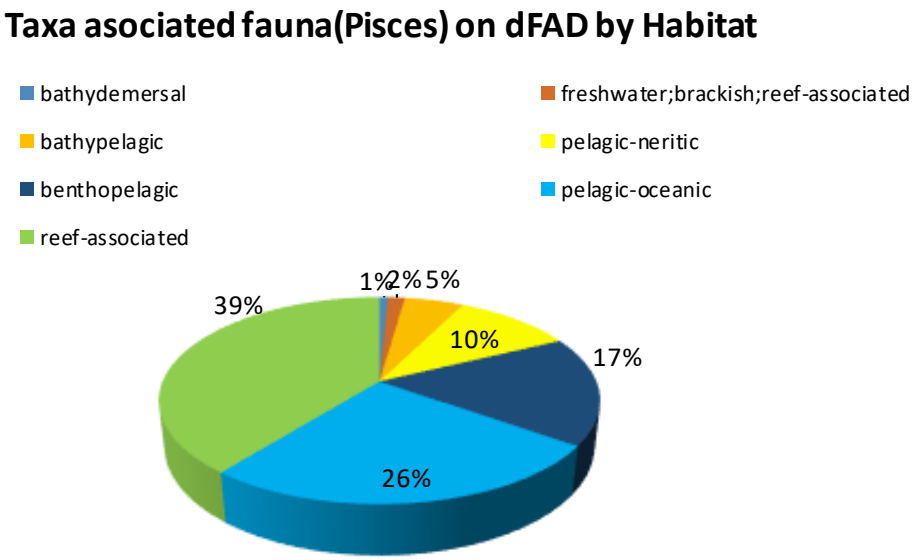

Figure 5.3.8 % relative of habitat of species cited under dFADs

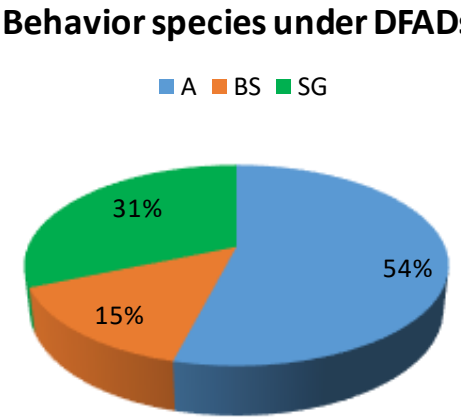

Figure 5.3.9. % relative by behavior of species cited under dFADs; A = alone; SG = Small Group; BS = large Group

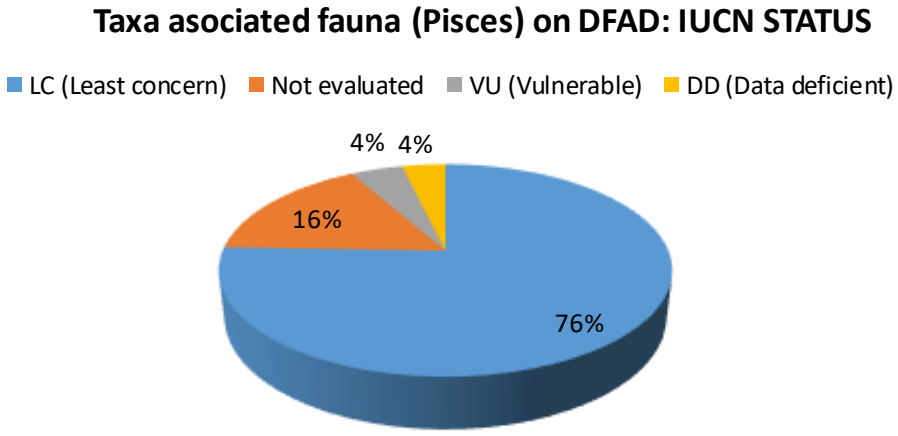

Figure 5.3.10. % relative of IUCN status of associated fish taxa under dFADs

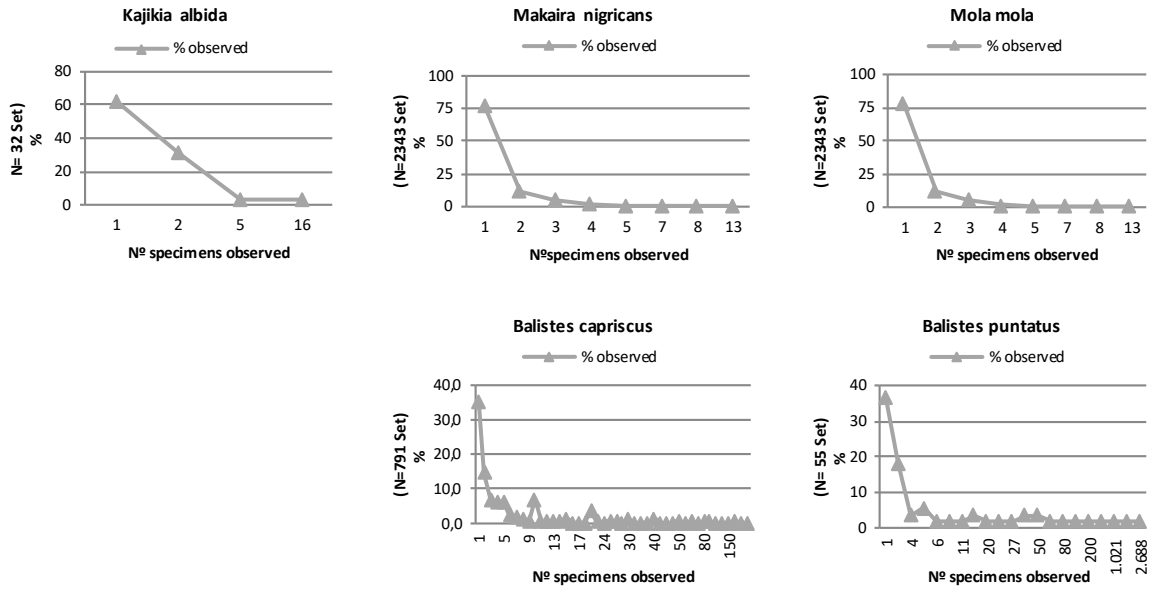

Figure 5.3.11. % occurrence of catches associated with dFAD fishing against the number of specimens caught in each catch of species termed vulnerable under IUCN status

Index	N	Media	Desv. típ.	Mín.	Máx.
N_abundance	7684	614,690	2089,877	1	65350
Species_richness	7684	5,080	2,403	1	16
Margalef's index	7110	1,029	0,465	0,115	3,667
H'_Shannon diversity	7110	1,002	0,458	0,112	2,884
Pielou's index_J'_Equitability	7110	0,625	0,228	0,112	1,000
Simpson diversity	7110	0,551	0,204	0,100	1,000

Table 5.3.1. Richness and biodiversity indices characterizing the associated bony fishes associated to dFADs

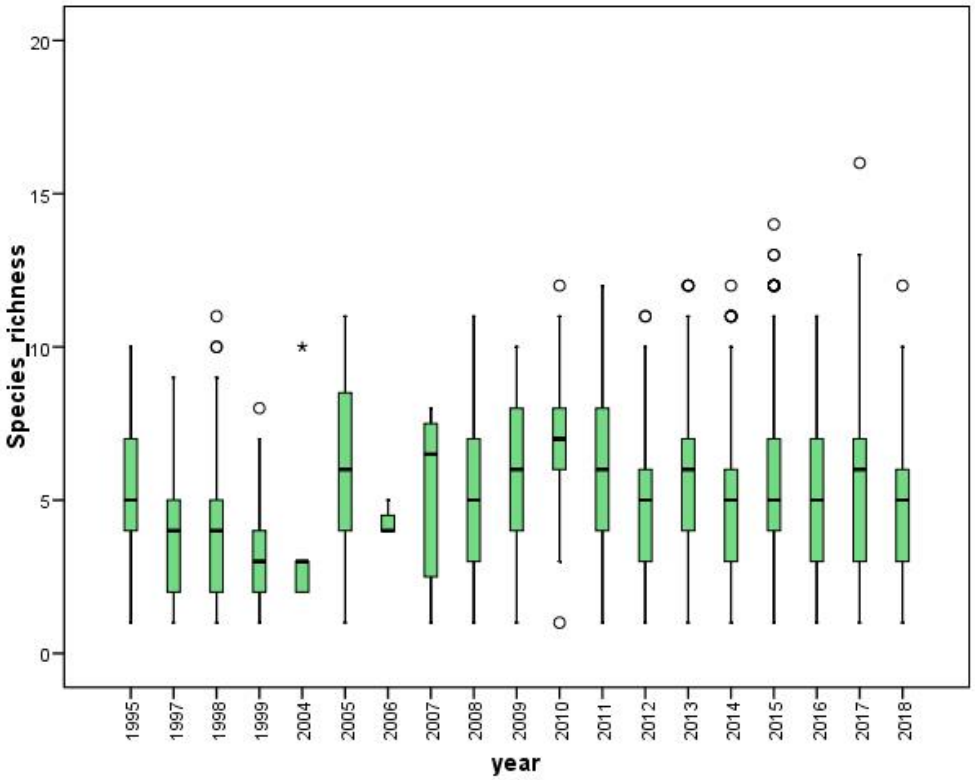

Figure 5.3.12. Richness index by year of fish associated under dFADs

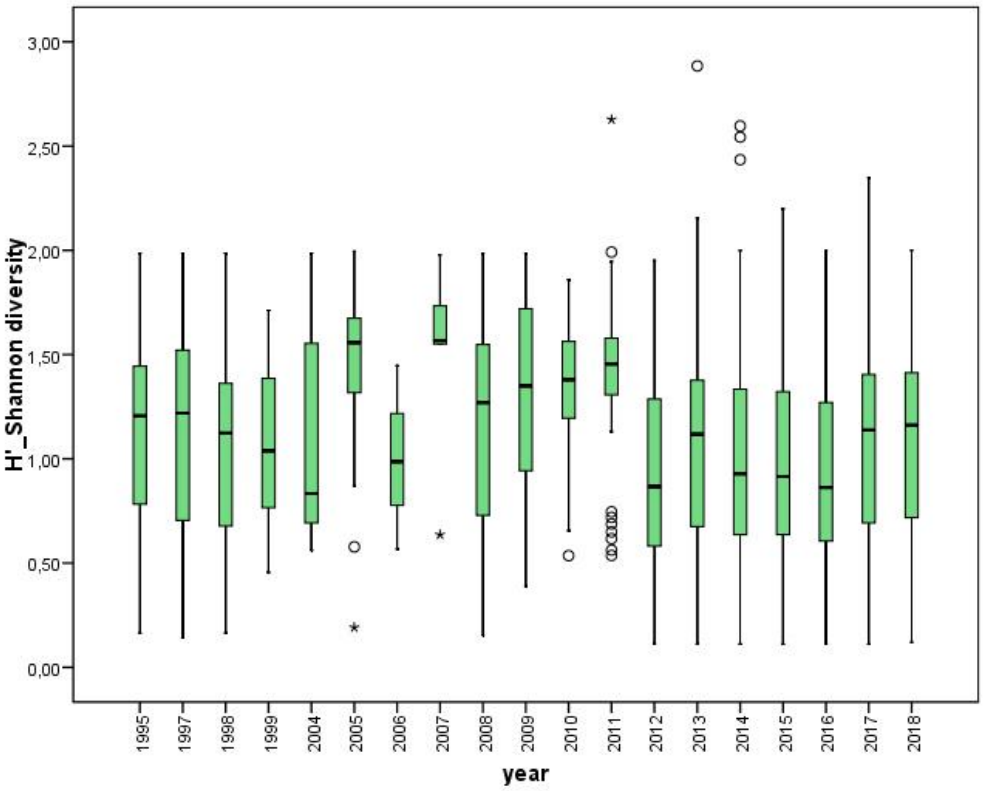

Figure 5.3.13. Shannon´s index distribution by year of fish associated under dFADs

The richness and biodiversity Shannon´s index ranged in more or less same level in all years studied. The indices showed very similar average value throughout the study period around 5 for richness or around 1.3 for biodiversity Shannon´s index respectively (**Figure 5.3.12** and **Figure 5.3.13**).

The non-metric multi-dimensional scaling (MDS) analysis of the species-samples matrix show low stress values. An MDS similarity analysis is presented, to know the similarity according to the Bray Curtis´s index between the years studied. The nineties clearly differ from the rest of the years (**Figure 5.3.14**).

Table 5.3.2. shows the pairwise comparisons through ANOSIM (similarity analysis) test. For each pair of year (groups), the first data column is of pairwise "R statistics". The R statistic varies between roughly 0: there are no differences, and 1: all dissimilarities between number of different fish species are larger than any dissimilarity among samples within either species. The R values range between R=-0.88 for pairwise 1995-1998 to R=0.371 for pairwise 2017-1999.

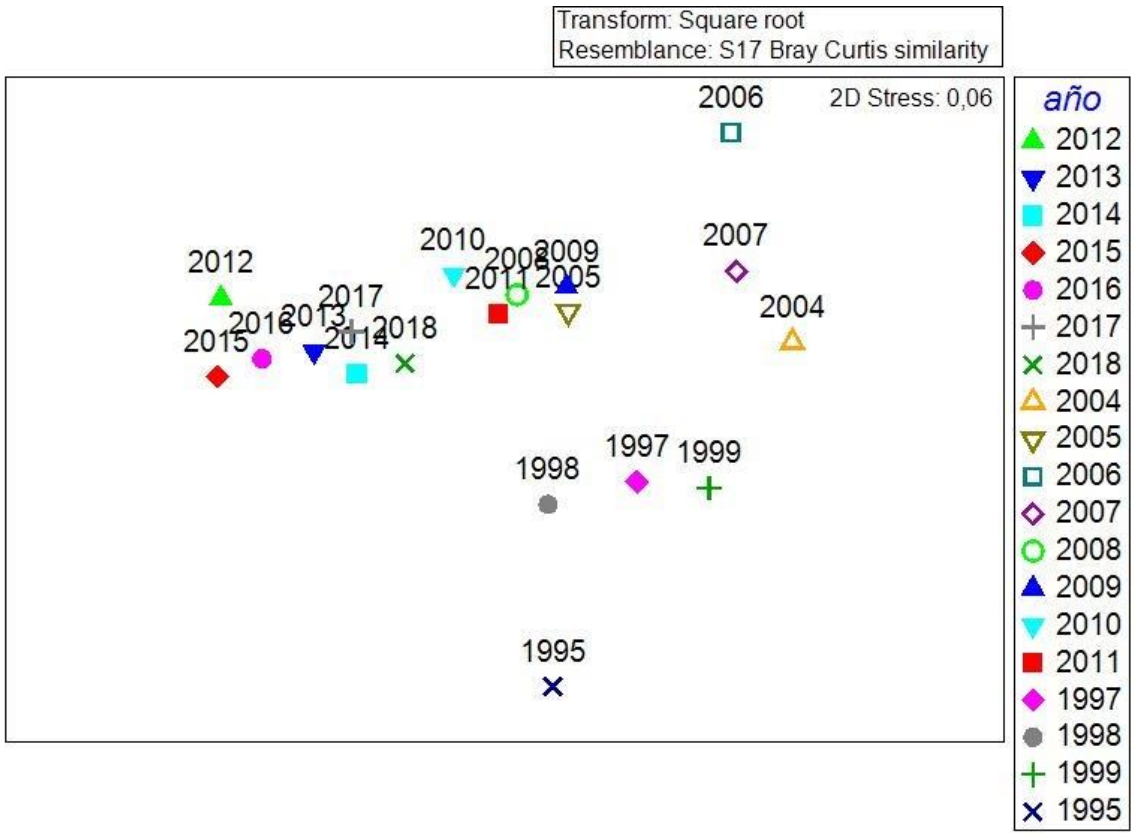

Figure 5.3.14. Non metric multi-dimensional scaling (MDS) similarity of Bray Curtis index by year

Pairs of years	R Statistic	Significance Level %	Possible Permutations	Actual Permutations	Number >= Observed
2015, 2016	0,02	0,1	Very large	999	0
2015, 2017	-0,028	99,5	Very large	999	994
2015, 2018	0,033	2,6	Very large	999	25
2015, 1997	0,221	0,1	Very large	999	0
2015, 1998	0,245	0,1	Very large	999	0
2015, 1999	0,361	0,1	Very large	999	0
2015, 1995	0,128	0,1	Very large	999	0
2016, 2017	-0,026	100	Very large	999	999
2016, 2018	0,014	17,5	Very large	999	174
2016, 1997	0,197	0,1	Very large	999	0
2016, 1998	0,21	0,1	Very large	999	0
2016, 1999	0,306	0,1	Very large	999	0
2016, 1995	0,114	0,1	Very large	999	0
2017, 2018	0,048	0,1	Very large	999	0
2017, 1997	0,248	0,1	Very large	999	0
2017, 1998	0,217	0,1	Very large	999	0
2017, 1999	0,371	0,1	Very large	999	0
2017, 1995	0,182	0,1	Very large	999	0
2018, 1997	0,124	0,1	Very large	999	0
2018, 1998	0,081	0,1	Very large	999	0
2018, 1999	0,262	0,1	Very large	999	0
2018, 1995	0,064	3,1	Very large	999	30
1997, 1998	-0,037	97,1	Very large	999	970
1997, 1999	0,131	0,3	Very large	999	2
1997, 1995	0,042	2,3	Very large	999	22
1998, 1999	0,087	2	Very large	999	19
1998, 1995	-0,088	100	Very large	999	999
1999, 1995	0,278	0,1	Very large	999	0

Table 5.3.2. Pairwise Tests used for the comparison of pairs of years

The Dominance plot (**Figure 5.3.15**) illustrates the number of taxa contributing to a given percentage of the catch. For each sample, or pooled set of samples, species are ranked in decreasing order of abundance. Their relative abundance is plotted against the increasing rank (x axis), the latter on a log scale. The y axis shows the cumulative relative abundance of each year and illustrates the behavior of annual biodiversity through the dominance curves of the entire study period. The trend of dominance curves of each year shows the same general trend; 10 species represent more than 80% of the species observed in each year. These species are: Canthidermis maculata, Caranx crysos, Elegatis bipinnulata, Acanthocybium solandri, Seriola rivoliana, Coryphaena hippurus, Carcharhinus falciformis, Sphyrna zygaena, Balistes capriscus, Kyphosus spp.

The dominance curves of the first years are somewhat different from those of the most recent years (**Figure 5.3.15**). If we restrict the analysis to the monitoring of only the 10 most common species, the dominance curves are closely matched between the years studied (**Figure 5.3.16**).

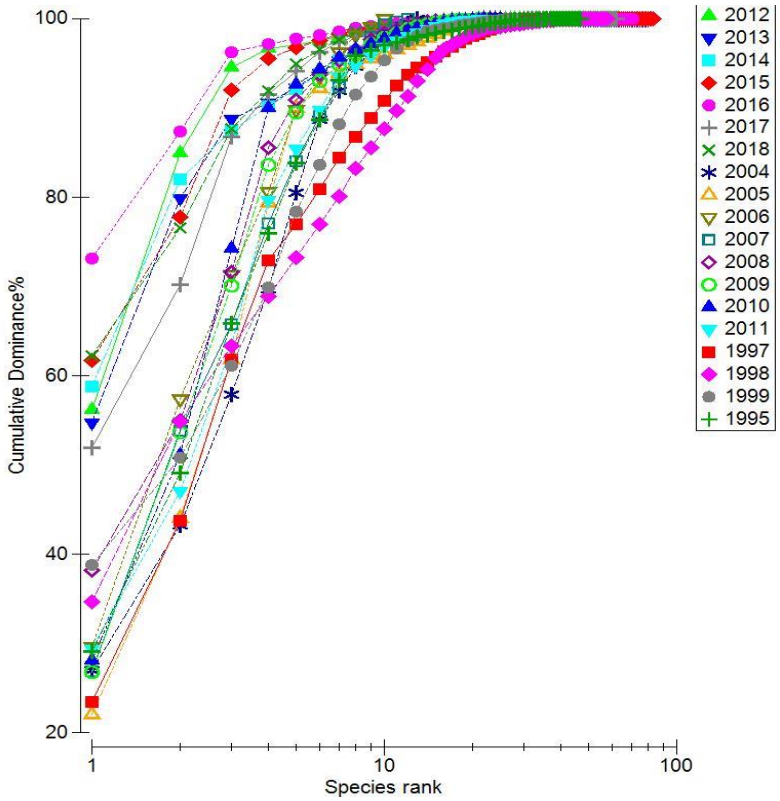

Figure 5.3.15. Cumulative Dominance % plot by taxa by year

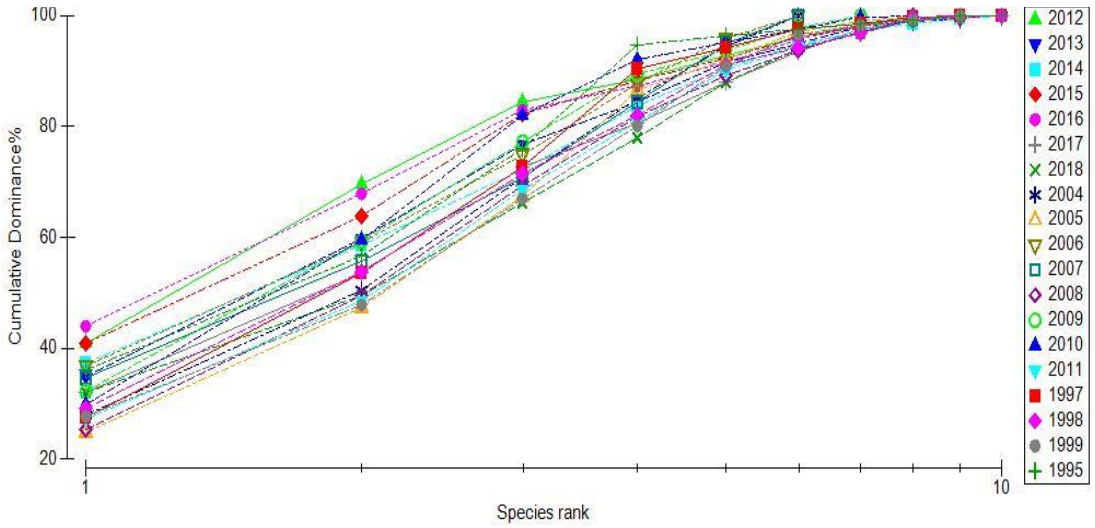

Figure 5.3.16. Dominance plot figure with filter ten main species

The dFAD location greatly influences the abundance and diversity of species associating with the structure. Several authors record the maximum diversity in dFADs that are located near natural reefs (Hammond et al., 1977; Workman et al., 1985; Beets, 1989). In addition, distance to the coast may also influence associated species and biomass, with more species and juvenile fishes in offshore areas than inshore (Wickham et al., 1973; Bortone et al., 1977; Feigenbaum et al., 1989; Castro et al., 1999). The general theory of many authors is: "*The larvae and juveniles phases or many species of fish are recruited under dFADs when they are found in coastal waters, and grow while drifting with these objects. During this period, the dFADs act as a substitute for a reef for non-pelagic species, until they reach an adequate size to enter the adult habitat*" (Klima an Wickham, 1971; Wickham and Russell, 1974; Workman *et al*., 1985; Hunter and Mitchell, 1967). This natural behavior of many fish species to be added under DFADs is the main drawback to reduce the Bycatch in fishery dFADs. Another factor influencing colonization of the dFADs is the soaking time (Kingsford 1992, Druce and Kigsford 1995, Moser et al., 1998).

In the currently study less than 30 % of the associated fauna captured as bycatch in sets of dFADs correspond to species that live in the oceanic pelagic environment. The remaining 70% corresponds to species not characteristic of this ecosystem. This may mean that the majority of species associated with dFADs may originate in non-oceanic habitats, many of them far from the pelagic-oceanic habitat, so their presence in this habitat is accidental or transitory.

The results obtained in the similarity MDS and in the dominance curves of species throughout the entire study period show differences curves for the first years with respect to the dominance curves of the most recent years. These differences might be explained by changes in fishing strategies on dFADs over time and by methodological differences between old and current observation programs. In the 1990s, the priority of the observer

programs were the obtaining of accurate information on bycatch and discards, while in recent years, the development of a voluntary "good practices programs", included in the current analysis, may have placed more focus on the timing and status of released specimens, which may have resulted in higher biodiversity indices. Despite this, the ANOSIM report R values very close to 0, showing high similarity between years no significant change over time apparent.

The richness indexes by set observed do not show declines over the 19 years of data. The average value of 5 species by set is more or less constant throughout all period. The same 10 most common species of bycatch remain the same species since early 1990s to the present. The Shannon biodiversity index shows minor oscillations throughout the entire study period, which could be explained by the previously mentioned methodological changes in the observation programs and due to changes in fleet behavior. In any case, the ranges of this biodiversity index have not changed and remain from 0.2 to values of 2 in the last 19 years. The dominance curves of the species observed throughout the study period do not show trends that show important changes in the community of associated fish. A similar dominance range over time is very characteristic with about 10 species covering 100% of the species mentioned in this fishing modality.

The information and results provided in the present study must be taken with great caution, as the balance and equality in the sampling have not been the same throughout the entire study period. Despite this, we argue that the impact on fish communities associated with fishing on dFADs is very limited, since such impacts covers very few species and its impact in terms of total catch is also considered very minor; summing this up would lead to a very slight negative impact of dFAD fishing.

Impact of dFADs on vulnerable ecosystems

To identify potential dFAD beaching events a beaching detection algorithm was created. This algorithm is based primarily on the spatial proximity of multiple positions from the same buoy and also on basic characteristics, such as water column depth, distance from land, and distance to ports. Subsequently, a global analysis of trajectory data from dFADs deployed by French PS boats over the period 2008-2017 has been conducted in order to achieve a good understanding of where and when beaching events occur.

Results indicate that the number of deployed buoys has continued to increase dramatically in recent years, especially in the Indian Ocean (**Figure 5.3.17A**). It must be noted that the percentage of the deployed dFADs that end up beaching increased until 2013, but surprisingly remains stable or even slightly decreases after 2013 (**Figure 5.3.17B**).

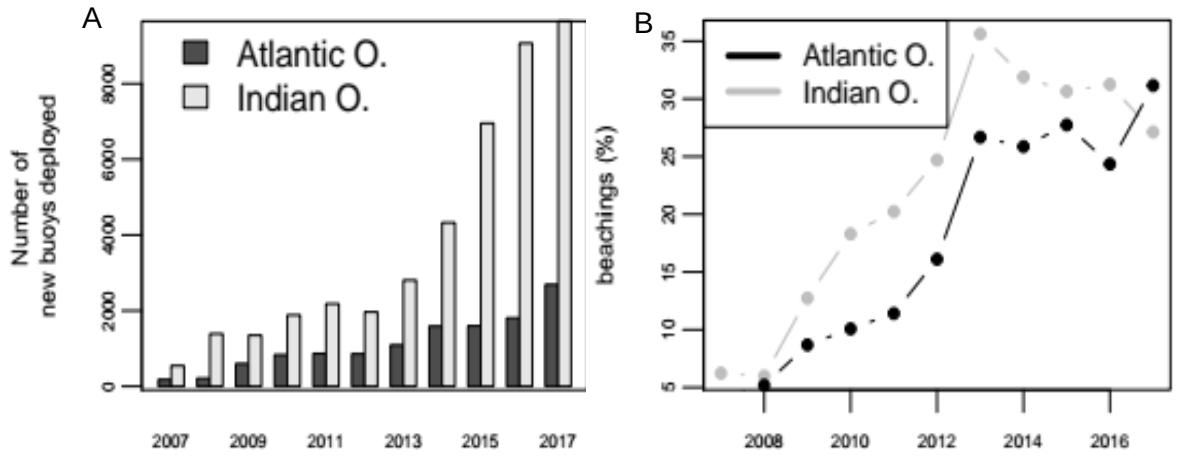

Figure 5.3.17. Number of new buoys deployed by the French PSs operating in the Indian and Atlantic oceans over the period 2007-2017 (left) and percentage of these buoys that beached (right)

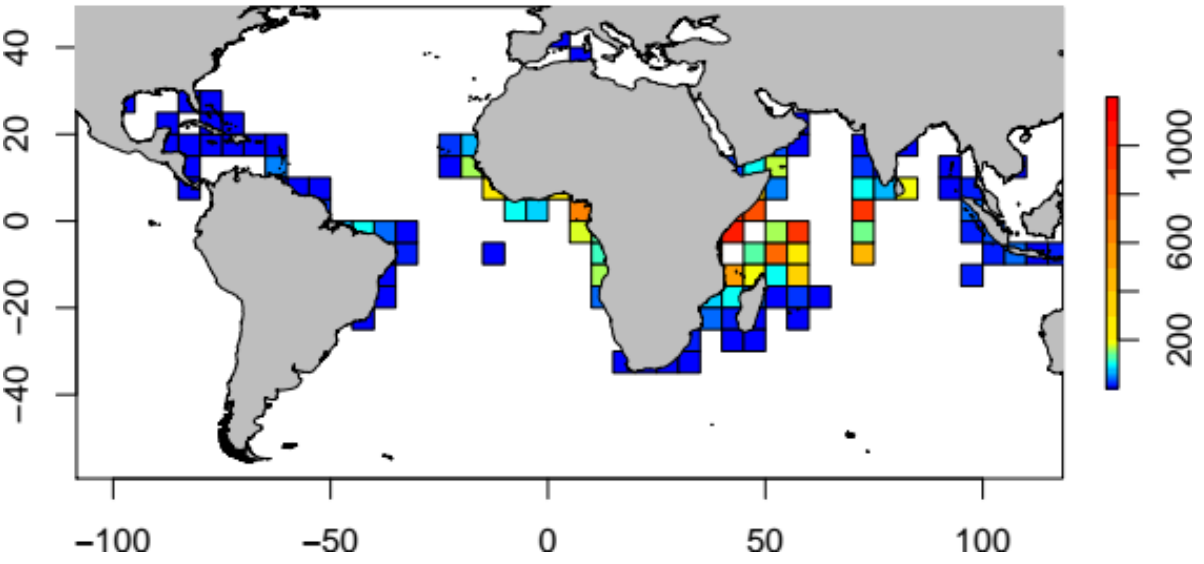

Figure 5.3.18: Density map of dFADs beaching for the French PSs over the period 2007-2017

Maps of beaching locations clearly identify coastal hotspots for dFAD beachings (**Figure 5.3.18**). For the Atlantic Ocean, beachings tend to occur along the coasts of Africa (Guinée-Sierra Leone et Cameroun-Gabon) but also in Brazil and the Caribbean. For the Indian Ocean they occur most often in Somalia, the Maldives, Sri Lanka and the Seychelles.

By backtracking from beaching locations we then produced maps identifying areas for which buoys crossing an area have a high beaching event probability within the next 3 months (**Figure 5.3.19.**).

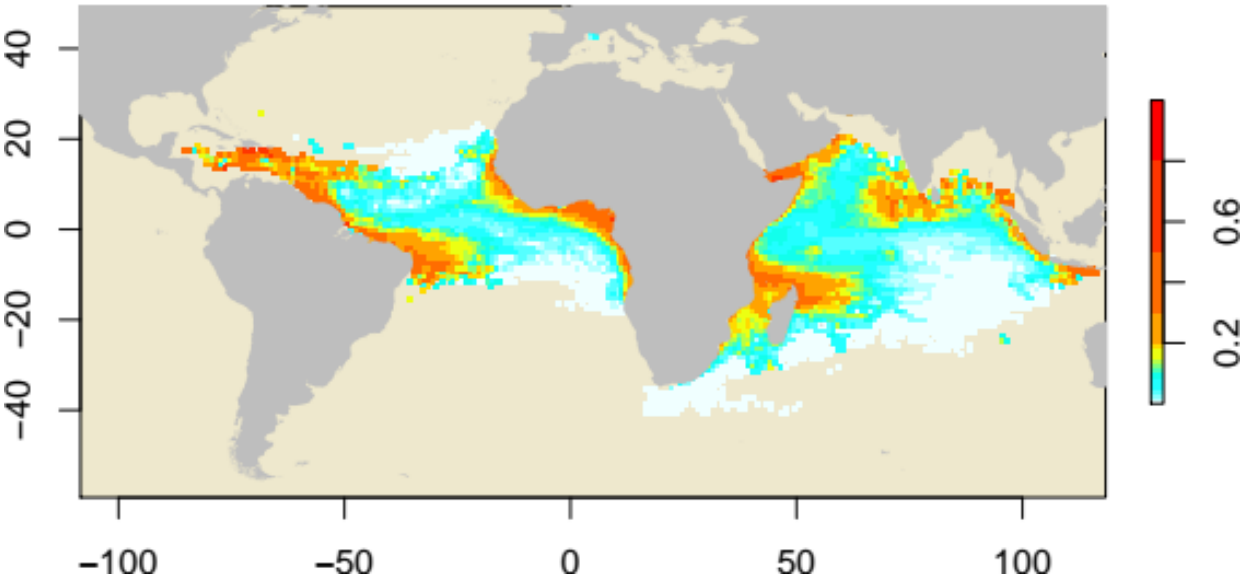

Figure 5.3.19. Map of the proportion of buoys that beached within 3 months following their last passage in each 1°*1° grid cell

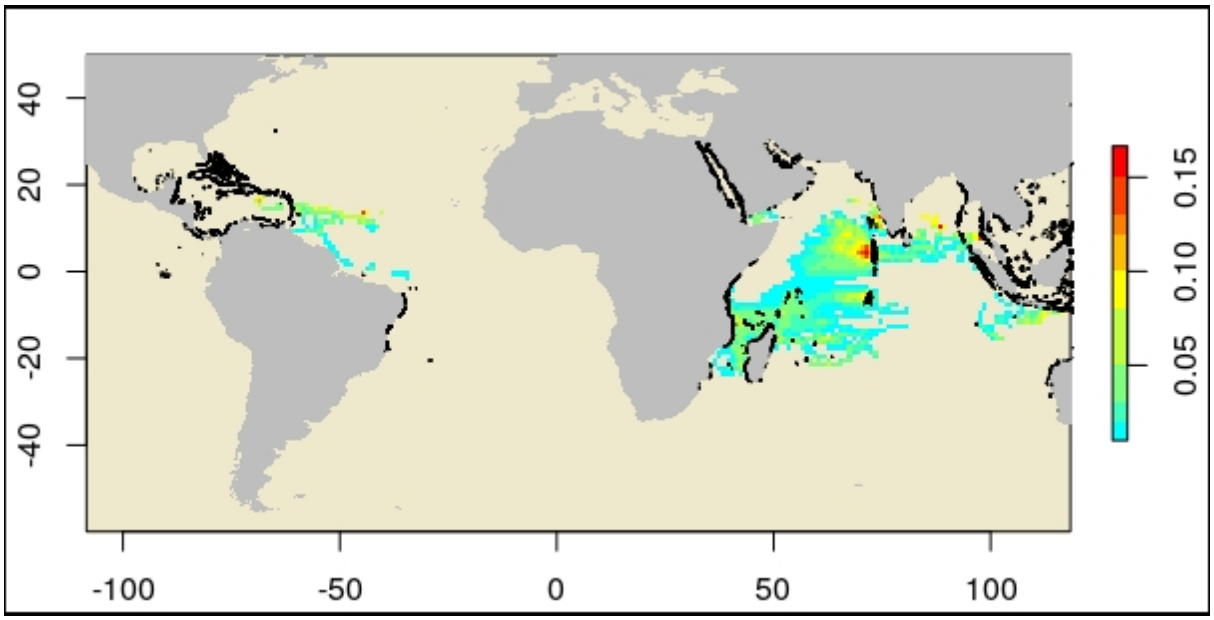

Figure 5.3.20. Map of the proportion of buoys that beached exclusively into Coral reefs within 3 months following their last passage in each 1°x1° grid cell

To highlight the potential impact of dFAD beaching in vulnerable areas, the same backtracking approach has also been conducted exclusively on buoys that beach into Coral reefs (**Figure 5.3.20**).

The analysis of the seasonality of these maps showed that risky areas in terms of probability of beaching events change with seasons and depend on monsoon regimes (see Schott et al., 2009). To reinforce these results showing the strong dependence of beaching events on the monsoon regimes, an additional study was conducted on the trajectories of beached dFADs in the Maldives. The analysis revealed significant differences in the origin and direction of arrival of the dFADs beaching in the Maldives (**Figure 5.3.21**).

The first period from January to April is characterized by beaching dFADs arriving mainly from the east of the Maldives (**Figure 5.3.21A**). This is consistent with transport by the South Equatorial Countercurrent (SECC) that drives the dFADs from the Western Indian Ocean, where they are primarily deployed to the east side of the ocean and then transported by the Northeast Monsoon Currents (NMC) that brings them back to the east coasts of the Maldives (see **Figure 5.3.22**).

For the second period (May –December), we noted that dFADs beached primarily from the west side of the islands with a difference in speed. The dFADs drift and cross the Indian Ocean faster in November and December than between May and October (**Figure 5.3.21A B**). This is also consistent with transport by the East African Coastal Current (EACC) that drives dFADs from the west side of the Indian ocean and brings them to the west coast of the Maldives (**Figure 5.3.22**).

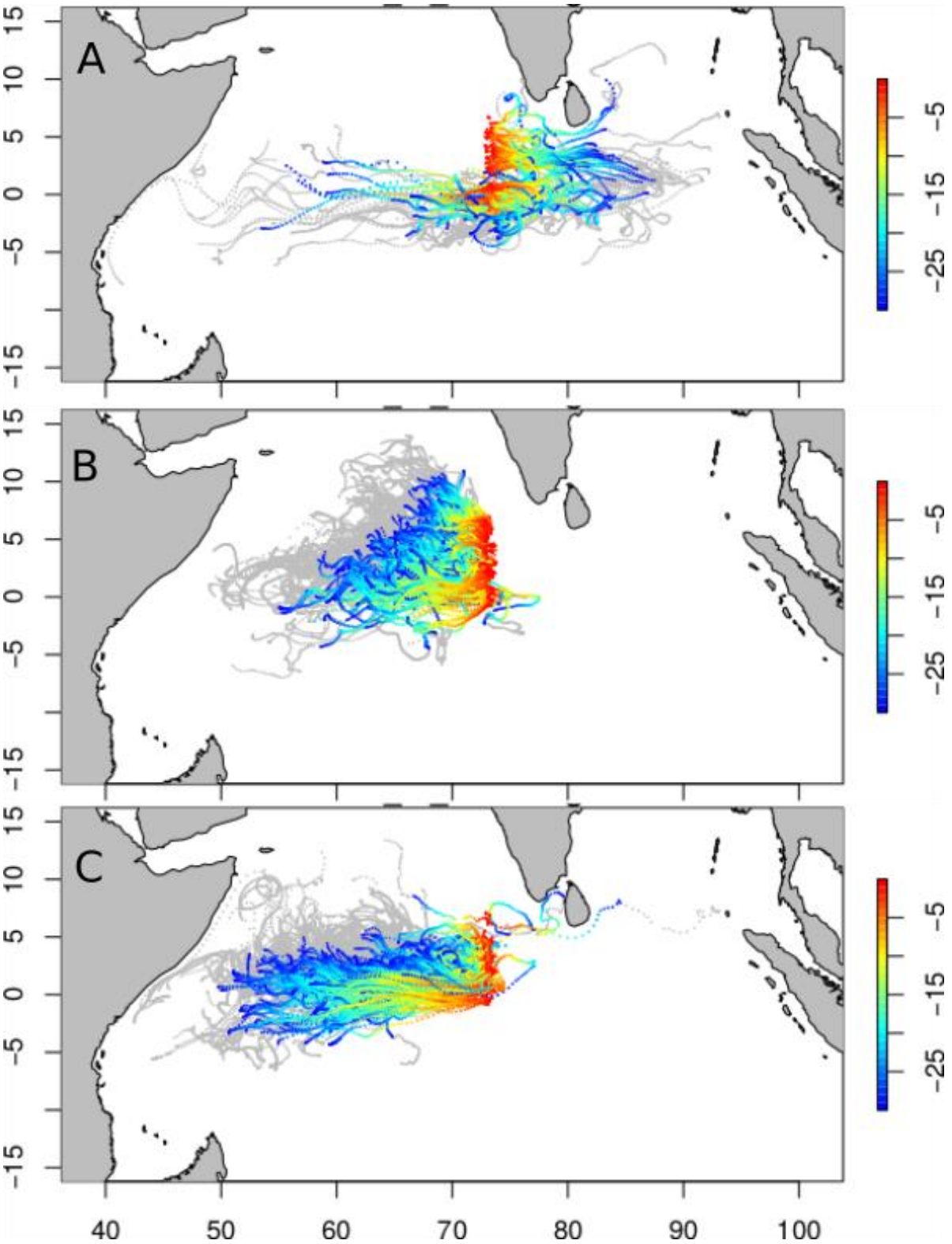

Figure 5.3.21. Maps of the trajectories of dFADs that beached in Maldives in the period 2008-2018. color bar shows the time period (days) before beaching. A) January-April; B) May-October; C) November-December.

A.

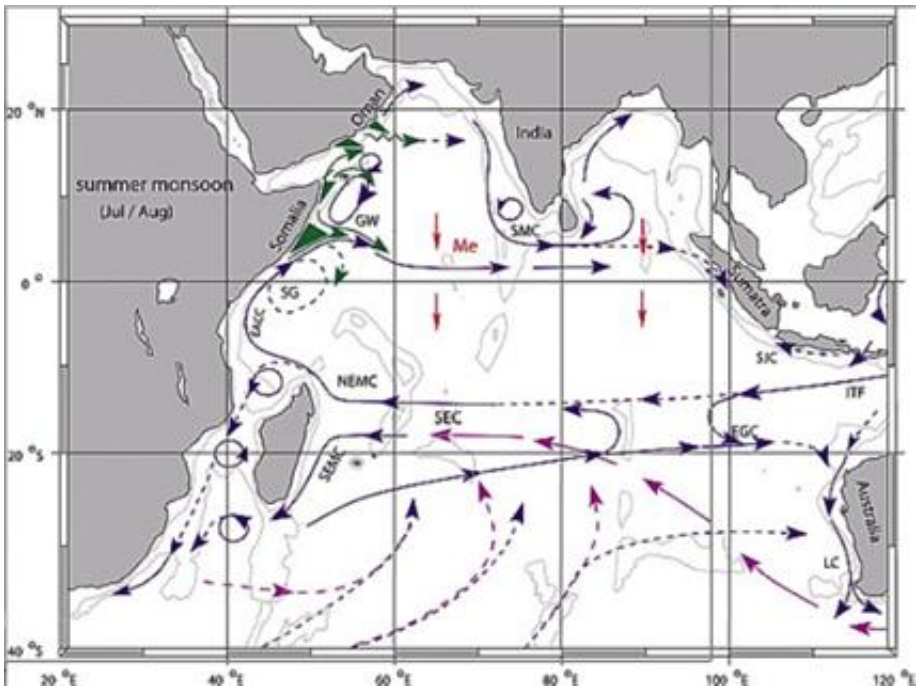

B.

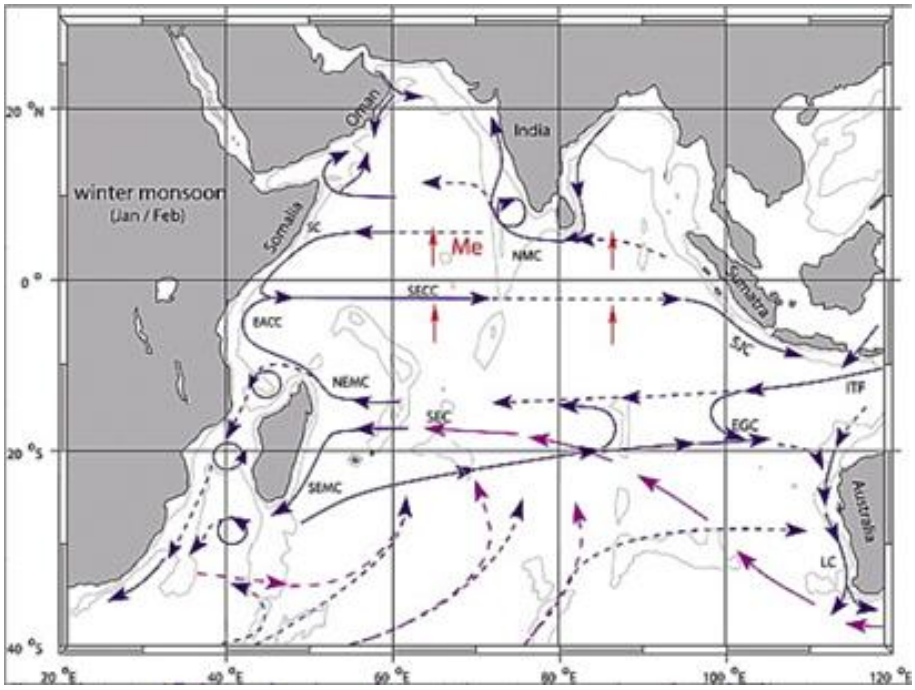

Figure 5.3.22 Schematic diagrams that summarize the near-surface flow field in the Indian Ocean during the (A) summer, and (B) winter monsoon periods from Schott et al, 2009.

5.3.3. Sub-task 3.2. Potential regulatory measures to reduce the impact of dFAD fishing on the ecosystem

Detection of hotspots of small BET catches

The 1°square*month distribution of dFAD catch for juvenile tropical tunas by PS vessels has been analyzed for the 2007-2016 period, with the aim to provide the scientific basis in support of possible improvements of the current regulatory measures based on the ICCAT multiyear conservation and management program (Rec-16-01). Moreover, the underlying objective of this work is to support the conception of regulatory measures, through the provision of scientific knowledge permitting a durable exploitation of SKJ while reducing the impact of dFAD fishing on BET and YFT populations. Based on a previous study (Deledda et al., 2018), the total dFAD catch by 1°square*month for the PS fleets operating in the Eastern Atlantic was either obtained from the ICCAT task II catch/effort data (e.g., EU fleet), or raised to ICCAT task I and re-estimated by month and 1°square for the other fleets (e.g., Ghana). Due to potential bias in the large sampling spatio-temporal strata currently used to correct the catch species composition reported in the European PS logbooks, a new stratification procedure has been used. Juvenile BET and YFT were discriminated from adults using the mean of the length at first maturity (LF50). Thus, the species composition in terms of juvenile BET and YFT for all size classes of SKJ was derived from the size frequency samples of dFAD sets collected at landings of the European and Ghanaian PS fleet. When a 1°square*month was fished and sampled, these proportions were directly combined to the total dFAD catch reported in logbooks to estimate the species composition of the dFAD catch in the same time-area unit. In contrast, when there was no sample corresponding to a fished 1°square*month, we combined the samples of the surrounding strata to estimate the missing information. To do this we performed a spatio-temporal variogram analysis to evaluate the level of correlation in time and space of the species composition. From the results of the autocorrelation analysis, we fixed spatiotemporal limits at 5° degrees and 2 months to combine the neighboring samples which are used to calculate the species composition of the fishing strata not sampled (**Figure 5.3.23**).

In comparison with the stratification scheme currently used, the method proposed preserves the sampling information at a much finer spatial and temporal scale, specifically appropriate for analyzing the tuna species composition of the catch.

The results of the spatio-temporal analysis highlight the non-random nature of the tuna distribution in the Atlantic Ocean. Major dFADs catches of juvenile bigeyes are observed from September to January (**Figure 5.3.24**).

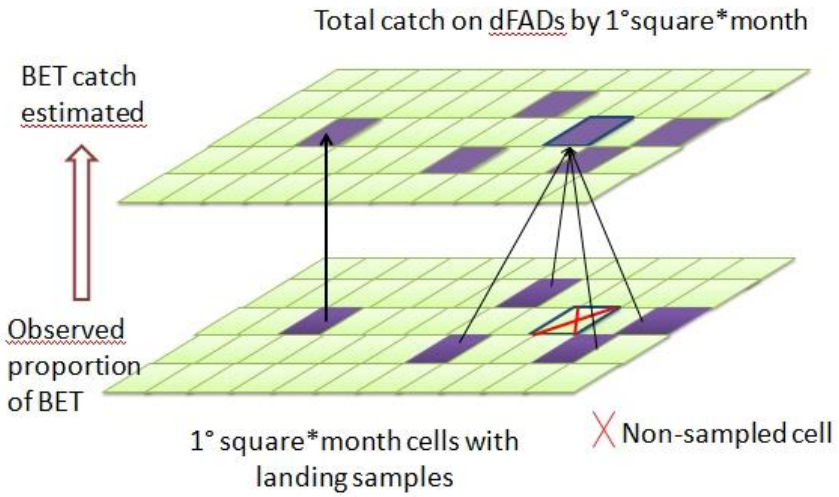

Figure 5.3.23. Calculation process used to estimate the dFAD juvenile (i.e., all year classes not yet mature) bigeye catch by 1°square*month from harbor samplings.

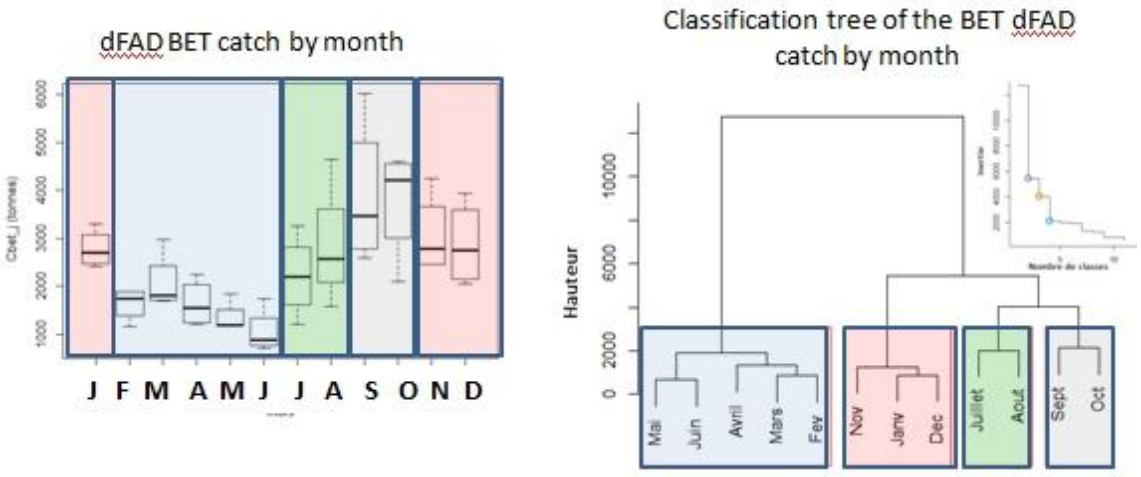

Figure 5.3.24. Seasonality of dFAD catches of juveniles BET (i.e., all year classes not yet mature) in the Atlantic Ocean.

Following this, an analysis of global and local Moran's indicators of spatial association permitted to highlight the hot spots of juvenile's BET dFAD catches at different fishing seasons during a typical year. From September to January, hotspots have been identified in the center of the Atlantic Ocean and then in the Gulf of Guinea from November to January. From February to June, two main hotspots areas were identified near the Mauritanian coast and in the center ocean area; this latter persists from June to August but it is slightly moving along the season (**Figure 5.3.25**).

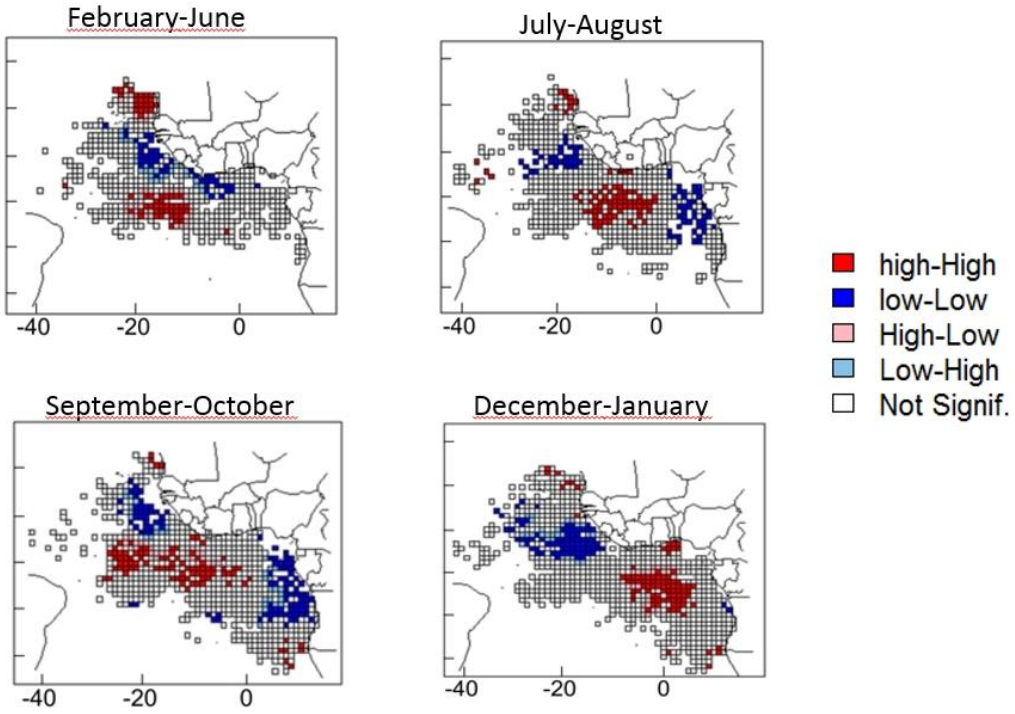

Figure 5.3.25. Preliminary analysis of hotspots detection of dFAD catch of juvenile (i.e., all year classes not yet mature) bigeyes. Hotspots are in red and coldspots in blue.

Analysis of support vessel activities during the months of the dFAD moratorium.

The analysis of support vessel activities before, during and after three January-February dFAD moratorium areas (i) from the African coast to 10°S latitude and between 5° W and 5° E longitude (Rec[14-01], in force during the 2016 fishing season) and (ii) from 5° N to 4° S latitude and from the parallel 20°W longitude to the African coast (Rec[15-01] and Rec[16-01], in force during 2017 and 2018, respectively), is one of the relevant points with regards to the efficiency of the assistance provided by these vessels to the PS vessels. These recommendations prohibit any fishing or support activity in association with objects, including FADs, in the closed areas during the first two months of the year. The Spanish PS fleet fishing activity has been supported by four supply vessels in the three years analyzed. The work on supply vessel activity has mainly comprised the compilation, depuration and analysis of the FAD logbooks received from the Spanish support vessels for the three moratoria established by ICCAT between 2016 and 2018. The lack of information from years before the closures, makes it difficult to evaluate more precisely how they have impacted supply vessels' activity. Moreover, data from FAD logbooks, particularly during the first years, had several quality issues that limit their usability (e.g., activity recorded by the purse seiners serviced, formatting issues, etc).

In spite of the above, the analysis of the FAD logbook information reported by the supply vessels allowed us to obtain information on the behavior of the fleet. As expected, no activities were recorded by support vessels in the spatio-temporal closure in any of the years (**Figure 5.3.26)**.

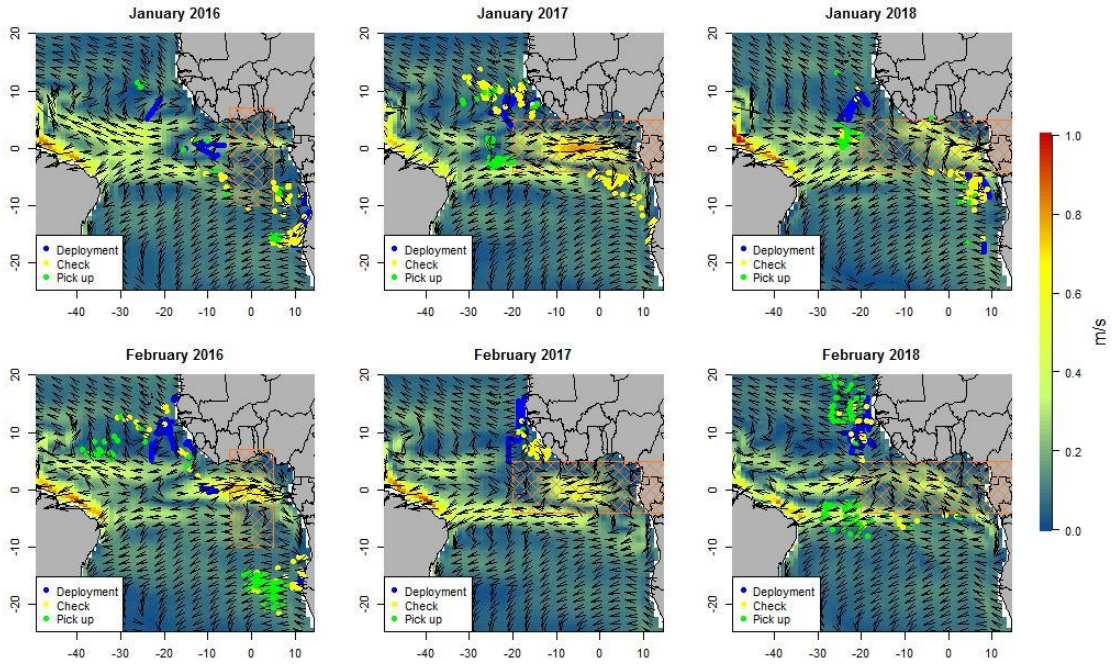

Figure 5.3.26- Summary of activities carried out by the Spanish support vessels during the closures in 2016-2018. The crossed areas indicate the region closed to FAD-related activities. The background quiver plot illustrates the average surface current fields by month[19].

The pattern of vessels' activity during the dFAD closures differed significantly between 2016 and the other two years, possibly due to the fact that the recommendations mentioned above affected different areas. In 2016, support vessels deployed dFADs off the coast of Angola, in the equatorial area west of the closure region (5ºW) and off the western coast of Africa between 5 and 15ºN. However, in 2017 and 2018, support vessels mainly deployed dFADs in this latter region, possibly due to the fact that dFADs deployed elsewhere out of the closure area might drift out of the fishing grounds, which are mainly distributed east of 20ºW. The Atlantic North Equatorial Countercurrent is typically weak in winter and most of the times the water flows westwards in this area, what explains the number of recoveries observed west of the closed area in 2017 and 2018. Due to the shortness of the time series, and the fact the areas closed differed between 2016 and the next two years, it is difficult to extract definitive conclusions. There were slight drops in the number of FADs deployed and serviced or checked by supply vessels during the closure months, as well as minor increases in the number

[19] data provided by the NOAA/OAR/ESRL PSD, Boulder, Colorado, USA, from their Web site at https://www.esrl.noaa.gov/psd/

of FAD retrievals as compared to the preceding and following months, though the series show high variability throughout the year (**Figure 5.3.27)**. Although further data are required, it seems the impact of the closures in supply vessels' activity is limited.

An important issue when analyzing dFAD data from FAD logbooks is the difficulty in tracking unique dFADs without the actual buoy transmission information, due to several circumstances, including the activity of non-Spanish flagged vessels over this dFADs (this activity, which can imply setting on these FADs, recovery, change of buoy is not reported) and issues related to dFAD miscoding and unreporting. As a consequence, as an example, the number of FADs deployed by supply vessels and later set by a PS vessel was unexpectedly low, and the information obtained is not considered representative in terms of total numbers. In this regard, the availability of information from both buoy tracking data and VMS could dramatically improve our understanding of FAD usage at all levels.

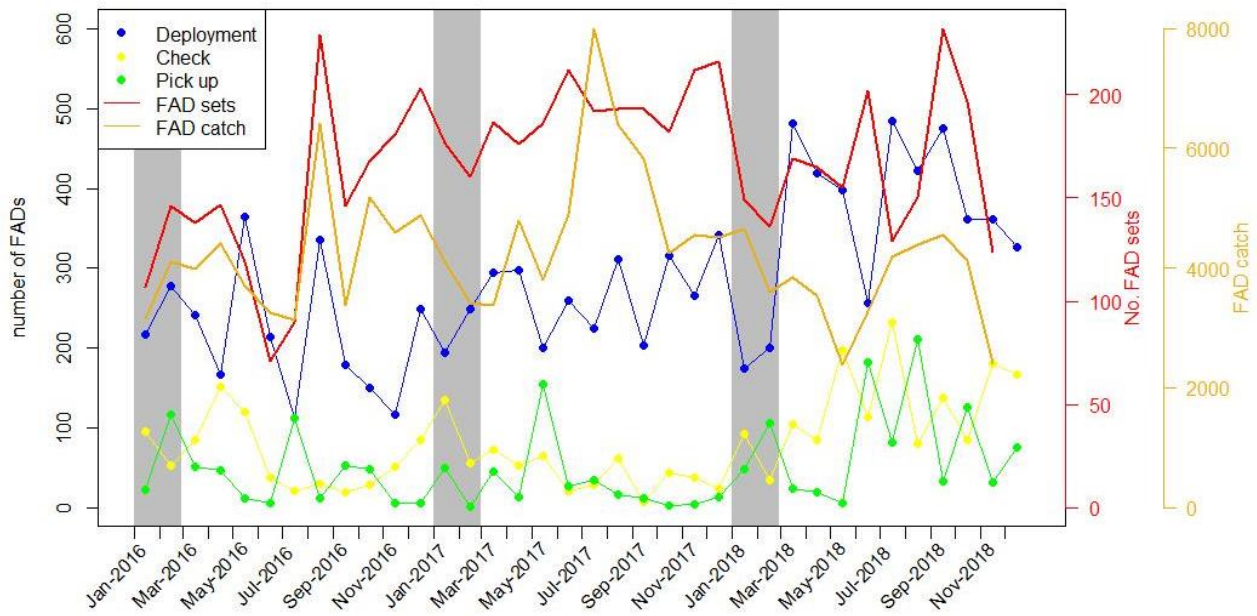

Figure 5.3.27- Time-series of supply vessel activity (deployments, checks/encounters and retrieval), FAD set numbers and total FAD catch by PS vessels.

The combination of FAD logbooks from PS vessels and supply vessels suggests that dFADs deployed in January and February out of the closed areas are not fished once the closure finishes in these areas. On the contrary, dFADs deployed in November-December can drift out of the closed areas and be fished in January-February although (**Figure 5.3.28).** As already noted, the numbers are likely underestimated. Just 9 of the buoys deployed in November and December in the closed areas in 2016 and 2017, out of 1600 deployements, were set out of the closed areas during the subsequent moratoria.

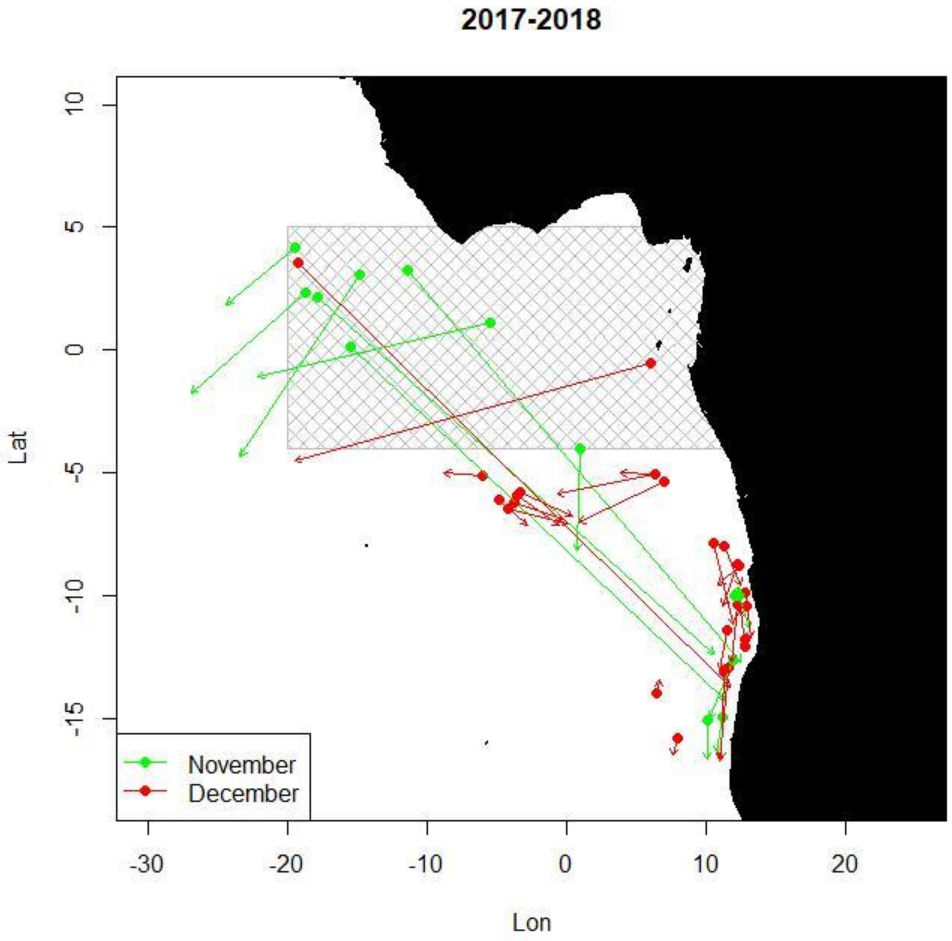

Figure 5.3.28. Spatial pattern of FADs deployed during November-December and set during the closure period. Tracks are not derived from buoy satellite transmissions (unavailable), but from FAD logbooks, so artifacts related to miscoding or unreporting are likely to occur. (e.g., FADs deployed in the closure area and set off Angola).

With the aim to evaluate if the buoys seeded into the moratorium area may be fished in the same area or at large distance after drifting, we calculated the proportion of buoys fished inside and outside the last two moratorium areas during the two months preceding the closure (i.e., November-December) after being seeded by the same vessel inside and outside the moratorium areas for the same months. Results are shown in **tables 5.3.3 A and B** for the Spanish purse seiners and French purse seiners, respectively.

Effective Moratorium	Period of deployment	N° buoys deployed		N° buoys then fished within the period of deployment	
				Inside	Outside
2016 from the African coast to 10°S; 5° W - 5° E	Nov–Dec 2015	Inside	NA	NA	NA
		Outside	NA	NA	NA
	Jan-Feb 2016	Inside	dFAD not authorized		
		Outside	979	0 (0.00)	11 (0.01)-
2017 and 2018 from 5° N - 4° S; 20°W-to the African coast	Nov–Dec 2016 and 2017	Inside	733	1 (0.00)	0 (0.00)
		Outside	1149	0 (0.00)	0 (0.00)
	Jan-Feb 2017 and 2018	Inside	dFAD not authorized		
		Outside	1642	0 (0.00°	12 (0.01)

Table 5.3.3A. Number and proportion of buoys seeded and fished by the same Spanish purse seiner according to the location at release and recapture with regards to the moratorium area.

Effective Moratorium	Period of deployment	N° buoys deployed		N° buoys then fished within the period of deployment	
				Inside	Outside
2016 from the African coast to 10°S; 5° W - 5° E	Nov–Dec 2015	Inside	99	5 (0.05)	5 (0.05)
		Outside	154	0 (0.00)	20 (0.13)
	Jan-Feb 2016	Inside	dFAD not authorized		
		Outside	158	0 (0.00)	4 (0.03)
2017 and 2018 from 5° N - 4° S; 20°W-to the African coast	Nov–Dec 2016 and 2017	Inside	916	110 (0.12)	10 (0.01)
		Outside	206	0 (0.00)	26 (0.13)
	Jan-Feb 2017 and 2018	Inside	dFAD not authorized		
		Outside	374	0 (0.00)	7 (0.02)

Table 5.3.3B. Number and proportion of buoys seeded and fished by the same French purse seiner according to the location at release and recapture with regards to the moratorium area.

For the French fleet among the buoys seeded in November-December inside the area, where the January-February moratorium will take place, the proportion of the buoys "recaptured" by the same vessel the same period of the year inside is equal (2015) or higher (2016-2017, together). The low percentage of "recapture" is likely due to the fact that fishers wait for several weeks before to fish on a recent dFAD deployed and also due to the presence of non-owned dFADs. However the

relative short distance travelled by the dFADs during these two months could be an argument to expand the moratorium period to November-December as it was the case in the past. The very low "recapture rate" of the dFADs seeded by the Spanish fleet causes concerns. Even if a part of the buoys seeded is then fished by other fleets, and consequently unreported, the dFAD activities reported by the Spanish fleet are likely incomplete and limit the analysis of spatial release-recovery of the dFADs equipped with buoys.

Efficiency of the current time-area moratorium on dFAD used to protect juveniles of bigeye

To encourage migratory species such as tropical tunas increased abundance, hotspot juvenile areas need to be protected to increase juvenile survival rate. In response to the significant decline in tropical tuna stocks (specifically BET) that followed from the development and intensive use of FADs by PS vessels in the mid-1990s, in addition to the technical improvement introduced on board vessels, a dFAD moratorium was first implemented in 1999 following the ICCAT recommendation (ICCAT, 1998). For twenty years and up to now, successive moratoria have targeted the floating object (FOB) fishery as a whole and modifications have been made to (1) the level of restriction, (2) the area and period considered (**Table 5.3.4.**). The moratorium now in place extends over 2,366,755 km^2 largely in the Gulf of Guinea and centered to the equator.

Rec	Lat N	Lat S	Lon E	Lon O	Imp (Period)	Start	End	Level
1998	5	-4	Afr.	-20	1999-2004 (3)	Nov	Jan	MFOB
2004 (Rec04-01)	5	0	10	-20	2005-2009 (1)	Nov	Nov	No-take
2008	5	-4	Afr.	-20	2010-2011 (3)	Nov	Jan	MFOB
2011	Afr.	-10	5	-5	2012-2015 (2)	Jan	Feb	MFOB
2015 (Rec15-01)	5	-4	Afr.	-20	2016-today (2)	Jan	Feb	MFOB

Table 5.3.4: Moratorium-type regulations over the last 20 years from ICCAT documentation. The current moratorium has been in place since Rec [-15-01] (ICCAT, 2015). With "imp" implementation years of the moratorium, the "period" corresponds to the number of months during which the moratorium is in effect. "Level" represents the level of restriction with "MFOB" for moratorium under floating objet (FOB) and "No take" for complete closure to fishing in the area. "Afr." Stands for African coast.

Due to time constraints and the recent situation of strong overexploitation of the stock of bigeye only the effectiveness of the current dFAD fishing moratorium Rec [15-01] was assessed using tagging data from the AOTTP (2016-2018) for both yellowfin and bigeye juveniles (Fork length <70 cm) by (1) computing the relative

risk of recapture, which depends on tagged tunas recapture rates inside and outside the moratorium area. Secondly, for both species, (2) shortest distance in kilometers at sea, cardinal directions and time at sea were computed for individuals tagged inside the moratorium area in 2017.

Tagged individuals whose size is less than 70 cm and 65 cm as juveniles for bigeye and yellowfin tuna respectively were considered in the analyses. These limits were based on the size distributions provided by sampling data (Ob73) collected at PSs landing ports (**Figure 5.3.29**).

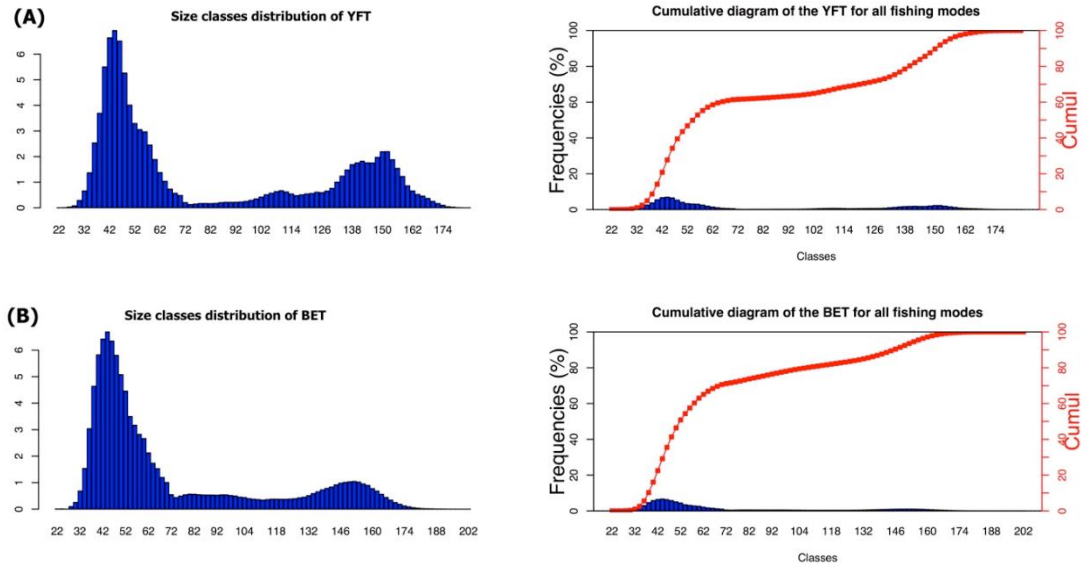

Figure 5.3.29: Size distributions (fork length in cm) of YFT and BET (B) reported in sample data from landing ports (source Ob7-IRD) of tuna PS vessels over the period 2007-2018. All fishing modes combined, the juveniles caught by PS vessels and measured during sampling (between 30 and 70 cm in fork length (FL)), represent 65% and 70% of yellowfin and bigeye tuna caught for, respectively, in the Eastern Atlantic Ocean.

Comparing the rate of recapture of juveniles within the moratorium and outside the moratorium strata through the use of relative risk allows a quantitative assessment of the effect of the moratorium (Lambert et al., 2006). Relative risk (RR) is a ratio of 2 proportions (i.e., rates) and is calculated from pi: pj, where pi and pj are the proportions of the animals in the groups that are recaptured depending on the location of release, "tagged outside" and "tagged inside" respectively. Thus, the relative risk (RR) is the ratio of these two proportions: $\boldsymbol{RR = pi/pj}$. When the relative risk is lower than 1, the recapture rate of fish tagged outside the moratorium will be lower than those tagged inside and we conclude that the moratorium is not statistically efficient in terms of protection of juveniles.

For this step, only tuna released during the moratorium months and recovered in 2017 have been selected. Then, the distance travelled and the number of months

at sea were calculated for tunas tagged inside the moratorium area. It must be kept in mind that the linear distances estimated between the release and the recapture locations likely underestimates the unknown true trajectories covered. Time at liberty (i.e., time at sea) is expressed here as the number of months between release and subsequent recapture. To better understand these quantities, stacked and stepped histograms of distance travelled and direction were configured into circular diagrams. The circular diagrams provide an ability to summarize three types of information according to the time spent at liberty (the number of months since 1 January 2017) of the tagged and recaptured tuna: (1) the x-axis represents the number of recaptured tuna, (2) the y-axis represents the directions taken by tagged and recaptured tunas according to the cardinal corner (between the point of capture and recapture), and (3) color represents the distance classes covered in kilometers (the shortest distance at sea between the release location and the recapture divided by quartile). These diagrams depict the number of recaptured individuals, the direction and the distance travelled (underestimated) by juveniles YFT and BET in 2017.

The results showed that recapture rates when juvenile YFT were tagged outside the moratorium area 18 times the recapture rate of tunas that were tagged inside the moratorium area (2017 and 2018 confounded) and 14.45 times for BET (**Table 5.3.5** and **5.3.6,** respectively).

Directions patterns can be evidenced with circular diagrams (**Figure 5.3.30** for YFT and **Figure 5.3.31** for BET).

Tagging location	N tagged	N recaptured	Recaptured (%)	Relative Risk	Chi.2	p
Outside	2912	282	9.68	18.73 ±(18.72,18.74)	251.45	< 2.2e-16
Inside	2635	15	0.57			
Total	5547	297	5.35			

Table 5.3.5: Rate of recapture and relative risk computed by zone (inside and outside the moratorium area) for juvenile of yellowfin tuna.

Tagging location	N tagged	N recaptured	Recaptured (%)	Relative Risk	Chi.2	p
Outside	2087	84	4.02	14.45 ±(14.4,14.5)	24.01	> 2.2e-16.
Inside	691	2	0.29			
Total	2778	86	3.10			

Table 5.3.6.: Recapture rates and Relative Risk computed by zone (inside and outside the moratorium area) for juveniles' bigeye tuna.

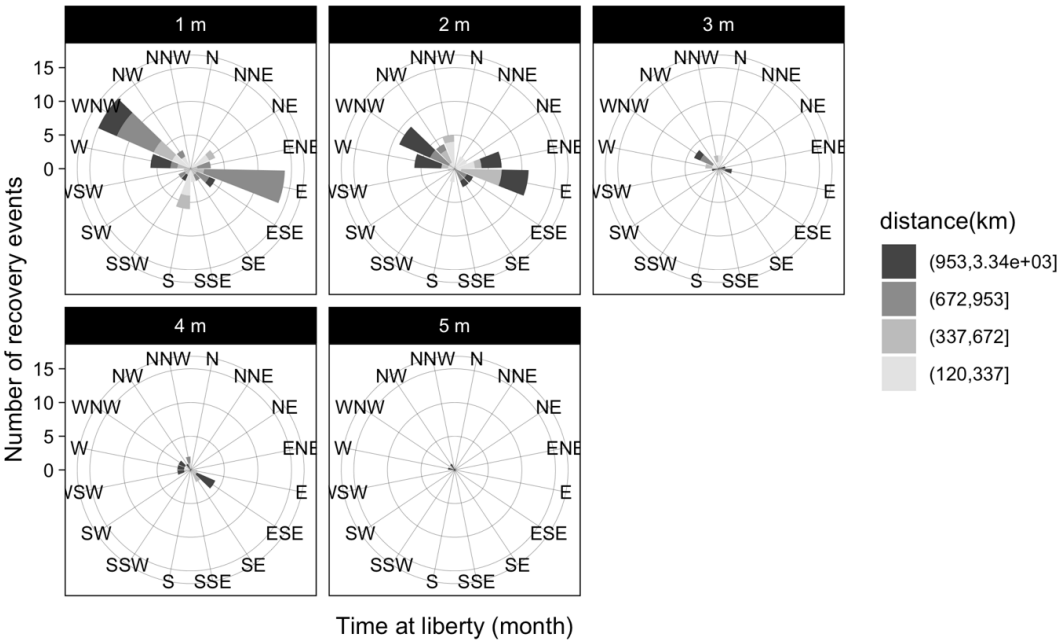

Figure 5.3.30: Distribution of directions taken by juveniles of YFT marked inside the moratorium and recaptured according to time at sea (in number of months) during the first half of the year (since the beginning of the moratorium in January 2017). On the Y-axis, the number of recoveries is between 0 and 15 and on the X axis, the cardinal directions are reported. The distance range travelled by the recaptured individuals is between 120 and 3000 km.

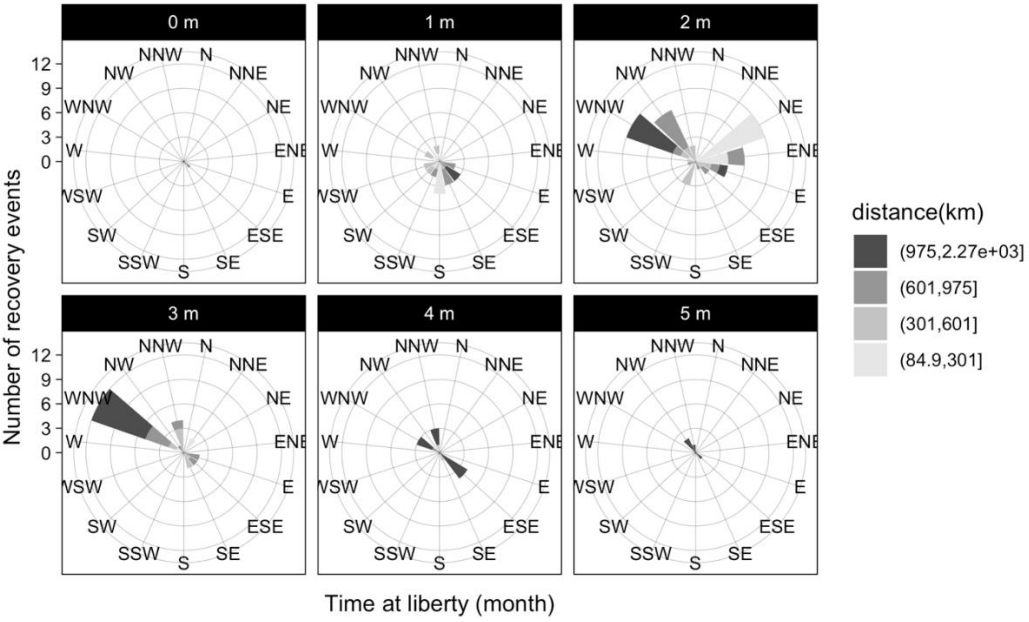

Figure 5.3.31 Distribution of directions taken by juvenile bigeye tuna tagged inside the moratorium and recaptured as a function of time at sea (in number of months) during the first 6 months of the year (since the beginning of the moratorium in January 2017). On the Y-axis, the number of individuals is between 0 and 12 and on the X axis, the cardinal directions are reported. The distance range travelled by the recaptured individuals from 85 to 2250 km.

Preliminary results obtained through this study show that the recapture rates of juvenile YFT and BET were relatively low during the moratorium period. The effectiveness assessment of the dFAD current moratorium through the relative risk is statistically significant for juvenile YFT, but not for BET (Deledda and Gaertner, 2019). Indeed, it was shown that for juvenile YFT tagged inside the moratorium area, the risk of being recaptured was more than 18 times the risk of being recaptured when tunas were tagged outside the moratorium. For juvenile YFT, an additional step dedicated to testing a border effect showed that 50% of the YFT tagged inside the moratorium were marked within 100 km of the northern edge of the moratorium (North Latitude = 5°). However, the 100 km wide band chosen to reduce the dFAD moratorium size was set arbitrarily in this study. This suggests that the selection of the wide band needs to be further statistically investigated in future analyses.

Our study still showed that very few individuals from amongst those that were deeply tagged in the moratorium were recaptured during the moratorium months. However, care must be taken to draw definitive conclusions from these preliminary results because the recapture rates over time (days), and therefore the evolution of relative risk according to the time spent at liberty, has not been assessed. Indeed, it would be interesting to assess the average time (during the moratorium) between tagging individuals inside the moratorium and recapture outside the moratorium. Once individuals have been identified out of the moratorium and the time at large, the distance at which they have been tagged from the edge will define the boundary area for which individuals have a larger relative risk of being recaptured.

From the circular diagram analysis, we showed that since the beginning of the moratorium period juvenile YFT were mainly recaptured in the east and west/northwest, with relatively long distances covered by tagged individuals (keeping in mind the 1 to 2 months' time at liberty considered). The major limitation of this step was to exclude the other years from the analysis and include releases, which were realized two or three months before the moratorium period. Future analysis should include these data to better assess the effect of the drifting FAD moratorium area. The average distances travelled and directions between release and recapture locations were not statistically tested and this point remains to be further developed. In addition, the uncertainty associated with the exact position of recoveries has not been studied and this could potentially change the results obtained. Overall, the information provided by tagging data coupled with commercial fishing data will allow for a better quantification of the moratorium effectiveness. The release-recapture data of the AOTTP offer many promising perspectives to understand why juvenile yellowfin and bigeye tuna juveniles migrate in some parts preferentially in the Eastern Atlantic Ocean.

Exploration of the duration of the season of FAD closures in the Atlantic Ocean on the reduction on small bigeyes

The following calculations estimate the catch of small bigeye (<60 cm FL) that would be avoided from purse seiners fishing on FADs if they would stop fishing on FADs during N months. These calculations are based on the reported catches by month averaged over the period 2014-2018. Bigeye juveniles catch on FADs range from the lowest catch in June (average of 938 tons) to the largest in October (average of 1,884 tons) [see **Figure 5.3.32**]. This means that the benefit of the reduction of juvenile catch will be different for each of the months of the year. For example, if the closure is in October, the reduction of juvenile catch would be larger than if it was in June. This pattern reinforces the results presented previously in **Figure 5.3.33** on the seasonality of dFAD catches of juveniles BET in the Atlantic Ocean in the chapter devoted to the detection of hotspots of juveniles bigeye catches on dFADs. It must be remember however that in both studies the current calculations are made in the context of the current spatio-temporal closure in January-February.

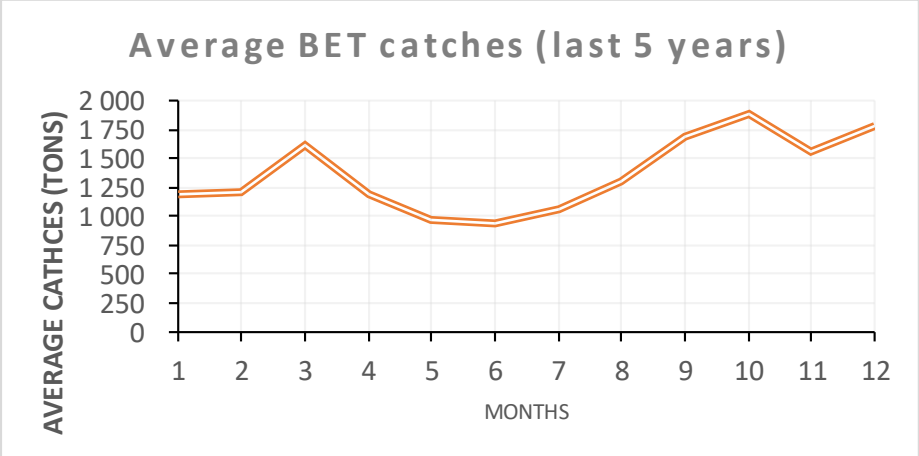

Figure 5.3.32. Monthly catch of small bigeyes on dFADs averaged over the period 2014-2018 in the Atlantic Ocean.

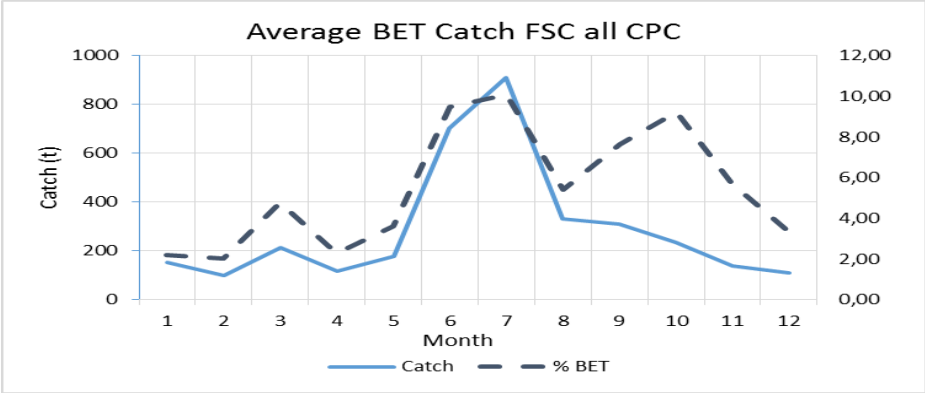

Figure 5.3.33. Monthly catch and percentage of bigeyes in free school, averaged over the period 2014-2018 in the Atlantic Ocean.

Also, these calculations do not include the increase of small bigeyes from Free School sets that would be expected should PS fleets decide to target free schools during the dFAD moratorium. However, we note that catch of bigeyes (all size) in free schools is low, on average no more than 800t in June (**Figure 5.3.33)**. Free schools are mainly constituted by large yellowfins (the percentage by month of bigeye catch in free school goes no further than 10%) thus the mortality on small bigeyes from free-schools is notably lower than on dFADs.

To explore the consequence of the duration of a total moratorium on dFADs on the stock of bigeye tuna in the Atlantic Ocean, we conducted a preliminary analysis as follows: We calculated the expected catch for a typical month by dividing the annual average catch of small bigeye (16,394.11 t over the period 2014-2018) by 12, then we multiplied this value by 2, 3, 4 and 5 months.

So, in brief, a total closure of 2-5 months would result in the reduction of small bigeye catch relative to current bigeye juvenile catch (**Table 5.3.7**). Proportion of reductions shown in the table are relative to the total PS-FAD (% of juvenile BET catches of PS-dFAD) and to all gears combined (% of juvenile BET catches ALL gears). Overall, we estimate that the benefit of 2-5 month total closures to activities on FADs could represent a reduction of bigeye juveniles of [9-23%].

Number of months of closure	2	3	4	5
Tons of small BET	2732.35	4098.53	5464.70	6830.88
% of small BET catches of PS-dFAD	16.67%	25.00%	33.33%	41.47%
% of small BET catches ALL gears	9.26%	13.89%	18.52%	23.16%

Table 5.3.7. Pattern of the small bigeye catch reduction according to different durations of the total moratorium on dFADs

5.3.4. Sub-task 3.3. Exploration of adaptive management framework for accounting for uncertainty in the monitoring and managing of the use of dFADs

The ecosystem approach for fisheries management (EAFM) is now a widely accepted concept, and its use is justified due to the increasing impacts on the ecosystem resulting from fisheries and other activities (Garcia et al., 2003). However, developing the available concepts and principles into operational management objectives is hampered by the climatic and socio-economic changes which continuously impact marine ecosystems. Today fishery managers are not only faced with the need to sustainably exploit tropical tuna resources, but also with the conservation of ecosystems, while providing food, income and safeguarding fishermen's livelihoods in a sustainable manner. Multi-species management, bycatch mitigation, and protection of vulnerable ecosystems must therefore be integrated to achieve ecological and socio-economic objectives.

The application of conventional research methods is often insufficient to support effective decision-making when decisions must be made regardless of the level of knowledge or uncertainty (McFadden et al., 2011). For many important problems, adaptive management (AM) is a promising means of facilitating decision making. The management situation for AM can be framed in terms of resources that are responsive to management interventions but subject to uncertainties about the impacts of those interventions (Williams, 2011). A generic model for adaptive management assumes that at any given time, resource change is influenced by the state of the resource, environmental conditions, and the management action taken at that time (**Figure 5.3.34**).

AM is a formal iterative process of resource management that acknowledges uncertainty and achieves management objectives by increasing system knowledge through a structured feedback process. The adaptive process to support iterative decision-making and to reduce uncertainty in natural system dynamics while concurrently meeting specified management goals and objectives, is often represented as a cycle of "plan, do, monitor and learn" (**Figure 5.3.35**). As illustrated, integral to the adaptive management process is both a decision component and an opportunity to learn.

Instead of focusing on tropical tuna management by using Management Strategy Evaluation (MSE) with (1) operating models sometime as sophisticated as the integrated models used for the Stock Assessments and (2) which omits the collateral effect of tropical fisheries on the epipelagic ecosystem, the AM process could offer an alternate approach to enable value judgments about how "highly migratory species" (HMS) resources could be managed and specifically how to control a sustainable use of the FAD-fishery.

Management involves not only predicting how ecological or physical systems are likely to respond to interventions, but also identifying what management options are available, what outcomes are desired, how much risk can be tolerated, and how best to choose among a set of alternative actions. For all of these reasons, it is fundamental to integrate from the beginning of an AM approach, the point of view of the different stakeholders (scientists, fishermen, government officials, and NGO representatives) in the co-design of the AM Strategies, e.g., to draw a simple conceptual model (e.g., box and arrow diagrams of potential impact pathways) that illustrates the 'big picture' associated with the sustainable management of HMS resources in the Atlantic Ocean and indicates where decisions or actions could be applied. In the case of the use of drifting FADs, alternative management measures could be mobile time-area closure for FAD fishing (see below), FAD set limitations, FAD per vessel limitations, support vessel limitations, time-area FAD seeding limitations, etc., bearing in mind that any one type of measure is unlikely to be able alone to perfectly control fishing mortality on juveniles of bigeye and yellowfin tunas.

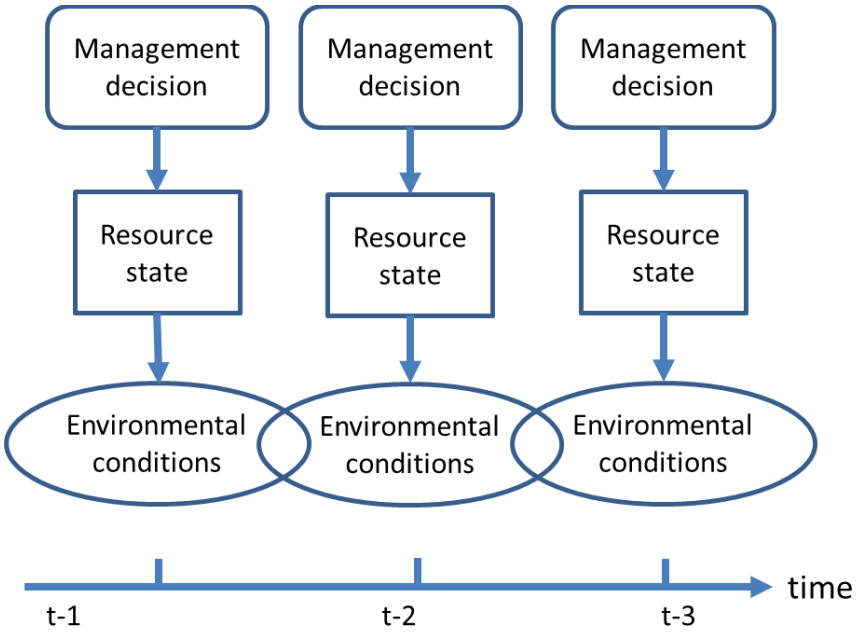

Figure 5.3.34. Dynamic resource system with changes influenced by fluctuating environmental conditions and management actions. Adapted from Walters and Holling (1990).

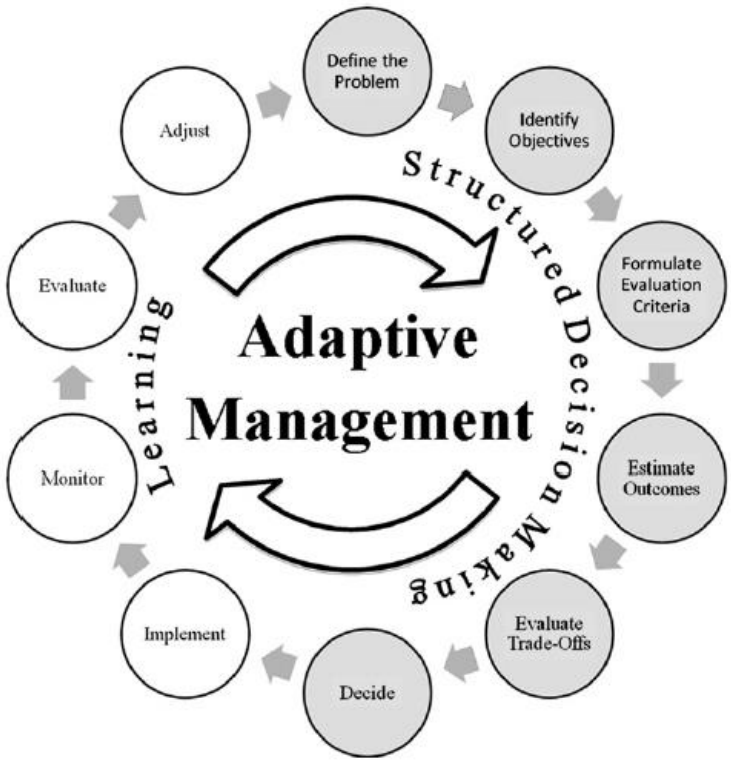

Figure 5.3.35. Adaptive management is characterized as learning by doing. The structured decision making (gray circles) used for identifying and evaluating alternatives and justifying complex decisions is combined with the learning steps (white circles) inherent in adaptive management (from Maxwell et al., 2015).

The process use computer models parameterized with stakeholder knowledge to synthesize and build consensus around management strategies and reach ecological consensus around alternatives for successful natural resource management. This could be done using simulation tools such as Multi-Agent Systems, which are particularly adapted to the exploration of hypotheses presented as "true", and to the representation of dynamic and complex systems which formalize situations of competition or interaction between field actors. Some modelling approaches depict a scientific posture shared by signatories in the use of simulation tools when dealing with complex systems. This posture is based on a cycling approach, in interaction with field processes, including discussion of assumptions and feedbacks on the field process. Confrontation between field and modelling processes must be permanent because of openness and uncertainty features of these systems. This approach is used with two possible aims: learn on systems or support collective decision processes in these systems, which corresponds to an objective of increasing knowledge either for the scientist or the field actors. Instead of proposing a simplification of stakeholder's knowledge, the model is seeking a mutual recognition of everyone's representation of the problem under study. Such mutual recognition lies on indicators which are gradually and collectively built during the implementation of the approach and constitutes the fundamentals of participatory modelling.

To summarize the process, scientists start building a preliminary model to explicit the theoretical as well as field-based knowledge. The confrontation of this first model with real circumstances leads to revise and to re-build it, taking gradually into account the features of the field situation, but also the questions that stakeholders are asking to themselves. The discussion of the model hypotheses, and the simulations implemented according to an experimental plan corresponding to the initial questions, allows to modify the formers and to formulate new questions. This process leads to the construction of a new model, which is either derived from the previous one following its confrontation with the real circumstances and its evolution, or an entirely new one. As this cycle repeats itself, we create a family of models representing the successive interactions between the researcher and the field. By recognizing the importance of identifying uncertainties in designing predictive expert ecosystem management models, this process aims to build a shared and well-accepted representation of the socio-ecosystem of the Atlantic, necessary to facilitate the development of policies and governance approaches to its collective management.

In AM, statistical methods play a critical role, since adaptive managers will need to monitor trends over time that show the system's responses to management policies or practices. Depending on the case study and the level of information and data available, the AM implementation can be based on simpler operative models than in MSE, using an optimum function and validated by statistical methods, e.g., before-after approaches, pressure–state–response ("PS") indicators, to assess if the regulation measure answers to the objectives fixed by the stakeholders.

To finish this guideline for the implementation of AM in tropical HMS fisheries, an additional point can be noted. It is recognized that traditional static management approaches implemented for reducing bycatch and other undesirable ecosystem impacts such as long duration fisheries area closures, often result in serious unanticipated economic impacts on ocean resource users related to shifts in fishing effort, changes in the size of non-target species caught, reduced catch of target species, and economic viability to fishing fleets. For this reason, as an extension of the AM, a Dynamic Ocean Management (DOM) approach should be explored with stakeholders (Hobday et al, 2014). In contrast to the dynamic nature of ocean organisms, conditions, and users, many ocean management approaches are static, whereas DOM uses real-time or near real-time data on the shifting physical, biological, socioeconomic, and other characteristics of the ocean and ocean resource users to generate responsive spatial management measures or strategies. DOM couples into the AM process by using spatio-temporal data to adapt management protocols in near real-time as conditions change. DOM is an area-based management approach that integrates and recognizes the interdependence across organisms, the environment, and associated processes (biological, oceanographic, social, or economic. The results of DOM in identifying the dynamic nature of both the related ecosystems, oceanography and presence of HMS are directly relevant to marine spatial planning and zoning efforts. In terms of time-area closure for FAD fishing, the benefits in terms of protection of juveniles of tropical tunas and vulnerable sharks, as well as in the good compliance of the regulated access area by fishermen could be compared between small mobiles time area strata and the current static FAD moratorium.

5.3.5. Difficulties encountered, and future work expected

The difficulties for this work package are due to the fact that some tasks are linked to the progress in intermediary results obtained in other tasks or other projects. With regards to the detection of hotspots of juvenile catch associated to dFADs, the study should be refined by accounting for the environmental factors and extended to the Indian Ocean. In addition, some information, such as the tagging data provided by the ICCAT-AOTTP, were continuously recovered over the duration of CECOFAD2 and will be used to gauge the usefulness of the different ICCAT moratorium on dFAD to protect juveniles of tropical tunas. With regards to the associated fauna, special attention will be given to underline the changes over time of quantitative/semi quantitative indicators in terms of occurrence/abundance of the associated species caught with tropical tuna under dFADs (e.g., before and after the development of dFAD fishing) as well as other metrics useful to characterize the risks due to this fishing practice on the epipelagic ecosystem.

6 Conclusions

With the aim to provide alternate abundance indices to the conventional longline, special attention has been paid during CECOFAD2 to the standardization of purse seiner CPUE series. The European purse seiner CPUE standardization for large yellowfin in free schools was successfully performed. Based on a 3-components model at the set scale level, the standardized index was used in the yellowfin stock assessment models in ICCAT and in a sensitivity analysis for the same species and fishing mode in IOTC. From a Spatial Capture-Recapture (SCR) model applied to the French fleet it was showed that the total density of dFAD equipped with buoys can be estimated and potentially included as an explanatory factor in dFAD CPUE standardization. However, the CPUE standardization for FAD-fishing is still in progress due to the difficulties to obtain information on the ownership of the buoys which could be used to discriminate the part of the fishing effort devoted to setting on dFAD belonging to each vessel (i.e., when the purse seiner is using the GPS of the buoy and goes directly towards the dFAD) to the proportion of foreign dFADs (i.e., encountered randomly), as well as to integrate the effect of the assistance provided by the support vessels to each purse seiner. In CECOFAD2 we also depicted the fishing activities devoted to dFAD by the European bait boat fleet operating off Senegal.

As an alternative to dFAD CPUE, direct indices of tuna abundance through the use of echo sounder buoys attached to dFADs in the Spanish fleet were investigated during CECOFAD2. The derived BAI, assumed to depict change over time of juvenile tunas, was integrated in the 2019 yellowfin stock assessment models conducted by ICCAT and IOTC in 2019. It should be noted however that this promising approach is still in progress and that additional refinements are needed to improve the relationship between the total catch per set and the school biomass estimated by the acoustic signal, previously to the set, as well as the proportion of the targeted species in the tuna school. It must be also noted that the BAI reflects the trend in the abundance over time for the aggregated population only. With this idea in mind, the continuous process of association and disassociation, as well as the residence time under dFADs, were also analyzed from echosounder data collected on French purse seiners. Preliminary results showed that newly deployed dFADs, equipped with a Marine Instruments buoy, are colonized by tuna aggregations after an average of 20.5 days in the Atlantic Ocean. The results also revealed, for the first time, that the continuous residence time of a tuna aggregation around a single dFAD is about 9 days and that an average of 7 days elapses between the aggregation departure and the later repopulation of the dFAD by other tunas. Based on individual observations, dFADs were shown to be occupied by tuna aggregation about 50 % of their soaking time after colonization.

An analysis conducted from the French observer data on the potential impact of dFAD-fishing revealed that silky shark (*Carcharhinus falciformis*) catches appeared

mostly localized around the Gabon and Angola coasts in the Atlantic Ocean while their distribution appeared more spread across all fishing regions in the Indian Ocean. Based on an empirical model that accounts for their association dynamics at dFADs, the relative abundance indices of silky sharks in the Indian Ocean over the 2007-2018 period globally showed an increasing trend with a magnitude depending on the area. This, however, depicts a relative trend over the period analyzed and not an indicator of the healthy level of the population. An analysis of potential changes in biodiversity of bony fishes associated with dFAD from the data collected by the scientific observers onboard Spanish purse seiners did not show evidence of significant impact of dFAD-fishing on this community of fishes. To assess the potential potential damage of lost DFADs on vulnerable coastal ecosystems, trajectory data from dFADs deployed by French purse-seiners over the period 2008-2017 were analyzed.

it was evidenced that the number of deployed buoys has continued to increase dramatically in recent years especially in the Indian Ocean. Consequently the percentage of the deployed dFADs that end up beaching increased until 2013, but surprisingly remains stable or even slightly decreases after 2013. Maps of beaching locations clearly identify coastal hotspots, such as the coasts of Africa (Guinea-Sierra Leone and Cameroun-Gabon), Brazil and the Caribbean, for the Atlantic Ocean, Somalia, Maldives, Sri Lanka and Seychelles, for the Indian Ocean. By backtracking from beaching locations, maps identifying areas for which buoys crossing an area have a high beaching event probability within the next 3 months have produced.

In order to better definition of an effective dFAD time area closure for protecting juvenile of bigeye in the Atlantic 0cean, a study was conducted to detect hotspots of catch of small bigeye. The spatio-temporal analysis permitted to identify hotspots from September to January in the center of the Atlantic Ocean and then from November to January in the Gulf of Guinea. This seasonal pattern was in agreement with an analysis of monthly purse seiner catches of small bigeyes on dFAD over the period 2014-2018. There is no evidence of an effect of the dFAD moratorium on a change in proportion of bigeye tuna caught in free schools. An analysis of Spanish support vessel activities before, during and after the 2 months of moratorium for the three moratoria established by ICCAT between 2016 and 2018 did not show evidence of an impact of the moratoriums on support vessel activities. It must be noted, when analyzing dFAD data from FAD logbooks, the difficulty in tracking unique dFADs without the actual buoy transmission information due to several circumstances; including the activity of non-Spanish flagged vessels over this dFADs and issues related to dFAD coding and recording, The release-recapture data of the AOTTP offer many promising perspectives to understand why juvenile yellowfin and bigeye tuna juveniles migrate in some parts preferentially in the Eastern Atlantic Ocean. To assess the efficiency of the current dFAD fishing moratorium Rec [15-01] tagging data from the AOTTP (2016-2018) for both yellowfin and bigeye juveniles (Fork length <70 cm) were used for

comparing the rate of recapture of juveniles within and outside the moratorium strata through the use of relative risk of recapture; Preliminary results suggest that the moratorium has been effective for protecting juveniles of yellowfin. The effect is less evident for bigeye due to the low number of releases-recaptures.

To help fishery managers to take decisions combining the sustainable exploitation of the tropical tuna resources and the conservation of the ecosystems while providing food income and safeguarding fishermen's livelihoods in a sustainable way, we propose a guideline for implementing an adaptive management (AM) approach for facilitating decision making in terms of management of highly migratory species (HMS) resources to support an ecosystem approach to fisheries. To reach this objective we propose a methodology to integrate the opinions of different stakeholders (scientists, fishermen, government officials, and NGO representatives) since the co-design of common objectives and indications where actions could be applied, to the assessment of the progress resulting from the implementation of management measures.

7 References

Ailloud, L. E., Lauretta, M. V., Hoenig, J. M., Walter, J. F. & Fonteneau, A. (2014). Growth of Atlantic bluefin tuna determined from the ICCAT tagging database: a reconsideration of methods. Collect. Vol. Sci. Pap. ICCAT 70, 380–393.

Ariz J, Chavance P., Delgado de Molina A. and H. Murua, (2010). European scheme of observers on board purse seiners in the Indian Ocean.IOTC/2010/ROS/03, 45 p.

Bacheler, N. M., Paramore, L. M., Burdick, S. M., Buckel, J. A. & Hightower, J. E. (2009). Variation in movement patterns of red drum (Sciaenops ocellatus) inferred from conventional tagging and ultrasonic telemetry. Fishery Bulletin 107, 405.

Baidai, Y., M. J. Amande, D. Gaertner, L. Dagorn, and M. Capello. (2018). Recent advances on the use of supervised learning algorithms for detecting tuna aggregations under fads from echosounder buoys data. IOTC-2018-WPTT20-25_Rev1. Mahé.

Baidai Y., Dagorn L., Amande M., Gaertner D., and Capello M. (2019a). Aggregation processes of tuna under drifting fish aggregating devices (DFADs) assessed through fisher's echosounder buoy in the Atlantic Ocean. SCRS/2019/149.

Baidai Y., Dagorn L., Amande M.J., Gaertner D. and Capello M. (2019b) Aggregation processes of tuna under drifting fish aggregating devices (dFADs) assessed through fisher's echosounder buoy in the indian ocean. IOTC-2019-WPTT21-55

Baidai Y., Dagorn L., Amande, M.J., Gaertner D., Capello M., 2019b. Mapping tuna occurrence under drifting fish aggregating devices from fisher's echosounder buoys in Indian Ocean. OTC-2019-WPTT21-56_Rev1

Baidai Y., Dagorn L., Amande, M.J., Gaertner D., Capello M., 2019c.Mapping tuna occurrence under drifting fish aggregating devices from fisher's echosounder buoys in Atlantic Ocean. SCRS/2019/150

Bates, D., Mächler, M., Bolker, B., & Walker, S. (2015). Fitting Linear Mixed-Effects Models Using lme4. Journal of Statistical Software, 67(1), 1–48. https://doi.org/10.18637/jss.v067.i01

Beets, J. (1989).Experimental evaluation of tish recruiment to combinations of fish aggregating devices and benthic artificial reefs.Bull. Mar. Sci. 44 (2): 973-983. (9)

Belkin, I. M., & O'Reilly, J. E. (2009). An algorithm for oceanic front detection in chlorophyll and SST satellite imagery. Journal of Marine Systems, 78, 319–326.

Bertrand, A., Josse, E., & Massé, J. (1999). In situ acoustic target-strength measurement of bigeye (Thunnus obesus) and yellowfin tuna (Thunnus albacares) by coupling split-beam echosounder observations and sonic tracking. ICES Journal of Marine Science, 56(1), 51-60.

Bortone, S.A., Hastings, P.A. & Collard, S.B. (1977). The pelagic-Sargassum ichthyofauna of the Eastern Gulf of Mexico. Northeast Gulf Science, 1(2):60-67. (14)

Boyra, G., G. Moreno, B. Sobradillo, I. Perez-Arjona, I. Sancristobal, and Demer D. (2018). "Target strength of skipjack tuna (Katsuwanus pelamis) associated

with fish aggregating devices (FADs)." ICES Journal of Marine Science 75(5): 1790-1802.

Breiman, L. (2001). Random forests. Machine Learning 45(1):5–32.

Brill, R. V., Block, B. A., Boggs, C. H., Bigelow, K., Freund, E. V., & Marcinek, D. J. (1999). Horizontal movements and depth distribution of large adult yellowfin tuna (Thunnus albacares) near the Hawaiian Islands, recorded using ultrasonic telemetry : implications for the physiological ecology of pelagic fishes. Marine Biology, 133, 395–408.

Capello, M., Robert, M., Soria, M., Potin, G., Itano, D., Holland, K., Deneubourg, J.L., agorn, L., (2015). A methodological framework to estimate the site fidelity of tagged animals using passive acoustic telemetry. PLoS One 10.

Carruthers, T. (2018) A multispecies catch-ratio estimator of relative stock depletion. Fisheries Research 197 (2018) 25–33

Castro, J.J. Santiago, J.A., & Hernández-García, V. (1999) Fish associated with fish aggregation devices off the Canary Islands (Central-East Atlantic). In: Massutí, E. & Morales-Nin (eds.). Biology and fishery of dolphinfish and related species. Sci. Mar. 63 (3-4): 191-198. (18)

Deledda G, Gaertner D, Demarcq H. (2018) Combining dFADs catch data and ecological factors for detecting hot spots of juveniles' bigeye tuna. SCRS/2018/038

Deledda-Tramoni G., Gaertner D. (2019) Assessing the effectiveness of the current moratorium on dFADs using conventional tagging data from the AOTTP. Preliminary results. Collect. Vol. Sci. Pap. ICCAT, 76(6): 126-138

Davies TK, Mees CC, Milner-Gulland E. Modelling the spatial behaviour of a tropical tuna purse seine fleet. (2014) PloS one.; 9(12):

Diallo.A, Tolotti, M.T., Sabarros, P., Dagorn, L., Deneubourg, J-L., Capello, M., (2018). Can we derive anabundance index for the silky shark based on its associative behavior with floating objects? IOTC-2018-WPEB14-32_Rev1 14th IOTC Working Party on Ecosystems and Bycatch (WPEB). Cape Town, South Africa.

Diallo.A, Tolotti, M.T., Sabarros, P., Dagorn, L., Deneubourg, J-L., Murua, H., Ruiz Gondra, J., Ramos Alonso, L., Abascal Crespo, F.J., Pascual Alayón, P.J., Capello, M., (2019). Silky shark population trend in the indian ocean derived from its associative behaviour with floating objects. IOTC-2019-WPEB15-23_Rev1 15th IOTC Working Party on Ecosystems and Bycatch (WPEB). La Reunion.

Druce, B. E., & Kingsford, M. J. (1995). An experimental investigation on the fishes associated with drifting objects in coastal waters of temperate Australia. Bull. Mar. Sci. 57 (2):378-392. (30)

Duparc A, Cauquil P, Depestris M, Dewals P, Gaertner D, Hervé A, Lebranchu J, Marsac F, Bach P. (2018) Assessment of accuracy in processing purse seine tropical tuna catches with the T3 methodology using French fleet data. In: Report of thte 20th session of the IOTC Working Party on Tropical Tunas. Victoria, Seychelles:IOTC. (IOTC-2018-WPTT20-16). p. 1–19.

FAO. (2016). Workshop on Impacts of Marine Protected Areas on Fisheries Yield, F. C. and E. & Food and Agriculture Organization of the United Nations. Report of the FAO Workshop on Impacts of Marine Protected Areas on Fisheries Yield, Fishing Communities and Ecosystems: Rome, Italy, 16-18 June 2015.

Feigenbaum, D., Fridlander, A., & Bushing, M. (1989).Determination of the feasibility of fish attracting devices for enhancing fisheries in Puerto Rico.Bull. Mar. Sci 44(2): 950-959. (34).

Fonteneau, A. (1992). Pêche thonière et objects flottants: Situation mondiale et perspectives. In: Rapport de Synthèse sur Groupe de Travail IATTC "objets flottants et thons" presenté à la 12ème Semaine des Pêches dos Açores, mars1992: 31 pp.

Fonteneau A., (1993). Pêche thonière et objets flottants: situation mondiale et perspectives. Rec. Doc. Sci. ICCAT, 40(2), 459-472

Fonteneau A., Diouf T., (1994). An efficient way of bait-fishing for tunas recently developed in Senegal. Aquat. Living Resour., 7(3), 139-151.

Fonteneau, A., Lucas, V., Tewkai, E., Delgado, A., & Demarcq, H. (2008). Mesoscale exploitation of a major tuna concentration in the Indian Ocean. Aquatic Living Resources, 21(2), 109-121

Fonteneau A., Gaertner D., Maufroy A. and Amandè M. J. (2015). Effects of the ICCAT FAD moratorium on the tuna fisheries and tuna stocks. Collect. Vol. Sci. Pap. ICCAT, 72(2): 520-533 (2016)

Foote, K. G. (1983). Linearity of fisheries acoustics, with addition theorems. The Journal of the Acoustical Society of America, 73(6), 1932–1940. https://doi.org/10.1121/1.389583

Garcia, S.M., Zerbi, A., Aliaume, C., Do Chi, T., Lasserre, G. (2003) The ecosystem approach to fisheries. Issues, terminology, principles, institutional foundations, implementation and outlook. FAO Fisheries Technical Paper. No. 443. Rome, FAO.71 p

Guéry L., Deslias C., Kaplan D., Marsac F., Abascal F., Pascual P., and Gaertner D. (2019a) Accounting for fishing days without set in the CPUE standardization of yellowfin tuna in free schools for the EU purse seine fleet operating in the Eastern Atlantic Ocean during the 1991-2018 period. SCRS/2019/066

Guéry L., Kaplan D., Marsac F., Floch L., Deslias C., Abascal F., Baez J.C., and Gaertner D. (2019b) Accounting for fishing days without set, fishing concentration and piracy in the CPUE standardization of yellowfin tuna in free schools for the EU purse seine fleet operating in the Indian Ocean during the 1991-2017 period. Doc. WPTT.

Goujon, M. (1998). Accord des producteurs de thon congelé pour la protection des thonidés de l'Atlantique : résultats pour la flottille française. Collect. Vol. Sci. Pap. ICCAT, 49(3), 477-482.

Hall, M. (1992). The association of tuna with floating objects and dolphins in the Eastern Pacific Ocean. VII. Some hypotheses on the mechanisms governing the associations of tunas with floating objects and dolphins. In: International workshop on fishing for tunas associated with floating objects. (11-14February 1992. La Jolla, California): 6 pp. (47)

Hallier J-P, Delgado de Molina A. (2000). Baitboat as a tuna aggregating device. Biology and behavior of pelage fish aggregations. In Pêche thonière et dispositifs de concentration de poissons, Caribbean-Martinique, 15-19 Oct 1999 553-578.

Hallier, J.P., and Gaertner, D. (2008) Drifting fish aggregation devices could act as an ecological trap for tropical tunas. Marine Ecology Progress Series 353: 255-264.

Hammond, F. L., Myatt, D. O., & Cupka, D. M. (1977). Evaluation of midwater structures as a potential tool in the management of the fisheries resources

on South Carolina´s artificial fishing reefs. S. Carolina Mar. Res. Center Tech. Rept. Ser., 15:1-19.

Hampton, I. (1996). Acoustic and egg-production estimates of South African anchovy biomass over a decade: comparisons, accuracy, and utility. ICES Journal of Marine Science, 53(2), 493–500.

Hilborn, R., Stokesb K., Maguirec J. J., Smithd T., Botsforde L. W., Mangelf M., Orensanzg J., Parmah A., Ricei J., Bellj J., Cochranek K. L., Garcial S, Hallm S. J., Kirkwoodn G.P., Sainsburyo K, Stefanssonp G, Waltersq C. 2004. When can marine reserves improve fisheries management? Ocean & Coastal Management 47, 197–205. Hobday, A.J., Maxwell, S.M., Forgie, J. et al. (2014) Dynamic ocean management: integrating scientific and technological capacity with law, policy and management. Stanford Environ.Law J. 33:125–165.

Holland, K., Brill, R., & Chang, R.K.C. (1990) Horizontal and vertical movements ofyellowfin and bigeye tuna associated with fish aggregating devices. Fish. Bull.88(3) 493-507. (53)

Hunter, J.R., & Mitchell, C.T. (1968). Field experiments on the attraction of fish tofloating objects. J. Cons. Perm. Int. Explor. Mer 31:427-434.

ICCAT. (1998). Recommendation by ICCAT Concerning the Establishment of a Closed Area/Season for the Use of Fish Aggregation Devices (FADs). Collect. Vol. Sci. Pap. (ICCAT) Rec-98-01

ICCAT. (2004). Recommandation de l'ICCAT sur un programme de conservation et de gestion pluri-annuel pour le thon obèse. Collect. Vol. Sci. Pap. (ICCAT). Rec-04-01.

ICCAT (2015). Recommandation by ICCAT on a multi-annual conservation and management program for tropical tunas. Collect. Vol. Sci. Pap. (ICCAT). Rec-15-01.

IUCN , (2019). La Lista Roja de especies amenazadas de la UICN. Versión 2019-2

Josse, E., Bach, P., & Dagorn, L. (1998). Simultaneous observations of tuna movements and their prey by sonic tracking and acoustic surveys. In Advances in Invertebrates and Fish Telemetry (pp. 61–69).

Kaplan DM, Chassot E, Amande´ JM, Dueri S, Demarcq H, Dagorn L, et al.(2014) Spatial management of Indian Ocean tropical tuna fisheries: potential and perspectives. ICES Journal of Marine Science: Journal du Conseil. 71(7):1728–49

Kaplan, D., Bach, P., Bonhommeau, S., Chassot, E., Chavance, P., Dagorn, L., Davies T., Dueri, S., Fletcher, R., Fonteneau, A., Fromentin, J.M., Gaertner, D., Hampton, J., Hilborn, R., Hobday, A., Kearney, R., Kleiber, P., Lehodey, P., Marsac, F.., Maury, O., Mees, C., Ménard, F., Pearce, J., Sibert, J. (2013). The true challenge of giant marine reserves. Science, 340 (6134) : 810-811.

Katara I., Gaertner D., Marsac F., Grande M., Kaplan D., Urtizberea A., Guery L., Depetris M., Duparc A., Floch L., Lopez L., Abascal F., (2018). Standardization of yellowfin tuna CPUE for the EU purse seine fleet operating in the Indian Ocean. IOTC–2018–WPTT20–36

Kingsford, M.J. (1992). Drift algae and small fish in coastal waters of noth eastern New Zealand. Mar. Ecol. Prog. Ser. 80 (1): 41-55

Kingsford, M.J. (1993) Biotic and abiotic structure in the pe1agic environment: Importance to small fishes. Bull. Mal: Sci. 53(2), 393-415.

Klima, E. F., & Wickham, D. A. (1971).Attraction of coastal pelagic fishes with artificial structures. Trans. Am. Fish. Soc. 100:86-99

Lambert, D. M., Lipcius, R. N. & Hoenig, J. M. (2006). Assessing effectiveness of the blue crab spawning stock sanctuary in Chesapeake Bay using tag-return methodology. Marine Ecology Progress Series 321, 215–225.

Lo, N. C., Jacobson, L. D., & Squire, J. L. (1992). Indices of Relative Abundance from Fish Spotter Data based on Delta-Lognornial Models. Canadian Journal of Fisheries and Aquatic Sciences, 49(12), 2515–2526

Lopez, J., Moreno, G., Boyra, G., Dagorn, L., (2016). A model based on data from echosounder buoys to estimate biomass of fish species associated with fish aggregating devices. Fish. Bull. 114.

Lopez, J., Moreno, G., Ibaibarriaga, L., & Dagorn, L. (2017). Diel behaviour of tuna and non-tuna species at drifting fish aggregating devices (DFADs) in the Western Indian Ocean, determined by fishers' echo-sounder buoys. Marine Biology, 164(3), 44. McFadden, J. E., T. L. Hiller, and A. J. Tyre. (2011). Evaluating the efficacy of adaptive management approaches: Is there a formula for success? Journal of Environmental Management 92:1354-1359.

Maclennan, D., Fernandes, P. G., & Dalen, J. (2002). A consistent approach to definitions and symbols in fisheries acoustics. ICES Journal of Marine Science, 59(2), 365–369.

Marsac, F, (2008) Outlook of ocean climate variability in the West tropical Indian Ocean, 1997-2008. IOTC-2008-WPTT-27

Maufroy A, Kaplan DM, Bez N, Molina D, Delgado A, Murua H, Floch L, Chassot E (2017) Massive increase in the use of drifting Fish Aggregating Devices (dFADs) by tropical tuna purse seine fisheries in the Atlantic and Indian oceans. ICES J Mar Sci 74:215–225.

Maunder, M. N., & Punt, A. E. (2004). Standardizing catch and effort data: a review of recent approaches. Fisheries Research, 70(2–3), 141–159.

Maxwell S,M, et al (2015)) Dynamic ocean management: Defining and conceptualizing real-time management of the ocean. Mar Policy 58:42–50

Moreno, G., L. Dagorn, G. Sancho, and D. Itano. (2007). Fish behaviour from fishers' knowledge: the case study of tropical tuna around drifting fish aggregating devices (DFADs). Canadian Journal of Fisheries and Aquatic Sciences 64(11):1517–1528.

Moreno, G., Boyra, G., Sancristobal, I., & Restrepo, V. (2019). Towards acoustic discrimination of tropical tunas associated with Fish Aggregating Devices. PloS ONE, 14(6), 24

Moser, M.L., Auster, P.J., & Bichy, J.B. (1998). Effects of mat morphology on large Sargassum-associated fishes: observations from a remotely operated vehicle(ROV) and free-floating video comcorders. Env. Biol. Fish. 51:391-398.

Murua J, Itano D, Hall M, Dagorn L, Moreno G, Restrepo V. (2016) Advances in the use of entanglement reducing Drifting Fish Aggregating Devices (DFADs) in tuna purse seine fleets. ISSF Technical Report 2016–08 International Seafood Sustainability Foundation, Washington, DC, USA.

Nelson, P. A. (2003). Marine fish assemblages associated with fish aggregating devices (FADs): Effects of fish removal, FAD size, fouling communities, and prior recruits. Fishery Bulletin 101(4):835–850.

Ohta, I., Kakuma, S., (2005). Periodic behavior and residence time of yellowfin and bigeye tuna associated with fish aggregating devices around Okinawa Islands, as identified with automated listening stations. Mar. Biol. 146, 581–594.

Ortuño Crespo, G. and Dunn, D. C., (2017). A review of the impacts of fisheries on open-ocean ecosystems. – ICES Journal of Marine Science, 74: 2283–2297.

Oshima, T. (2008). Target strength of Bigeye, Yellowfin and Skipjack measured by split beam echo sounder in a cage. IOTC, WPTT-22, 4.

Orue, B., Lopez, J., Moreno, G., Santiago, J., Boyra, G., Uranga, J., Murua, H., (2019a). From fisheries to scientific data: A protocol to process information from fishers' echo-sounder buoys. Fisheries Research 215 38–43

Orue, B., Lopez, J., Moreno, G., Santiago, J., Soto, M., Murua, H., 2019b. Aggregation process of drifting fish aggregating devices (DFADs) in the Western Indian Ocean: Who arrives first, tuna or nontuna species? PLOS ONE.

O'Reilly J.E., Maritorena, S., Mitchell G. , Siegel, D., Carder, K., Garver, S. , Kahru, M., McClain, C.R. (1998) Ocean color chlorophyll algorithms for SeaWiFS. J. Geophys. Res., 103: 24937-24953

Pascual-Alayón P., Amatcha H., N'Sow F., Ramos Mª L, Abascal F. J. y Rojo V. (2017). Estadística de las pesquerías españolas atuneras, en el océano atlántico tropical, período 1990 a 2016. SCRS/2017/199

Pascual-Alayón P., Rojo V., Amatcha H., N' Sow F., Ramos Mª L y Abascal F. J. (2019). Statistics of the European and associated purse seine and baitboat fleets in the atlantic Ocean (1991-2018). SCRS/2019/076

Petit C, Pallares P, Pianet R. (2000). New sampling and data processing strategy for estimating the composition of catches by species and sizes in the European purse seine tropical tuna fisheries. 2000.

Potier, M., Marsac, F., Lucas, V., Sabatié, R., Hallier, J. P., & Ménard, F. (2004). Feeding partitioning among tuna taken in surface and mid-water layers: the case of yellowfin (Thunnus albacares) and bigeye (T.obesus) in the western tropical Indian Ocean. Western Indian Ocean Journal of Marine Science, 3(1):51-62

Robert, M., Dagorn, L., Lopez, J., Moreno, G., & Deneubourg, J.-L. (2013). Does social behavior influence the dynamics of aggregations formed by tropical tunas around floating objects? An experimental approach. Journal of Experimental …, 440, 238–243.

Røttingen, I. (1976). On the relation between echo intensity and fish density. FiskDir. Skr. Ser. Havunders., 16(9), 301–314.

Santiago, J., Uranga J., Quincoces I., Orue B.,Grande M., Murua H., Merino M., Urtizberea A., Pascual P.,, Boyra G., (2019a). A novel index of abundance of juvenile yellowfin tuna in the indian Ocean derived from echosounder buoys.

Santiago, J., Uranga J., Quincoces I., Orue B.,Grande M., Murua H., Merino M., Urtizberea A., Pascual P.,, Boyra G., (2019b). A novel index of abundance of juvenile yellowfin tuna in the indian Ocean derived from echosounder buoys.

Schott FA, McCreary JP. (2001) The monsoon circulation of the Indian Ocean. Prog Oceanogr. 51(1):1–123.40.

Simmonds, E. J., & MacLennan, D. N. (2005). Fisheries acoustics: theory and practice. Blackwell Science.

Taquet, M. (2004). Le comportement agrégatif de la dorade coryphène (Coryphaena hippurus) au)tour des objets flottants. Thèse de Doctorat de l'Université de Paris 6, Océanologie biologique, 168p.

Walters C J, Holling C S. (1990). Large-scale management experiments and learning by doing. Ecology 71: 2060–2068

Wickham, D., Watson, J., & Ogren, L. (1973).The efficacy of midwater artificial structures for attracting sport fish. Trans. Amer. Fish. Soc. 3: 563-673. (131).
Wickham, D. A., & Russell, G. M. (1974). An evaluation of mid-water artificial structures for attracting coastal pelagic fishes.Fish. Bull. 72 (1): 181-191.
Williams, B.K., (2011). Adaptive management of natural resources-framework and issues. Journal of Environmental Management. 92: 1346-1353
Workman, I.K., Landry, A.M.Jr., Watson, J.W.Jr., & Blackwell, J.W. (1985). A midwaterfish attraction device study conducted from Hydrolab. Bull. Mar. Sci.37(1):377-386.

8 List of Acronyms

aCAT = aggregated Continuous Absence Time

aCRT = aggregated Continuous Residence Time

AIC = Akaike's Information Criterion

AM = Adaptive Management

ANABAC = Asociación Nacional de Armadores de Buques Atuneros Congeladores

ANOSIM = Analysis of similarities

AOTTP = Atlantic Ocean Tropical Tuna Program

AUC = Area Under the Curve

AZTI = AZTI-Tecnalia Research Institute

BAI = Buoy-derived Abundance Index

BET = Bigeye tuna

BIC = Bayesian Information Criterion

CEFAS = Centre for Environment, Fisheries and Aquaculture Sciences

Chl-a = Chlorophyll-a

CPUE = Catch per unit of effort

DCF = Data Collection Framework

dFAD = man-made drifting fish aggregating device

DG MARE = Directorate-General for Maritime Affairs and Fisheries

DOM = Dynamic Ocean Management

EAFM = Ecosystem Approach for Fisheries Management

EEZ = Exclusive Economic Zone

EU = European Union

FOB = Floating Object, including natural objects (e.g., floatsam, log) and artificial objects (FAD), see table 1 Annex 3 in ICCAT Rec[16-01]

FSC = Free school

FL = Fork Length

GAMM = Generalized Additive Mixed Models

GLM = Generalized linear model

GLMM = Generalized Linear Mixed Model

GMT = Greenwich Mean Time

GPS = Global Positioning System

GSHHG = Global Self-consistent Hierarchical, High-resolution Geography

HMS = Highly Migratory Species

ICCAT = International Commission for the Conservation of Atlantic Tunas

ID = Identification

IEO = Instituto Español de Oceanografia

IOTC = Indian Ocean Tuna Commission

IRD = Institut de Recherche pour le Développement

IUCN = International Union for Conservation of Nature

LASSO = least absolute shrinkage and selection operator

LMM = Linear Mixed Model

LSmeans = least square means s

M3I = Marine Instruments' M3i, equipped with double power supply system by rechargeable batteries by solar panels and back up package of alkaline batteries.

MCS = Monitoring, Control and Surveillance

MDS = Multidimensional scaling

MODIS = Moderate Resolution Imaging Spectroradiometer

MRAG = Marine Resources Assessment Group

MSE = Management Strategy Evaluation

NGO = Non-Governmental Organization

NTB = non-tracked buoy

OCUP = Observateur Commun Unique et Permanent

OPAGAC= Organización Productores Asociados Grandes Atuneros Congeladores

ORTHONGEL = Organisation des Producteurs de Thon Congelé et Surgelé

PS = Purse seiner

RECOLAPE = Strengthening regional cooperation in the area of large pelagic fishery data collection (RECOLAPE)

RF = Random Forest

RR = Relative risk

SA = Stock Assessment

SCR = Spatial Capture-Recapture

SCRS - Standing Committee on Research and Statistics (ICCAT)

SKJ = Skipjack

SST = Sea Surface Temperature

TAAF = Terres australes et antarctiques françaises

TS = Target Strength

VMS = Vessel Monitoring System

WP = Working Package

WPTT = Working Party on Tropical Tuna (IOTC)

YFT = Yellowfin tuna

GETTING IN TOUCH WITH THE EU

In person

All over the European Union there are hundreds of Europe Direct information centres. You can find the address of the centre nearest you at: https://europa.eu/european-union/contact_en

On the phone or by email

Europe Direct is a service that answers your questions about the European Union. You can contact this service:

– by freephone: 00 800 6 7 8 9 10 11 (certain operators may charge for these calls),

– at the following standard number: +32 22999696, or

– by email via: https://europa.eu/european-union/contact_en

EA-02-20-650-EN-N

doi: 10.2826/621446